



**POLITECNICO  
DI TORINO**

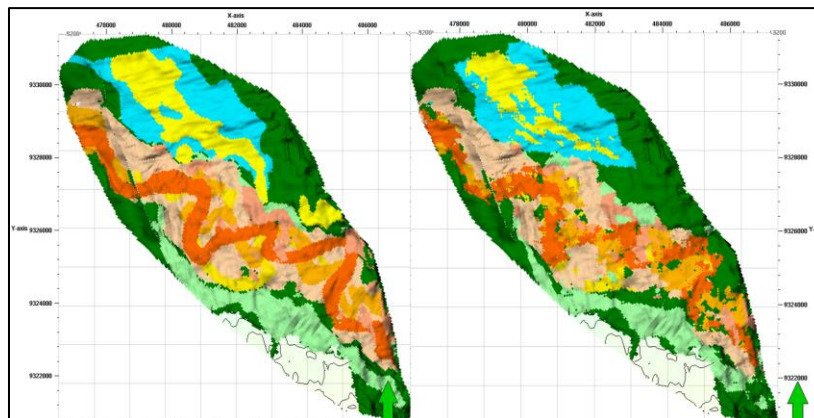
**THESIS**

# Offshore Angola oil field: Multiple Point Statistics (MPS) Modelling Approach

Eni Angola S.p.A – Reservoir Department

19 December 2018

Politecnico di Torino



## ABSTRACT:

Aim of these work is to implement the Multiple Point Statics “MPS” technology (using the Schlumberger Petrel 2017.1 software) to an Angolan offshore oil field already in production, comparing the results with the one coming from the existing standard modeling technique. This is achieved extending the stochastic simulation approach to the sedimentological model by means of the MPS algorithm.

Considering that the MPS is a modern modelling technique on the geostatistical panorama, the core concept is related with the aim of better representing the subsurface geology of the reservoir, by means of a deep analysis of the sedimentological model and the Environments of Deposition “EoD”. This can be achieved by the wide integration of data from the training image and secondary data (probabilistic data).

The Environments of Deposition (EoDs) coming from the sedimentological interpretation are used to build the Training Images (conceptual models) for each zone and the depositional model, instead of being the product of a deterministic interpretation, is the result of a MPS simulation. Moreover, the existing EoD property is converted into a probabilistic trend and used to condition the simulation.

The substitution of the vertical boundaries among the EoDs with more realistic depositional interfaces slightly reduces the global sand content – and the STOIP accordingly – but it improves the geological imaging of the field and the hydraulic communication among the depositional bodies.

The lithological facies and the petrophysical properties are distributed following the same approach of the current model (standard modelling approach) in order to properly evaluate the impact of the MPS algorithm on the STOIP.

Therefore, the reduction of the static hydrocarbon volume in place does not necessarily lead to a reduction of the ultimate recovery, due to a possible more efficient horizontal and vertical dynamic efficiency. The dynamic test (in both terms of HM and forecast) represents the most relevant way forward of the work, considering that the field is already in production since almost 2 years.

## AUTHOR:

JERSON PAIVA

STEFANO LO RUSSO	ILARIO FRANCO	19 December 2018
	ANDREA TOMASI	
PoliTo Supervisor	eni Supervisors	Date

## TABLE OF CONTENT

ABBREVIATIONS & ACRONYMS .....	7
1 THESIS SUMMARY .....	8
1.1 Introduction .....	8
1.2 Conclusion and recommendations.....	9
2 FIELD OVERVIEW.....	10
2.1 Geological settings .....	10
2.2 Development plan .....	12
2.3 Current reservoir 3D model .....	14
2.3.1 SiS (Sequential Indicator Simulation) Facies model .....	14
2.3.2 SGS Petrophysical properties model .....	21
2.3.3 Volumetric.....	24
3 MULTIPLE POINT STATISTICS (MPS) .....	26
3.1 MPS Simulation Technology .....	26
3.2 MPS application to an Angolan offshore field .....	28
3.2.1 EoD Probability Volumes .....	29
3.2.2 Training Image generation .....	36
3.2.3 MPS Geo-body Facies (EoD) model .....	49
3.2.4 SIS Facies distribution property model .....	66
3.2.5 SGS Petrophysical properties model .....	67
3.2.6 Volumetric (STOIIP) .....	72
3.2.7 Static volumes comparison (Current vs. MPS workflow) .....	74
4 UNCERTAINTY AND OPTIMIZATION ANALYSIS.....	76
4.1 Risk analysis (RA) purpose .....	76
4.2 Standard model RA workflow .....	76
4.3 MPS model Risk Analysis workflow.....	78
4.4 Result comparison .....	81
5 CONCLUSION AND WAY FORWARD .....	83
REFERENCES .....	87

## LIST OF TABLES

Table 1- PVT Properties .....	10
Table 2- Zone A and AB Facies Fraction .....	18
Table 3- Zone C Facies Fraction .....	18
Table 4- Zone CD Facies Fraction .....	18
Table 5- Zone D, E and F Facies Fraction .....	19
Table 6- Petrophysical distributions (mean value) by facies .....	21
Table 7- STOOIP volumes (Standard model) by zone .....	25
Table 8 – Pseudozones A and AB - MPS Facies Model .....	50
Table 9 – Pseudozones C and CD - MPS Facies Model .....	50
Table 10 – Pseudozones D and E - MPS Facies Model .....	51
Table 11 – Pseudozones F - MPS Facies Model .....	51
Table 12- Zone C MPS Facies Fraction .....	57
Table 13 – Pseudozones C - MPS Facies Model (simulation 3) .....	58
Table 14- Geo-bodies Facies Fraction per zone for all simulations .....	65
Table 15 - STOOIP per pseudozones .....	73
Table 16- Pseudozones STOOIP St. Deviation from the standard model .....	75
Table 17- STOOIP Standard Deviation from the reference standard model .....	75
Table 18- RA variables to be simulated .....	76
Table 19- EoD and facies fractions algorithm .....	77
Table 20 – Training Image input facies fractions .....	78
Table 21- Training image D, E and F facies fraction algorithm .....	79
Table 22- Standard model RA STOOIP P10, P50 and P90 .....	81
Table 23- MPS model RA STOOIP P10, P50 and P90 .....	82

## LIST OF FIGURES

Figure 1 – Standard model workflow .....	8
Figure 2 – Block map .....	10
Figure 3 – Structure horst schematic and LM22 Top map .....	11
Figure 4 – LM22 internal architecture (seismic & sedimentology) .....	12
Figure 5 – LM22 completion scheme .....	12
Figure 6 – Development wells - log correlation .....	13
Figure 7 – Pressure points analysis .....	13
Figure 8 – Petrel static modelling workflow .....	14
Figure 9 – Cluster analysis result .....	15
Figure 10 – Zones and Pseudozones from 3D model .....	16
Figure 11 – Geo-bodies (EoD) - Zones A, AB, C, CD, D and E .....	16
Figure 12 – Geo-bodies (EoD) - Zones F and E .....	17
Figure 13 – EoD vertical cross section .....	17
Figure 14 – Facies modelling window .....	20
Figure 15 – Facies distribution map view and vertical section .....	20
Figure 16 – Facies Histogram (Standard model) .....	21
Figure 17 – NTG property distribution .....	22
Figure 18 – Porosity distribution settings .....	22
Figure 19 – Porosity distribution .....	23
Figure 20 – Porosity distribution settings .....	23
Figure 21 – Water Saturation distribution .....	24
Figure 22 – Static model work flow .....	24
Figure 23 – Cross section through the reservoir .....	25



Figure 24 – Training Image concept.....	26
Figure 25 – Multiple Point configurations .....	26
Figure 26 – Standard Model geo-body conceptual cross section .....	27
Figure 27 – MPS Model geo-body conceptual model .....	27
Figure 28 – MPS model channel margins in conceptual cross section .....	28
Figure 29 – Petrel static MPS modelling workflow.....	28
Figure 30 – Zone A and AB – EoD probability map .....	29
Figure 31 – Zone C and CD - EoD probability map .....	29
Figure 32 – Zone D and E - EoD probability map .....	29
Figure 33 – Zone F - EoD probability map.....	30
Figure 34 – Channel Axis 3 – EoD probability volume (3D property).....	30
Figure 35 – Mud filled channel 3 – EoD probability volume (3D property) .....	31
Figure 36 – Rich of Axis – EoD probability volume (3D property) .....	31
Figure 37 – Crevasse – EoD probability volume (3D property).....	32
Figure 38 – Frontal Splay – EoD probability volume (3D property) .....	32
Figure 39 – Channel4 – EoD probability volume (3D property) .....	33
Figure 40 – Channel D – EoD probability volume (3D property) .....	33
Figure 41 – Channel North – EoD probability volume (3D property) .....	34
Figure 42 – Channel 2 – EoD probability volume (3D property) .....	34
Figure 43 – Channel 1 – EoD probability volume (3D property) .....	35
Figure 44 – smoothness principle applied on the MPS external constraint concept.....	35
Figure 45 – Training Image work flow .....	36
Figure 46 – Training Image grid input .....	37
Figure 47 – Training Image facies modelling window.....	38
Figure 48 – Zone A- Channel axis 3 and mud filled channel inputs .....	39
Figure 49 – Zone A Training Image 3D grid.....	39
Figure 50 – Zone AB- Mud filled inputs.....	40
Figure 51 – Zone AB Training Image 3D grid.....	40
Figure 52 – Zone C- Channel 4 and Channel axis 3 inputs.....	41
Figure 53 – Zone C- Rich off Axis and Frontal Splay inputs .....	41
Figure 54 – Zone C Training Image 3D grid .....	42
Figure 55 – Zone CD Rich off Axis inputs .....	42
Figure 56 – Zone CD Training Image 3D grid .....	43
Figure 57 – Zone D Channel D input .....	43
Figure 58 – Zone D Training Image 3D grid .....	44
Figure 59 – Zone E Channel E North and Rich off axis input .....	44
Figure 60 – Zone E Training Image 3D grid.....	45
Figure 61 – Zone F Channel 4 and Channel axis 3 inputs .....	45
Figure 62 – Zone F Channel 2 and Channel 1 input .....	46
Figure 63 – Zone F Training Image 3D grid.....	46
Figure 64 – Zone C, facies interpretation – Seismic.....	47
Figure 65 – Zone C- Channel 4 and Channel axis 3 inputs (second simulation) .....	47
Figure 66 – Zone C Training Image 3D grid (second simulation) .....	48
Figure 67 – Zone D- Channel D inputs (second simulation) .....	48
Figure 68 – Zone D Training Image 3D grid (second simulation).....	49
Figure 69 – MPS Facies modelling concept .....	52
Figure 70 – Pseudozones A and AB – MPS model (simulation 1) .....	53
Figure 71 – Zone C and CD – MPS model (simulation 1) .....	53
Figure 72 – Pseudozones D and E – MPS model (simulation 1) .....	53
Figure 73 – Pseudozone F – MPS model (simulation 1) .....	54
Figure 74 – Pseudozones A and AB – MPS model (simulation 2) .....	54
Figure 75 – Pseudozones C and CD – MPS model (simulation 2) .....	55
Figure 76 – Pseudozones D and E – MPS model (simulation 2) .....	55

Figure 77 – Pseudozones F – MPS model (simulation 2).....	55
Figure 78 – Cross section – MPS model .....	56
Figure 79 – Pseudozone A and F, Facies Interpretation - Seismic.....	56
Figure 80 – Pseudozones A and AB – MPS model (simulation 3) .....	58
Figure 81 – Zone C and CD – MPS model (simulation 3) .....	59
Figure 82 – Pseudozones D and E – MPS model (simulation 3) .....	59
Figure 83 – Pseudozone F – MPS model simulation 3) .....	60
Figure 84 – Pseudozones A and AB – MPS model (simulation 4) .....	60
Figure 85 – Pseudozones C and CD – MPS model (simulation 4) .....	61
Figure 86 – Pseudozones D and E – MPS model (simulation 4) .....	61
Figure 87 – Pseudozones F – MPS model (simulation 4).....	61
Figure 88 – Cross section – MPS model (simulation 3).....	62
Figure 89 – Pseudozones A and AB and C Cross section – simulation progress .....	63
Figure 90 – Pseudozones D and F Cross section – simulation progress .....	64
Figure 91 – Facies model settings .....	66
Figure 92 – Facies distribution result.....	66
Figure 93 – NTG Properties distribution settings .....	67
Figure 94 – NTG distribution .....	67
Figure 95 – Porosity Properties distribution settings .....	68
Figure 96 – Porosity distribution .....	68
Figure 97 – Porosity model distribution per facies .....	69
Figure 98 – Porosity Properties distribution settings .....	69
Figure 99 – Water Saturation distribution .....	70
Figure 100 – Water saturation changes as a function of the porosity .....	70
Figure 101 – Water Saturation evolution analysis .....	71
Figure 102 –standard model EoD, facies and NTG distribution .....	71
Figure 103 –MPS model EoD, facies and NTG distribution .....	72
Figure 104 – Petrel MPS static model workflow.....	73
Figure 105 – STOOIP analysis per pseudozone .....	74
Figure 106 – STOOIP analysis .....	75
Figure 107 – Uncertainty and optimization window RA Standard model .....	78
Figure 108 – Uncertainty and optimization window RA MPS 3rd model .....	80
Figure 109 – Standard model uncertainty analyze histogram P10, P50 and P90.....	81
Figure 110 – MPS model uncertainty analyze histogram P10, P50 and P90.....	82
Figure 111 – MPS Concept model (with stacked geo-bodies) .....	84
Figure 112 – MPS model.....	85

## ABBREVIATIONS & ACRONYMS

Term / Acronym / Abbreviation	Explanation / Definition
GOIP or GIIP	Gas Initially in Place
OOIP or OIIP	Oil Initially in Place
OCIP or CIIP	Condensate Initially in Place
FOPR	Field Oil Production Rate
FOPT	Field Oil Production Total
FGPR	Field Gas Production Rate
FGPT	Field Gas Production Total
FWPR	Field Water Production Rate
FWPT	Field Water Production Total
FWCT	Field Water Cut
FGOR	Field Gas Oil Ratio
P10	10 <sup>th</sup> percentile, there is 10% probability of being equal or lower than the P10 value
P50	50 <sup>th</sup> percentile or median, there is 50% probability of being equal or lower than the P50 value
P90	90 <sup>th</sup> percentile, there is 90% probability of being equal or lower than the P90 value
LM22	Lower Miocene 22
FF	Facies Fraction
MSTB	Millions of Stock Tank Barrels
SCF	Standard Cubic Feet
BOPD	Barrels of Oil Per Day
SiSim	Sequential Indicator Simulation
GRFS	Gaussian Random function Simulation
EoD	Environment of Deposition
TI	Training Image
MPS	Multiple Point Statistics
RA	Risk Analysis
CPI	Computed Petrophysical Interpretation
SneSim	Single normal Equation Simulation
RB/MSCF	Reservoir Barrel /Millions Standard Cubic Feet
RB/STB	Reservoir Barrel / Stock tank Barrel
STOOIP,STOIIP	Stock Tank Oil Originally In Place, Stock Tank Oil Initially In Place

# 1 THESIS SUMMARY

## 1.1 Introduction

The scope of this work is extending the stochastic simulation approach to the sedimentological model by means of the recently developed modeling technology called Multiple Point Statistics “MPS”. The environments of deposition, coming from the sedimentological interpretation, will be used to build the training images (conceptual models) for each zone and the sedimentological model, instead of being the product of a deterministic interpretation, will be the result of a MPS simulation. The facies and the petrophysical properties will be distributed following the same approach of the standard model (Figure 1). Hundreds of realizations will be run and their average answer, in both terms of STOIIP and geological shapes, will be compared with the current model.

The current reservoir model has been subdivided into 8 pseudozones, belonging to the LM22 sequence. Each zone underwent a detailed sedimentological interpretation, which came out with the deterministic definition of different Environments of Deposition (EoD). 6 facies have been defined at well scale by means of a cluster analysis and then distributed into the grid by EoD through a SISim algorithm. The target proportion for each facies has been defined within each EoD and a sand probability volume has been applied as 3D trend for sandy facies. Finally, the petrophysical properties have been simulated by facies through statistical techniques. The above mentioned workflow is summarized in the schematic below, Figure 1.



Figure 1 – Standard model workflow

Multiple point Geo-statistics (MPS) is an innovative technology developed in the last decade by Stanford University. It has been designed to model very complex and curvilinear geological features. It goes over the traditional statistical approach based on the two-point correlation that is expressed by variograms, by using multiple-point configurations that are represented by training images, to infer statistics. They are 2D images or regular 3D grids able to reproduce the depositional environment that is object of the study. The MPS modelling results will be analyzed and compared with the standard model ones. The best case out of the different sensitivities with MPS simulation and the standard base case will undergo a risk analysis, in order to understand the impact on STOOIP of the parameters such as facies distribution and modeled geo-bodies percentages.

## 1.2 Conclusion and recommendations

The MPS technology is a modern modelling approach extremely indicated for complex and heterogeneous depositional systems. It is capable to reproduce complex geological shapes and spatial relationships, incorporating the geological principles, which leads to a better reservoir characterization and management

The out coming STOIIP from the MPS model is a conservative result in relation to the standard model, since a very detailed geological modelling in terms of both shapes and spatial relationship among the EoDs and geo-bodies is considered.

The detailed results of the work are listed here below:

- the MPS algorithm allows a better definition of the geological shapes and consequently a better simulation of the sedimentological model;
- the details of the TIs by means of the object modelling stochastic algorithm allows capturing and reproducing the stratigraphic and depositional principles (superposition, cross-cutting, intrusive relation);
- by modelling the EoDs in a stochastic manner, it is possible to easily update the sedimentological model once new wells are available;
- the Training Image definition is a time consuming iterative process, many sensitivities are needed to get the right spatial configuration and distribution;
- EoD probability volume (3D external trend property), plays a fundamental role in the EoD model definition. Through the weight factor the effects of the trend on the final simulation can be fine-tuned. This is an iterative process and it is clearly time consuming;
- MPS simulation is a time consuming algorithm in terms of both training image definition and facies simulation. This has to be taken into account especially while planning a Risk Analysis;
- Computational capacity is needed to run this kind of simulation and it is even more critical when performing a complete reservoir Risk Analysis.

To complete the study a reservoir dynamic simulation should be performed (initialization, History Match and forecast) in order to verify if the dynamic behavior of the field is better matched and forecasted by a static model, which reproduces with more details the geological features and their spatial relationships.

The outcome of the MPS model can optimize the pre-development prognosis of the field and lead to a better development campaign of the reservoir.

## 2 FIELD OVERVIEW

### 2.1 Geological settings

The structure is located in the North-Eastern part of the block (Figure 2), approximately 100 km from coast. The water depth is 550m and the field extension is about 50 km<sup>2</sup>. On average, the vertical gross thickness of LM22 level is about 250 m.

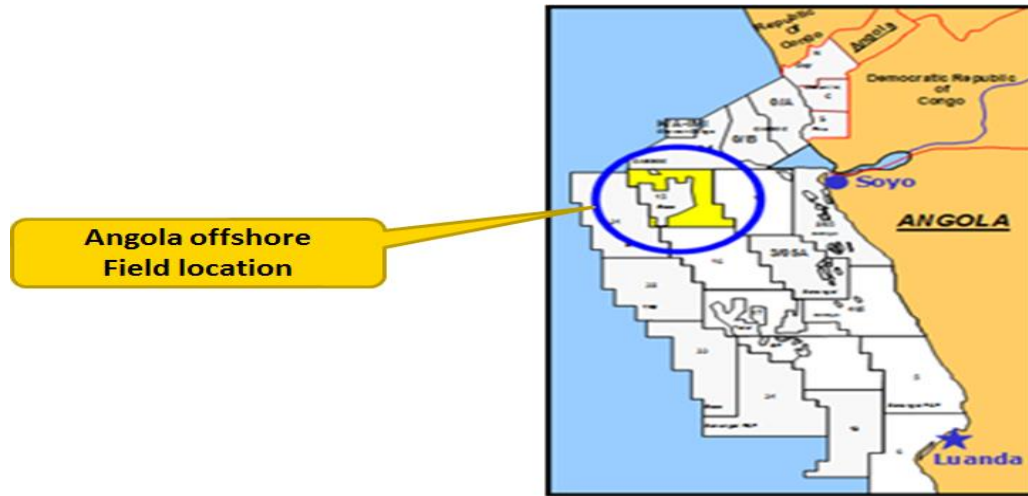


Figure 2 – Block map

The reservoir is characterized by a stack of Miocene turbidity channels, deposited with an East-West trend. The reservoir under analyze is the Lower Miocene 22 sequence, the so called “LM22”. Being the field a structural high (horst), the sand bodies, dipping towards West, are closing against the main structural component, represented by the bounding fault on the Eastern side. Reservoir seal is provided by the encasing deep-water shale settings.

The oil bearing reservoir “horst”, i.e. the Lower Miocene (LM22) interval, was discovered by the explorative well EXP-1 drilled in February 2010, which found a gas and oil bearing sequence with a Gas Oil Contact at -2818 m TVDSS and an Oil Down To at -3000 m TVDSS (Figure 3).

PVT	
API	36 °
Flash GOR	1046 scf/stb
Flash Bo	1.581 rb/stb @pb
Oil viscosity	0.35 cP
Sat Pressure (Pb)	4289 psia
Res. Pressure	4474 psia
Res. Temperature	120 °C

Table 1- PVT Properties



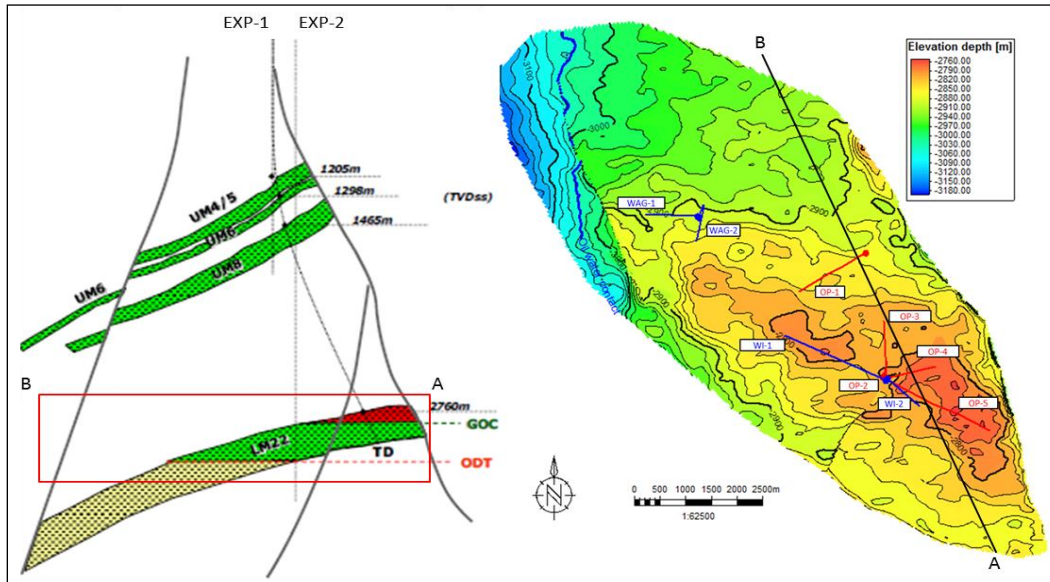


Figure 3 – Structure horst schematic and LM22 Top map

The reservoir is formed by terrigenous sediments, deposited during the Lower Miocene, within a large distal slope turbidity channel complex, which has been classified in the sedimentological study as a Weakly Confined Channel System. LM22 system represents a base of slope depositional setting. The main depositional trend is from SE to NW oriented at  $135^\circ$  degrees. The internal architecture of the sequences is quite complex, showing a lowering in amalgamation from the bottom to the top of the system.

The LM22 reservoir is believed to be an aggradational distributary system with amalgamated channels, slightly erosional at its base and with an overall fining upward trend. The system starts with thick sand layers at its base and becomes progressively mud dominated at the top. The channelized sequence, which shows different scales and sand content, presents depositional elements like channel (various infilling), crevasse, off-axis and frontal splay.

Due to the geophysical complexity of the field area, the sedimentological interpretation has been carried out on different volumes, basically Ip and VpVs, coming from 2013 inversion study. In order to recognize the depositional elements (EoDs), both geometries and amplitude values have been considered.



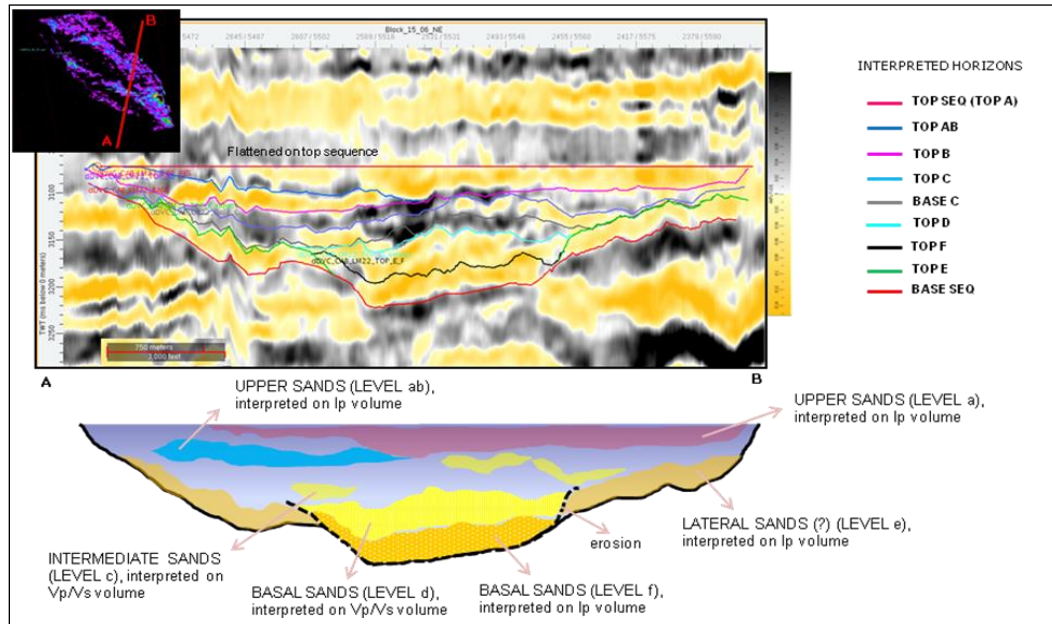


Figure 4 – LM22 internal architecture (seismic & sedimentology)

## 2.2 Development plan

The initial development plan foresaw ten wells: five oil producers, three WAG injectors and two WI wells. During the development of the field, the zone E was found with a low net pay and facies poorer than prognosis, leading to the revision of the development plan with nine development wells: five oil producers, two WAG injectors and two WI wells.

In accordance with the reference sedimentological setting on Figure 4, the completion scheme was optimized accordingly, giving priority to the basal sand packages (Figure 5).

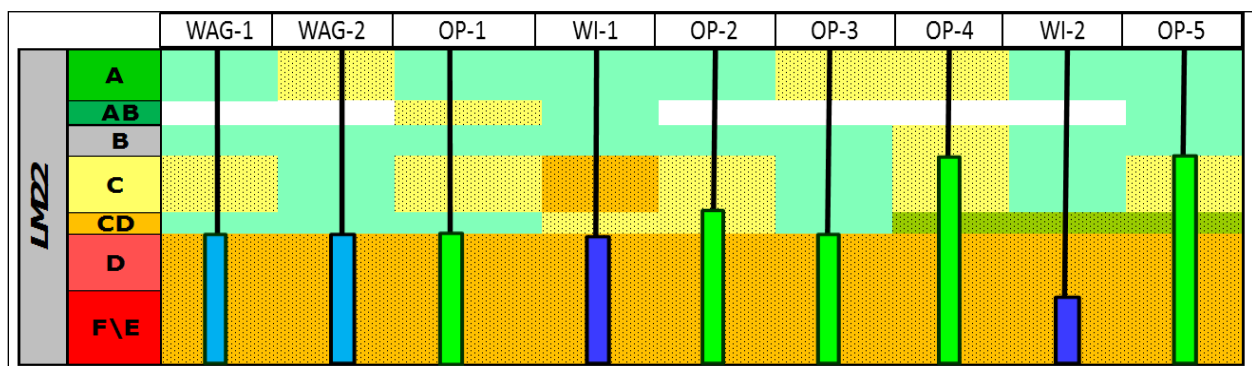


Figure 5 – LM22 completion scheme

The sedimentological model is reflected in the log-correlation of the development wells, where the different facies settings of each zone as well as the facies continuity through the zones can be appreciated.

Looking at the gamma ray log, the sand bodies can be clearly identified as well as the sedimentological behavior of each zone, i.e. the fining upward trend. The basal amalgamated sand bodies represent a stationary phase of the deposition (low aggradation) and are characterized by a high net sand content.

The resistivity log confirms the reservoir fluid content, distinguishing hydrocarbon from water and showing their contact.

The density/neutron log highlights the mineralized sand bodies and their relative porosity and density.

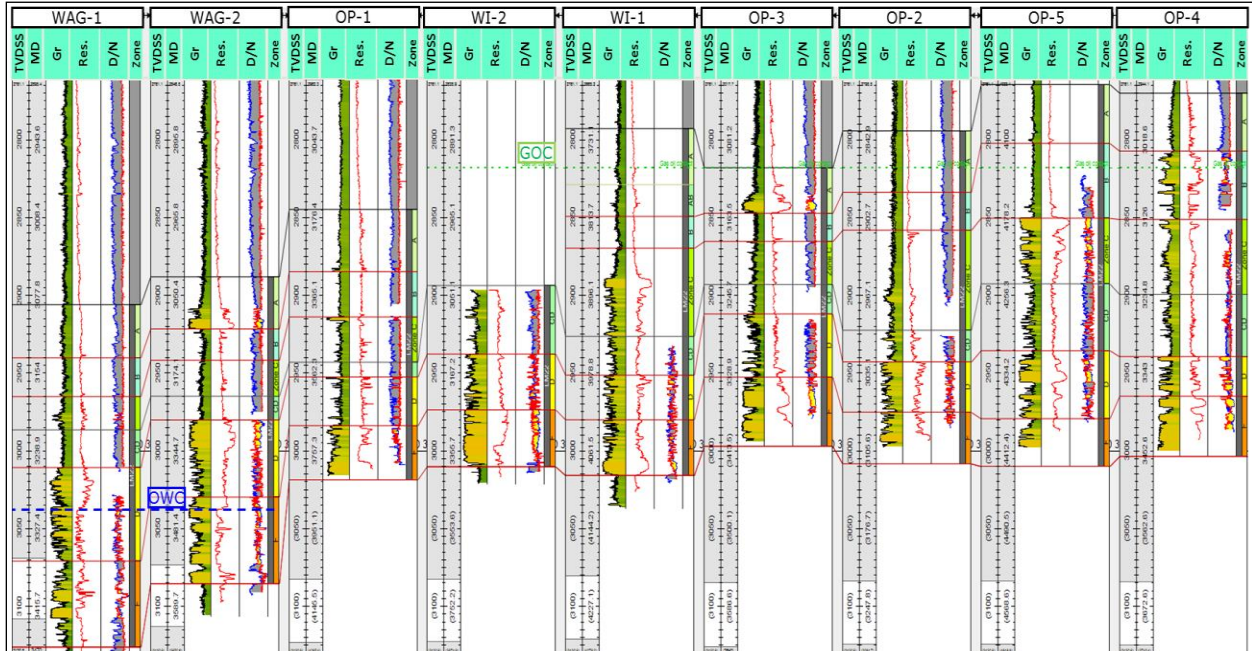


Figure 6 – Development wells - log correlation

The reservoir was subject to pressure point analysis during the drilling campaign, de-risking the regional uncertainties on the connectivity and fluid gradient of the reservoir.

The reservoir fluid gradients and the fluid contacts, Gas Oil Contact (GOC) and Oil Water Contact (OWC), were confirmed by the pressure point analysis as well as the channel connectivity (Figure 7).

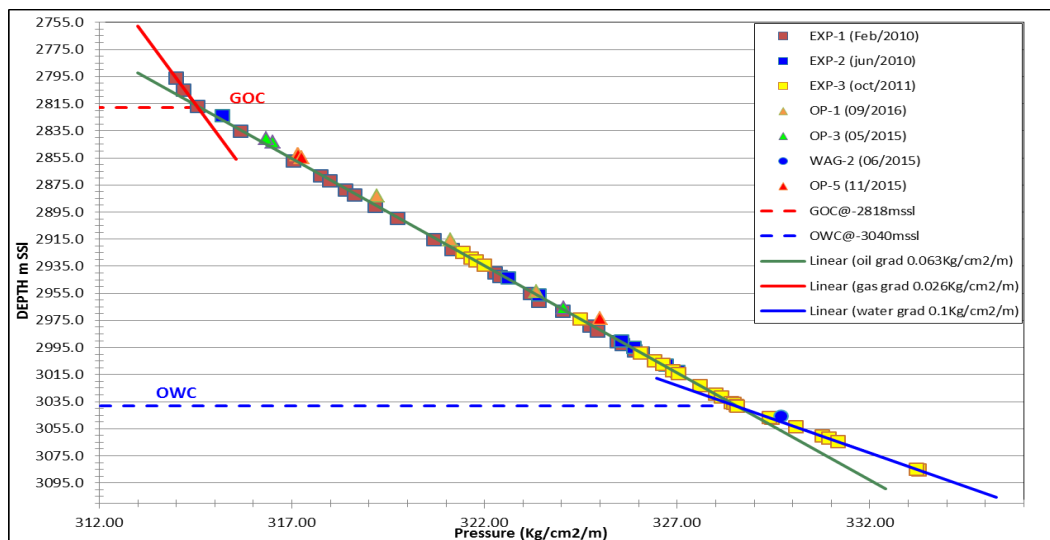


Figure 7 – Pressure points analysis

## 2.3 Current reservoir 3D model

The standard static model was developed basing on the following main data: well data (logs, well tops and facies) and seismic derived data (structural interpretation, EoDs and seismic inversion).

Well data:

- Memory log data are interpreted in order to get the CPI (computer processed interpretation);
- Basing on the log data and the CPI, a facies log is generated by means of a Cluster Analysis (CA) process;
- Facies and CPI log curves are upscaled in the 3D grid in order to use them for modelling purposes.

Seismic derived data:

- The structural analysis is performed on the seismic volumes in order to generate the structural grids (horizons) and the faults (fault sticks);
- The sedimentological interpretation is carried out on the amplitude extractions, made on the main horizons;
- EoD maps are generated from the sedimentological interpretation and a EoD 3D property is finally derived from these maps in order to be used to drive the facies simulation.

The above described sets of data are implemented in the following way:

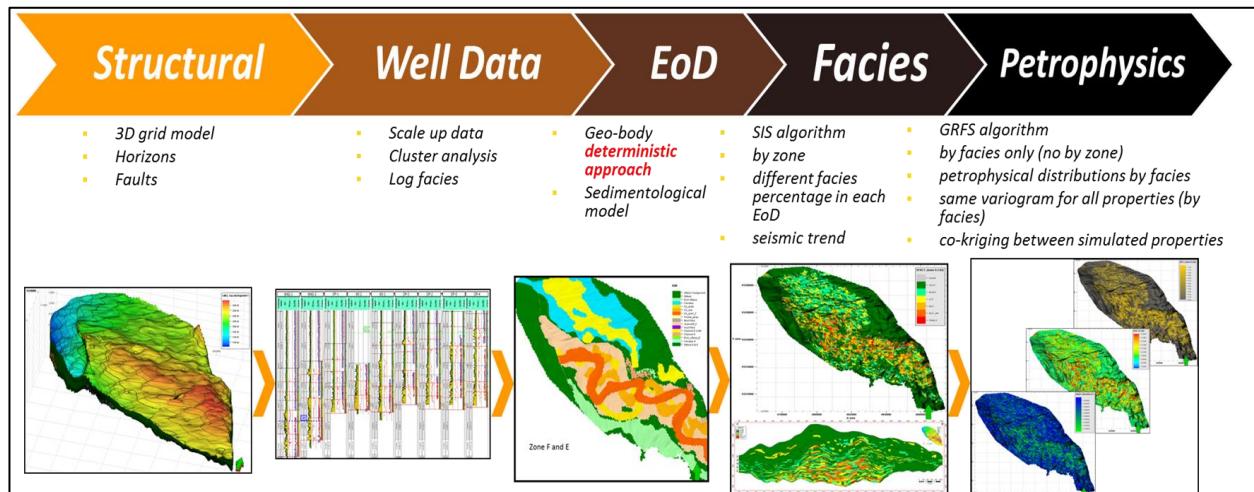


Figure 8 – Petrel static modelling workflow

### 2.3.1 SiS (Sequential Indicator Simulation) Facies model

The current reservoir model is based on the facies characterization coming from both the explorative wells (EXP-1 and EXP-2) and the development wells.

The cluster analysis was performed to discretize the petrophysical log response in the wells, simplifying the reservoir characterization. It is based on the multivariate statistics analysis, grouping objects according to similarity of the data. It consists of the following main steps:

- preliminary analysis and treatment of well logs and core data;
- statistical processing (unsupervised classification – 25/30 classes);
- Log-facies characterization (supervised classification – 4/7 classes).

The six facies coming out from the cluster analysis are listed here below:

- Log-facies 1: Very Low Concentration Turbidities (VLCT); shale section with very low sand content;
- Log-facies 2: Mixed Debrite (MXDT); representing a transition from shale to sandy facies, related to VLCT;
- Log-facies 3: Low Concentration Turbidities (LCT); laminated shaley-sands;
- Log-facies 4: High Concentration Turbidities (HCT); massive clean sand bodies;
- Log-facies 5: High Concentration Turbidities\_High Porosity (HCT\_HP); massive sand bodies with high porosity;
- Log-facies 6: Traction (TRACT); well sorted sand bodies with good porosity and permeability.

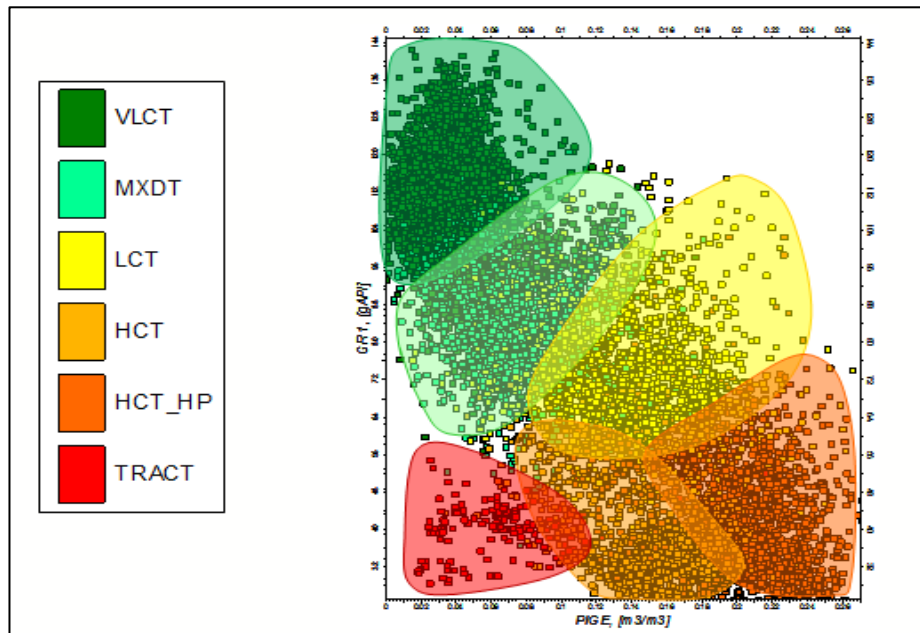


Figure 9 – Cluster analysis result

The facies distribution was carried out by zones and EoD, which means that different EoDs were modelled inside each zone of the model and then they were populated with different types of facies. In particular:

- Zone A was subdivided in two pseudozones: A and AB;
- Zone B was considered as constant VLCT;
- Zone D was subdivided in three pseudozones: D, E and F.

As it can be appreciated in the picture here below (Figure 10), the zones are delimited by horizons (black solid lines), while the pseudozones are defined only as index property (stair-step shape).



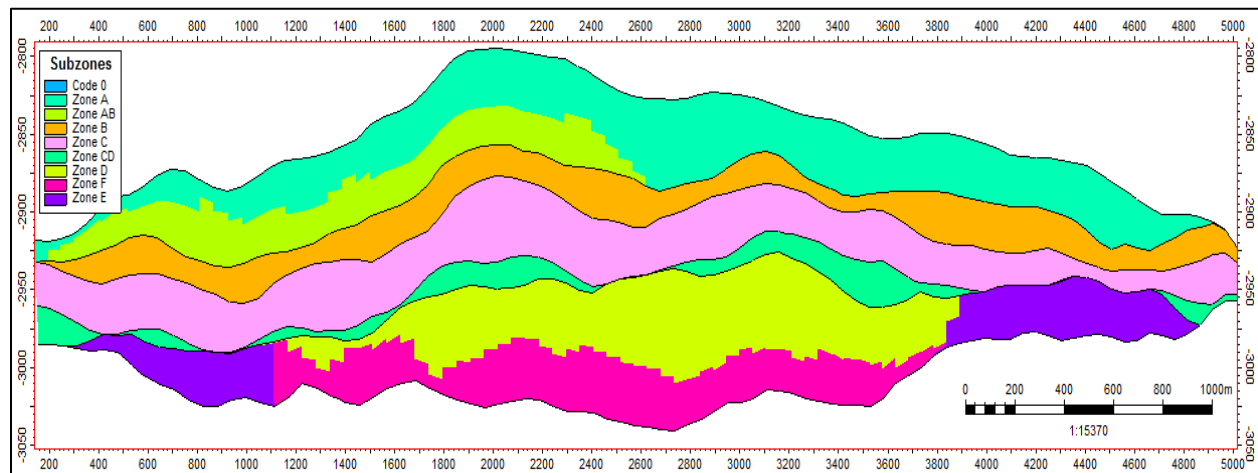


Figure 10 – Zones and Pseudozones from 3D model

Once the vertical zonation of the reservoir was defined, the sedimentological architecture was generated by modeling the interpreted EoDs inside each pseudozone as shown in the figures below.

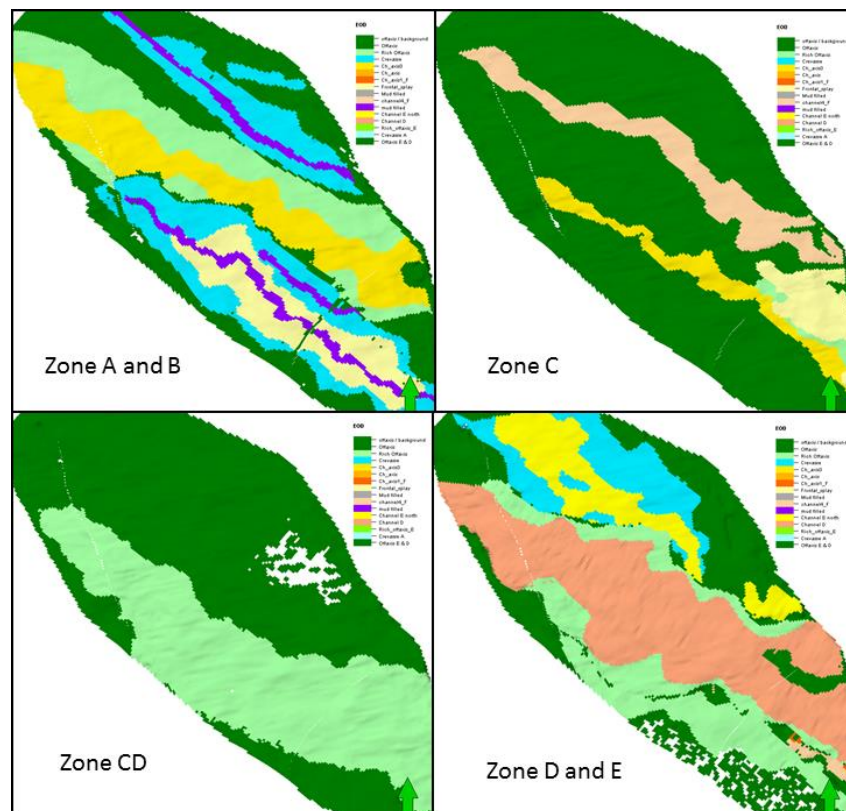


Figure 11 – Geo-bodies (EoD) - Zones A, AB, C, CD, D and E

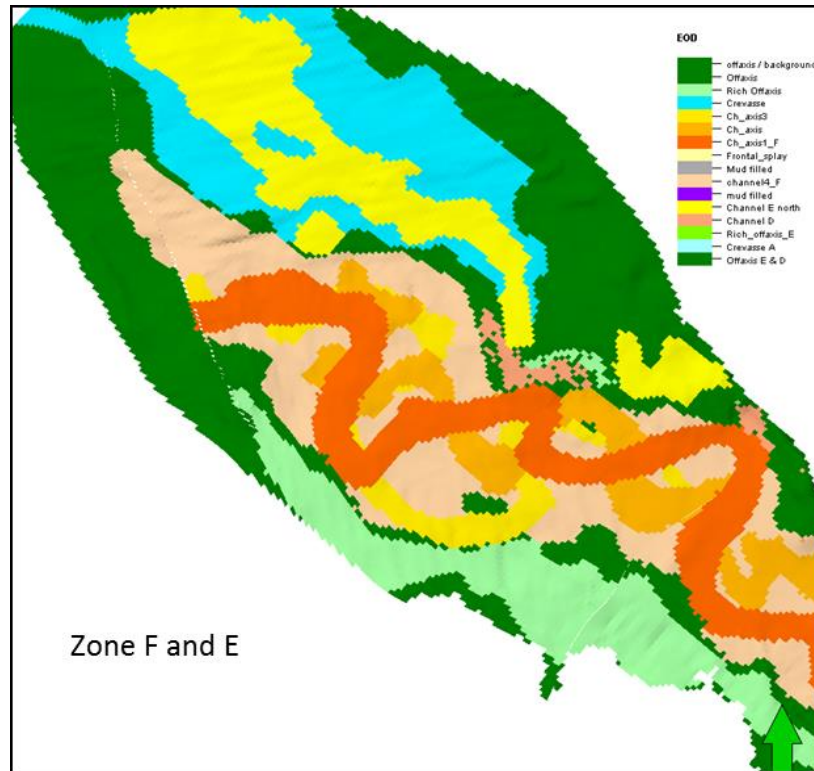


Figure 12 – Geo-bodies (EoD) - Zones F and E

On the standard model the EoD geo-bodies were modelled by pseudozone, simply assigning a value to the 3D property from a map. This means that they show strong and unrealistic vertical boundaries, with low lateral sinuosity. They involve the full thickness of the referred pseudozone, assigning the same EoD type between the top and bottom horizons (Figure 13).

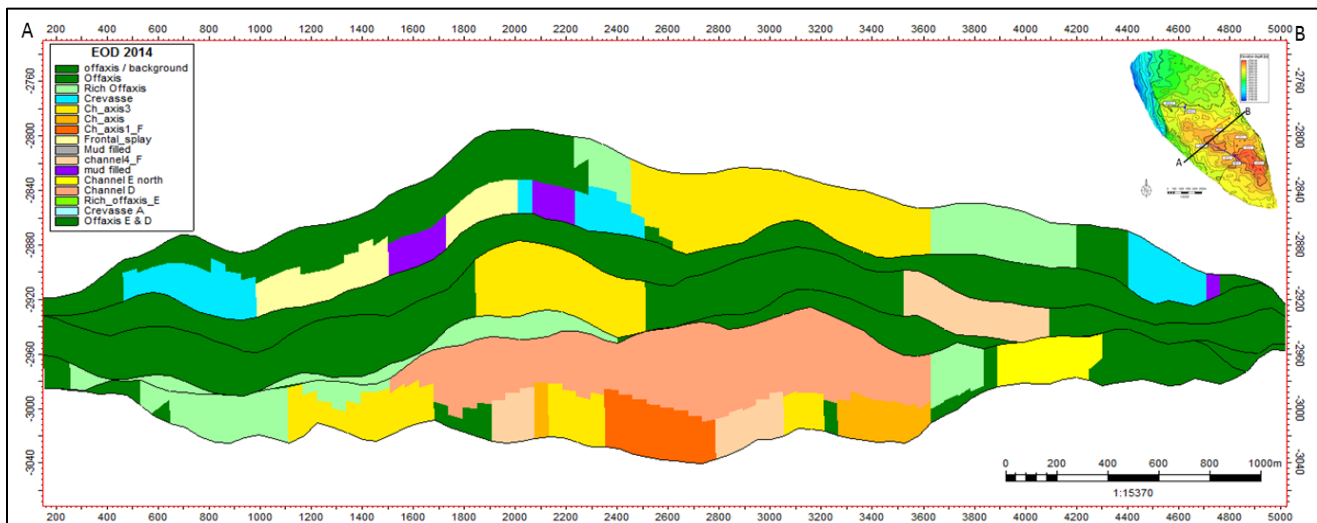


Figure 13 – EoD vertical cross section

Geobodeis Facies MPS		Facies	Fractions
Pseudozone A and AB	offaxis	VLCT	100
	Rich off Axis	VLCT	56.81
		MXDT	32.77
		LCT	9.44
	Crevasse	VLCT	83
		LCT	15
		HCT	3
	Channel axis 3	VLCT	72.72
		MXDT	8.03
		LCT	8.63
		HCT	2.17
	Frontal splay	HCT_HP	8.45
		VLCT	70
		LCT	24
	Mud filled	HCT	6
		VLCT	100

Table 2- Zone A and AB Facies Fraction

Geobodeis Facies MPS		Facies	Fractions
Pseudozone C	offaxis	VLCT	83
		MXDT	16
		LCT	1
	Rich off Axis	VLCT	81
		MXDT	11.4
		LCT	6.94
		HCT_HP	0.66
	Crevasse	VLCT	70
		LCT	22
		HCT	8
	Channel axis 3	VLCT	49.74
		MXDT	11.06
		LCT	33.64
		HCT	2.3
	Frontal splay	HCT_HP	10.33
		TRCT	2.46
		VLCT	26.27
		MXDT	33.67
		LCT	13.53
	Channel 4	HCT	13.87
		HCT_HP	12.66
		VLCT	82.5
		MXDT	10.23
		LCT	5
		HCT	6.27

Table 3- Zone C Facies Fraction

Geo-body Facies		Facies	Fractions
Pseudozone CD	offaxis	VLCT	95
		MXDT	3.35
		LCT	1.59
	Rich off Axis	VLCT	50.19
		MXDT	32.68
		LCT	10.1
		HCT	4.09
		HCT_HP	2.86

Table 4- Zone CD Facies Fraction



Geo-body Facies		Facies	Fractions
Pseudozone D, E and F	offaxis	VLCT	91.76
		MXDT	7.42
		LCT	0.82
	Rich off Axis	VLCT	50
		MXDT	27
		LCT	23
	Crevasse	VLCT	36.28
		MXDT	39.99
		LCT	22.38
		HCT	1.36
	Channel D	VLCT	26.28
		MXDT	17.25
		LCT	18.96
		HCT	10.65
		HCT_HP	26.73
	Channel axis 3	VLCT	27
		MXDT	15
		LCT	26
		HCT	10
		HCT_HP	22
	Channel axis	VLCT	18.56
		MXDT	13.92
		LCT	14.11
		HCT	28.66
		HCT_HP	23.26
	Channel axis1_F	TRACT	1.48
		VLCT	12.97
		MXDT	16.18
		LCT	9.71
		HCT	39.69
	Channel4_F	HCT_HP	14.26
		TRACT	7.19
		VLCT	45
		MXDT	15
	Channel E North	LCT	25
		HCT	15
		VLCT	20.3
		MXDT	56.39
		LCT	23.31

Table 5- Zone D, E and F Facies Fraction

The facies distribution was performed in each zone independently, by EoD, using the Sequential Indicator Simulation (SiS) algorithm. Different facies fractions (FF) were applied on each geo-body as shown in the tables here above.

The general settings applied on the facies modeling window (Figure 14) are the same for all the zones, with exception of the facies fractions within the different geo-bodies (Table 2, Table 3, Table 4 and Table 5). The distribution begins from the up-scaled facies log.

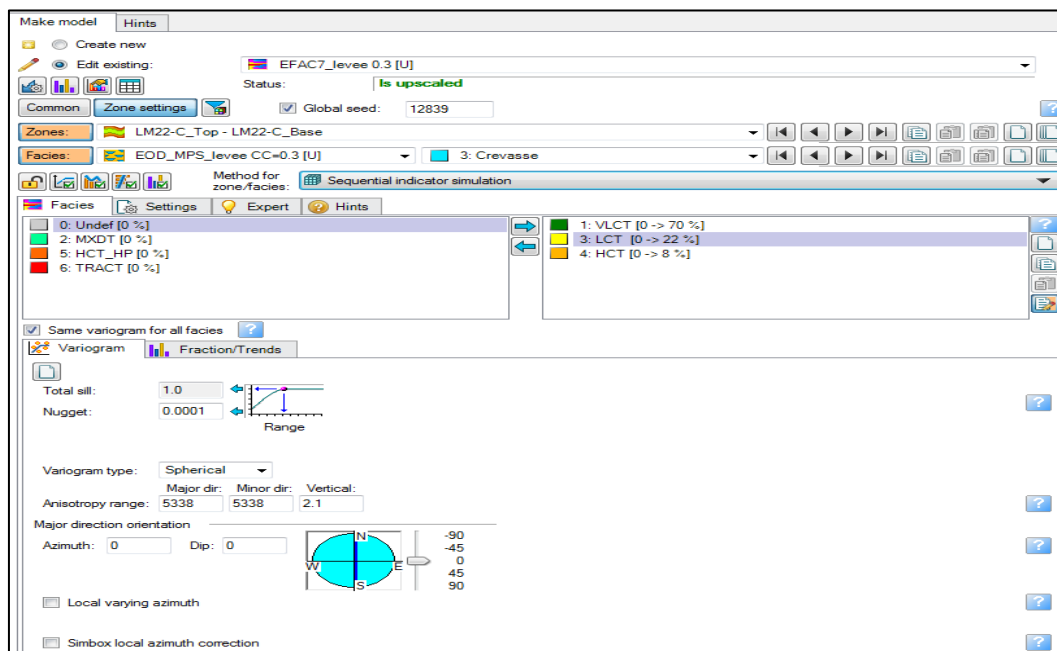


Figure 14 – Facies modelling window

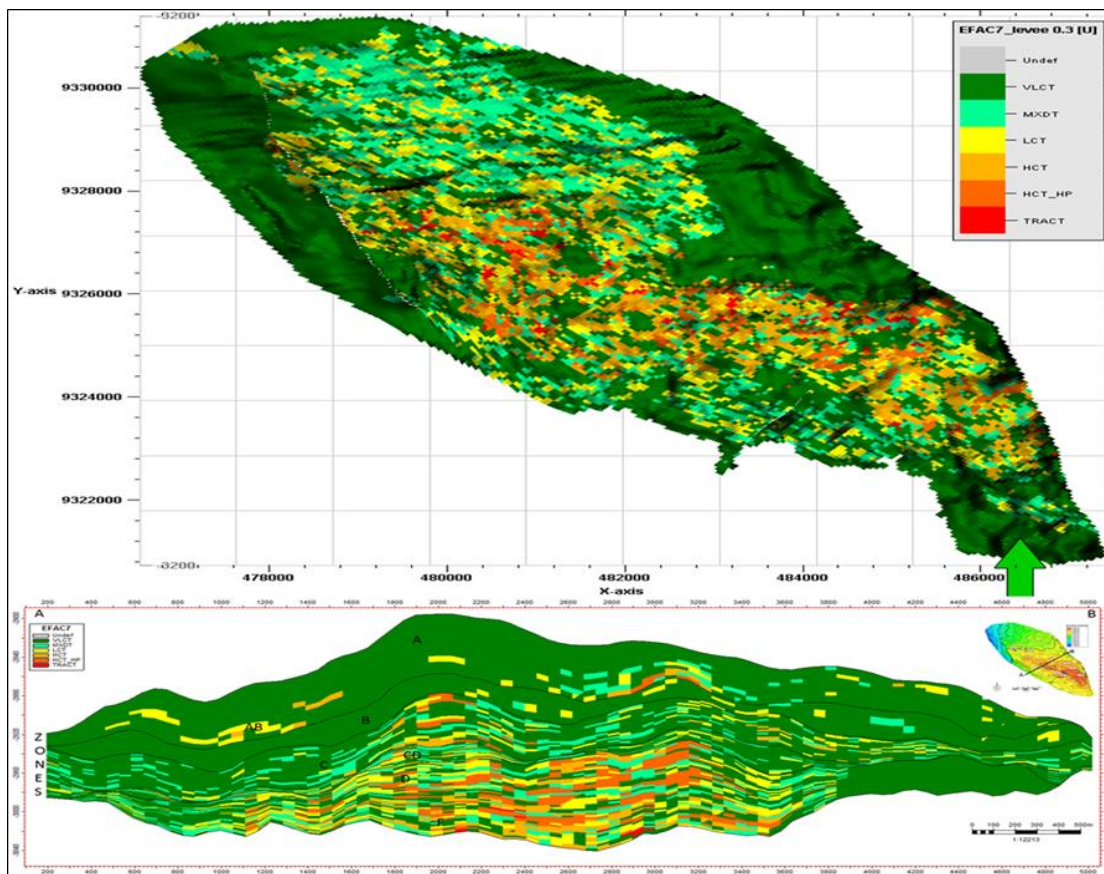


Figure 15 – Facies distribution map view and vertical section

The differences, in terms of global amount, among the well logs, the up-scaled cells and the facies distribution are shown in the histogram here below (Figure 16).

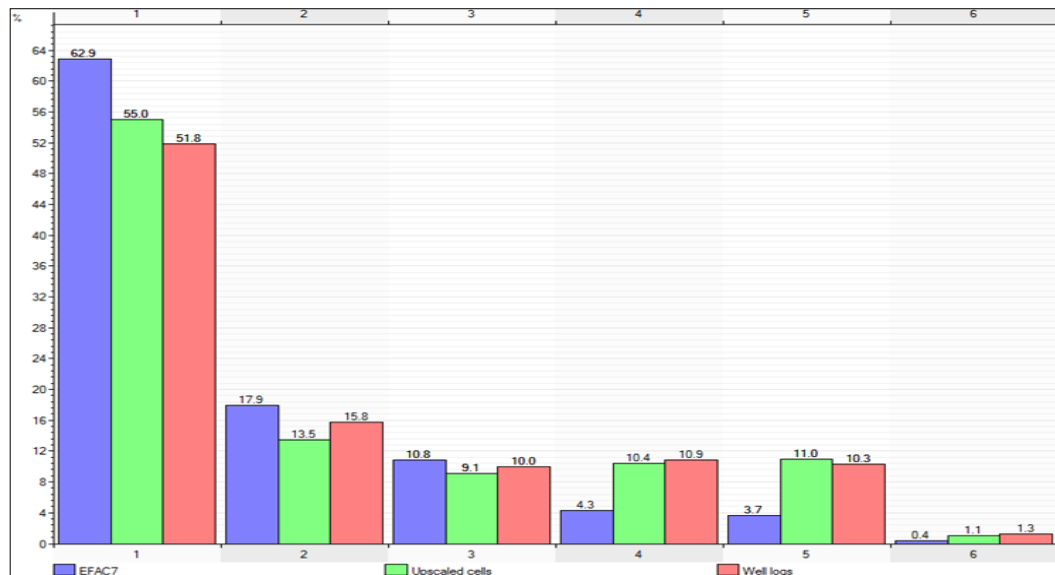


Figure 16 – Facies Histogram (Standard model)

### 2.3.2 SGS Petrophysical properties model

Basing on the performed facies distribution, the following petrophysical properties were distributed considering the main values referenced in Table 6: NTG, POROSITY and Sw.

Facies	NTG	Porosity	Sw
VLCT	0.05	0.07	0.49
MXDT	0.48	0.09	0.46
LCT	0.83	0.15	0.29
HCT	1	0.15	0.18
HCT_HP	1	0.2	0.18
TRACT	1	0.07	0.35

Table 6- Petrophysical distributions (mean value) by facies

NTG, Porosity and Water saturation were modelled considering the facies distribution already shown above (Figure 15).

NTG was modeled by means of the Gaussian Random Function Simulation (GRFS) algorithm for VLCT, MXDT and LCT. In the case of HCT, HCT\_HP and TRACTION facies, a constant value of one has been assigned.

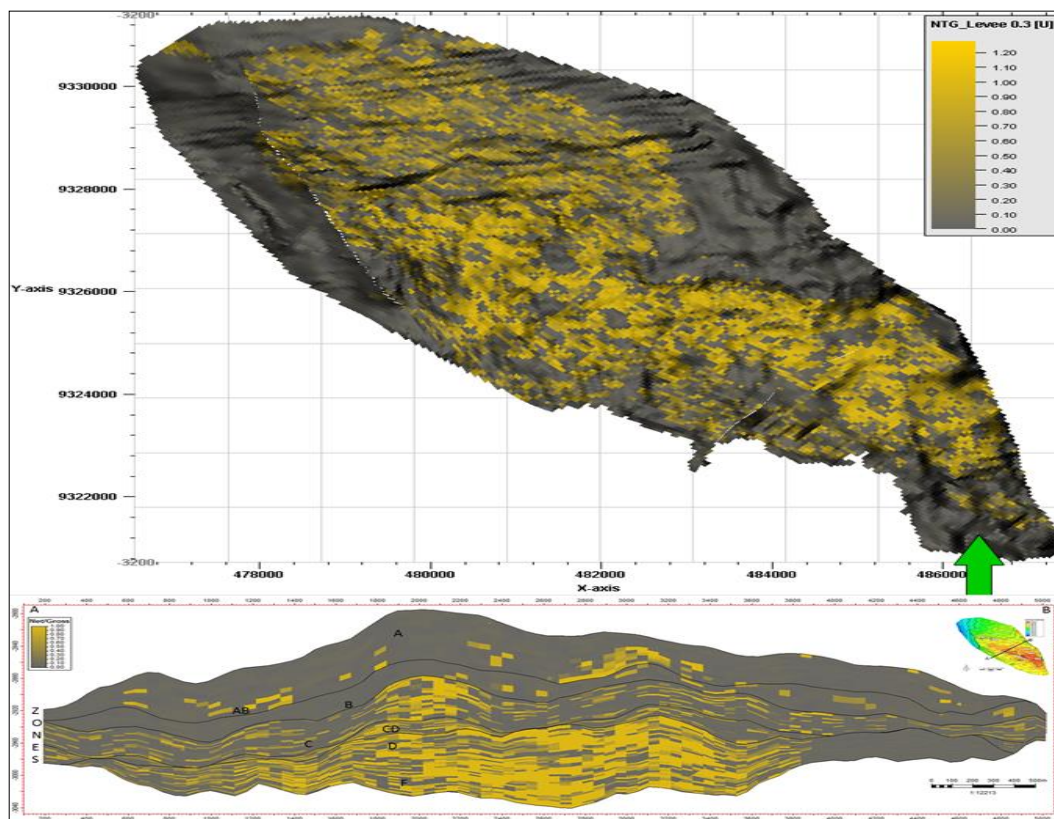


Figure 17 – NTG property distribution

Porosity was distributed by means of the GRFS algorithm, having as collocated co-Kriging property the NTG distribution shown here above (Figure 17).

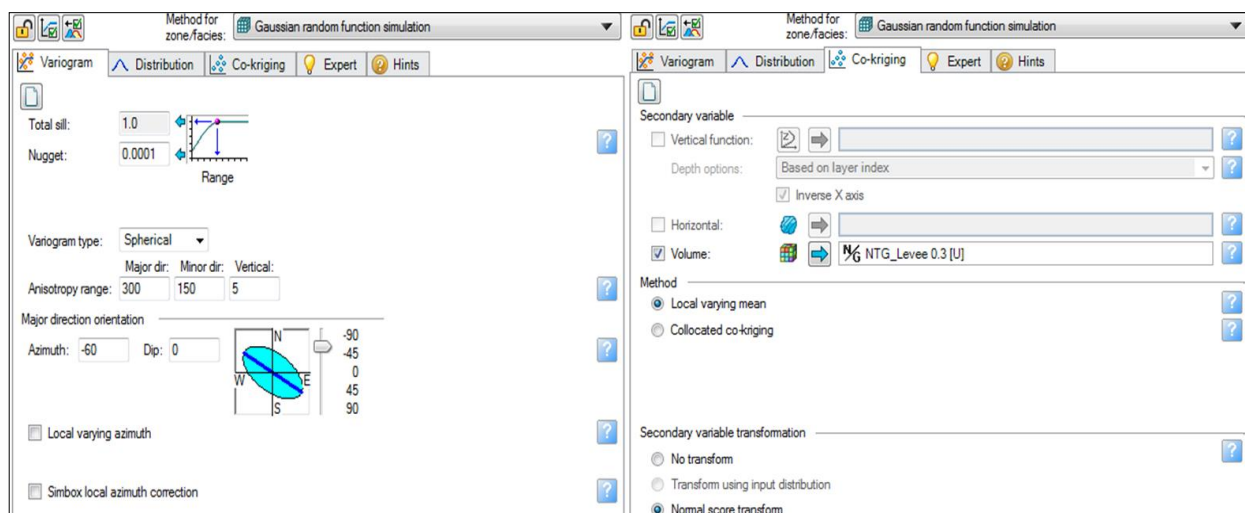


Figure 18 – Porosity distribution settings



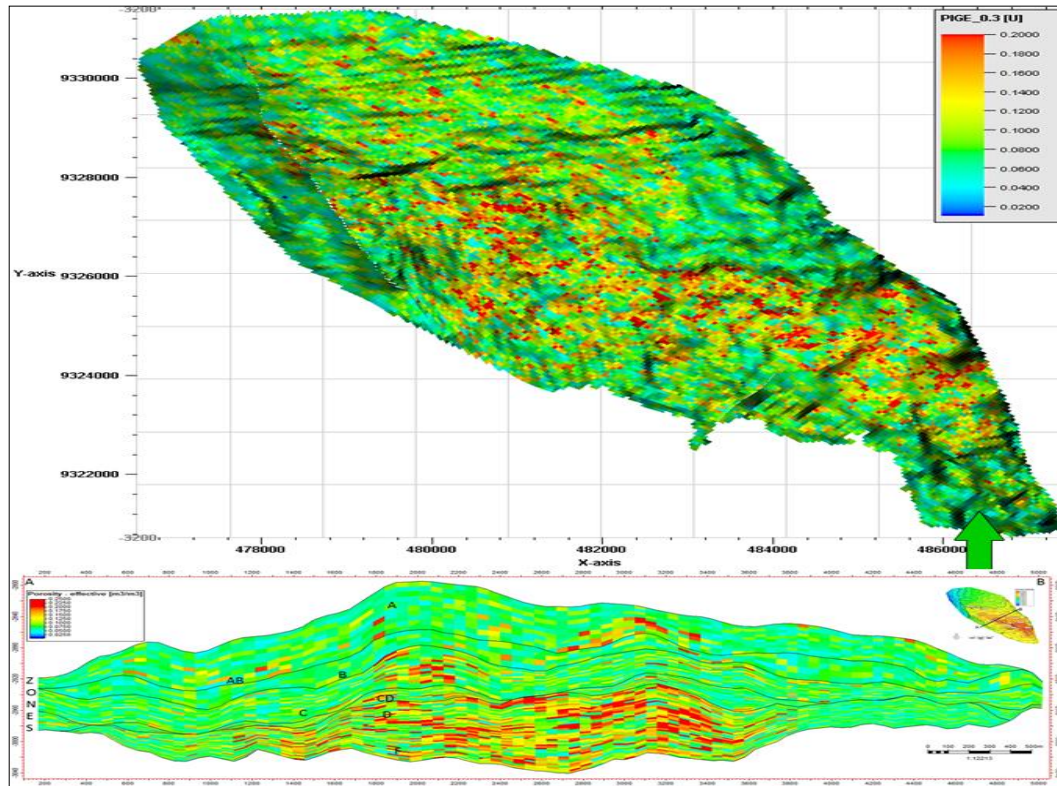


Figure 19 – Porosity distribution

The Water saturation distribution was performed by means of the GRFS algorithm, having as collocated co-Kriging property the Porosity distribution shown here above (Figure 19).

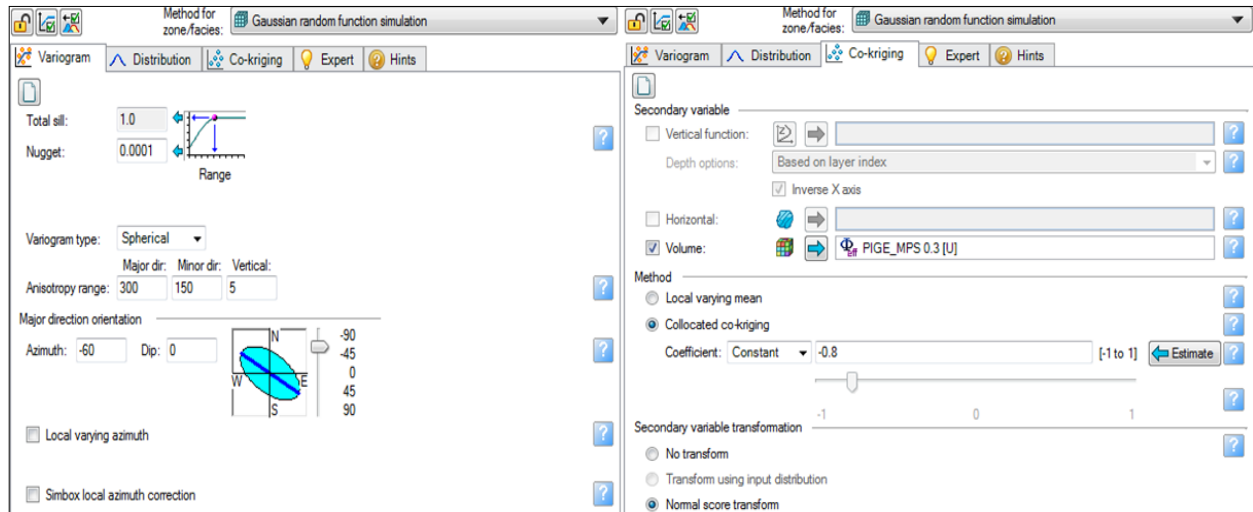


Figure 20 – Porosity distribution settings

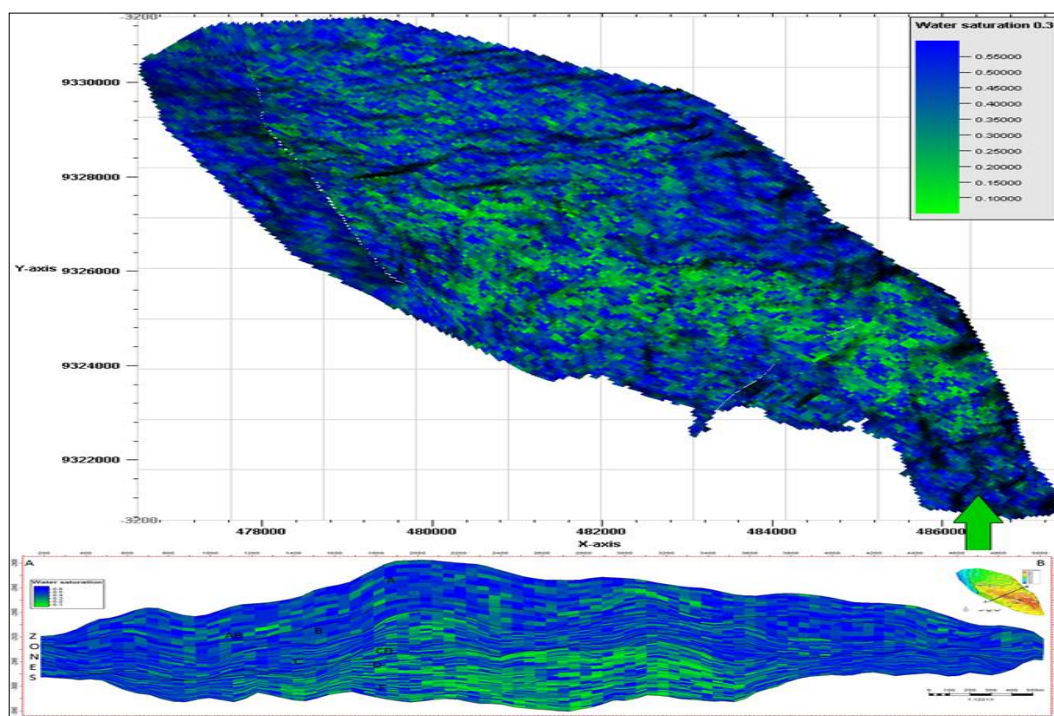


Figure 21 – Water Saturation distribution

### 2.3.3 Volumetric

Following the standard static modelling workflow, after the facies modelling and petrophysical modelling, the volume calculation was performed considering the reservoir fluids contacts and the formation volume factors for the gas and for the oil.

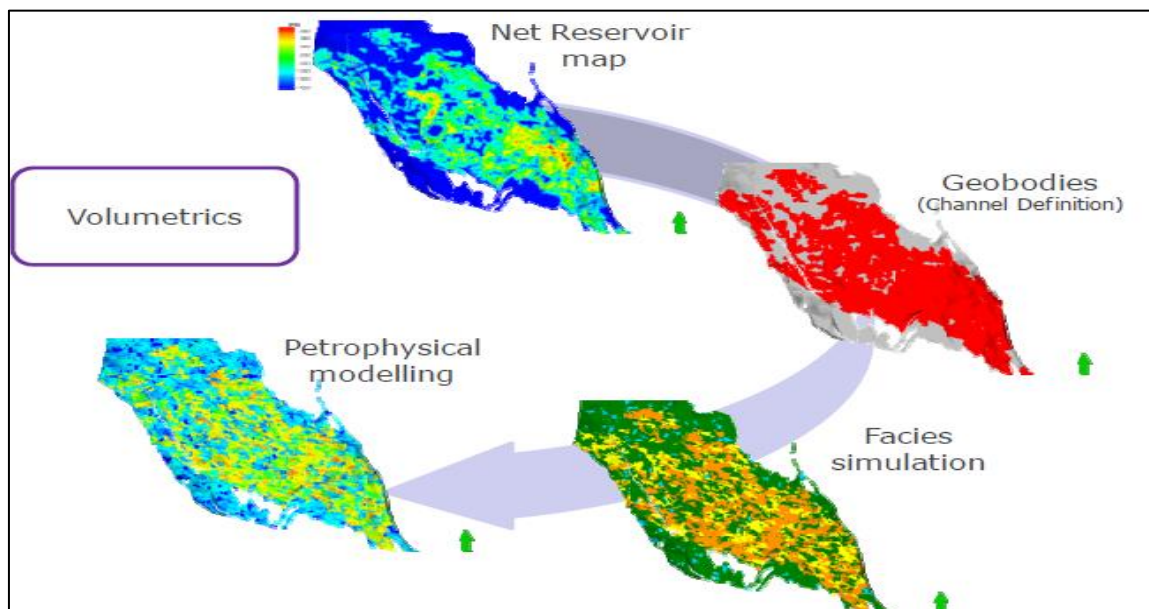


Figure 22 – Static model work flow

The Gas Oil Contact (GOC) is at -2818 meters subsea level (mssl), the Oil Water Contact (OWC) is at -3038 mssl and the perched water level on the south-eastern part of the structure is at 2997.5 mssl.

The oil formation volume factor ( $B_o$ ) is equal to 1.6 RB/STB and the gas formation volume factor ( $B_g$ ) is equal to 0.8 RB/MSCF.

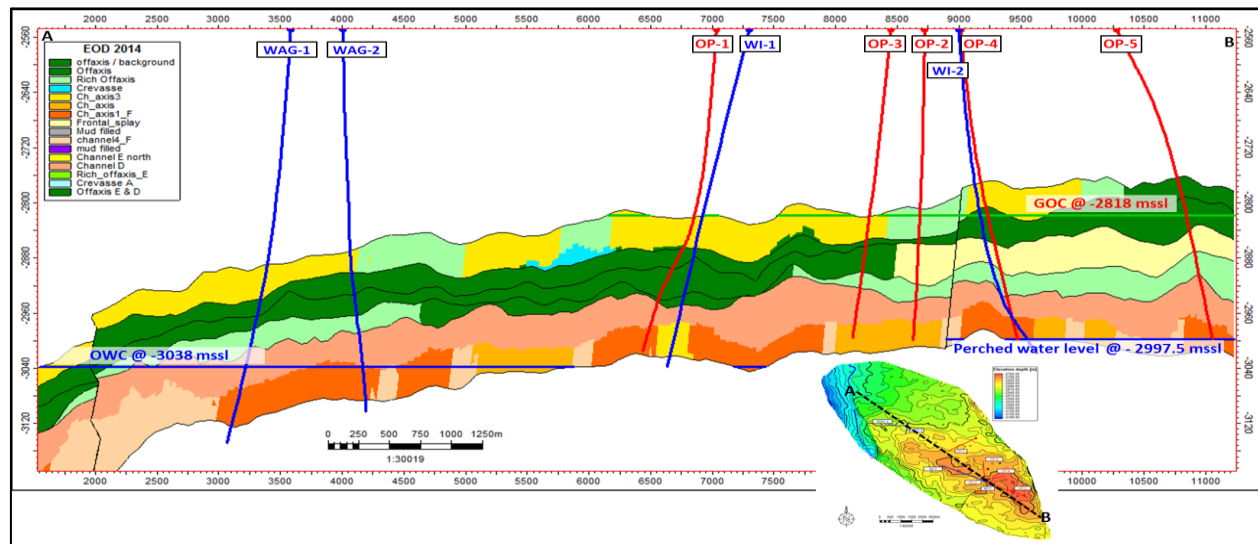


Figure 23 – Cross section through the reservoir

STOIIP[*10 <sup>6</sup> STB]	
Pseudozones	Standard simulation
Zone A	51.03
Zone AB	32.8
Zone B	43.53
Zone C	105.25
Zone CD	72.57
Zone D	191.86
Zone F	116.49
Zone E	38.57
Total STOOIP	652.1

Table 7- STOOIP volumes (Standard model) by zone

Considering all the settings applied for the STOOIP calculation, the results are been reported considering the STOOIP in each pseudozone. Emphasizing that the biggest volumes are in the basal levels D and F which represents 47% of the total STOOIP, level AB and E represent a smaller area fraction of the reservoir total coverage area, reflecting a smaller volume.



## 3 MULTIPLE POINT STATISTICS (MPS)

### 3.1 MPS Simulation Technology

The Sequential Gaussian Simulation (SGS) and the Sequential indicator Simulation (SIS) approaches, applied on stochastic reservoir modeling, are unable to deal with complex and heterogeneous spatial structures. Normally these methods cannot convey the connectivity and variability when the considered phenomenon contains definite patterns or structures (Tahmasebi 2018).

The MPS is an innovative stochastic facies modeling technology, developed in the last decades, which reproduces patterns from training images, represented by a discrete 3D property, in parallel honoring both up-scaled well data (hard data) and secondary data (incorporated if available) to constrain the spatial distribution and proportions.

MPS can reproduce a heterogeneous complex channel system, by making use of the training image concept and external constraints, which can be weighted in a fractional way accordingly (probability properties). The multiple point configurations algorithm is pixel based approach, it has the advantage over the object modelling method that it can condition to data more easily. As illustrated here below.

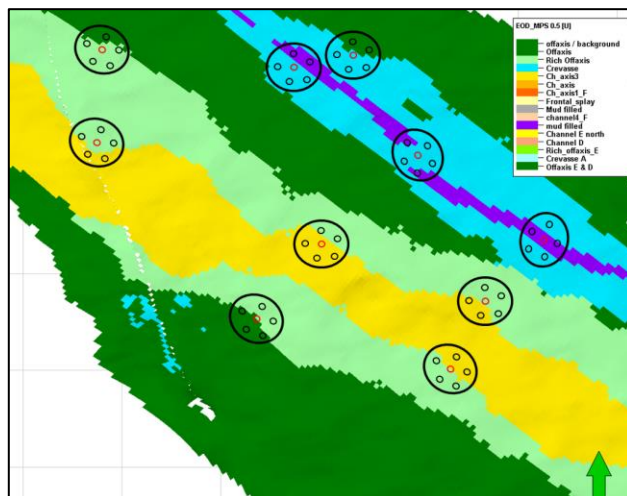


Figure 24 – Training Image concept

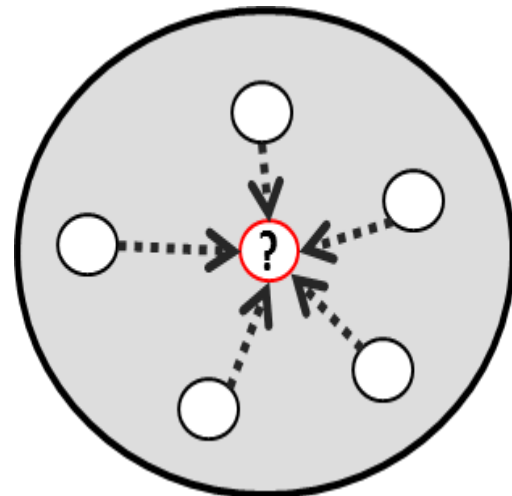


Figure 25 – Multiple Point configurations

In the MPS technology a few algorithms are mostly used (Lyster 2008):

- MPS-GS algorithm: quite recent method, it combines an initial image and the target statistics by making use of conditional distribution;
- SneSim Algorithm: also quite recent method, it is a sequential simulation method that uses conditional probabilities of facies and TI;
- FILTERSIM algorithm: uses filters to group similar patterns of facies reducing the dimension of the statistics.

A common algorithm is the Single Normal Equation Simulation (SNESim) approach, which structurally can be resumed by:

- consider the data jointly as a multiple point event; search training image for the closest replication of the multiple point data event;
- read the distribution of the central value over the these replicates;
- Draw from that distribution; if not enough replicates are found reduces the data event (Zhang 2006).

MPS makes use of a multiple point configuration that conceptually can better describe the geo-body, by increasing the sampling/identification of the geo-body orientation, basing on a Training image “TI” that theoretically honors the sedimentological model and the EoD.

By applying the MPS, the Geo-body obtained as result will consider the edges and roundness of the body, respectively channel shape, levee extension and thickness attenuation, roughness, superposition principle (erosion).

The frontal vertical cross section through a channel, in a schematic way, shows a completely different geometry, comparing with the channel EoD of the standard model Figure 26.

The MPS will generate a different geo-body geometry, which will directly affect the facies fraction within the model.

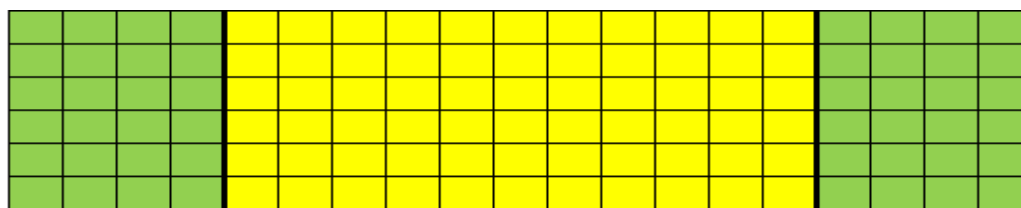


Figure 26 – Standard Model geo-body conceptual cross section

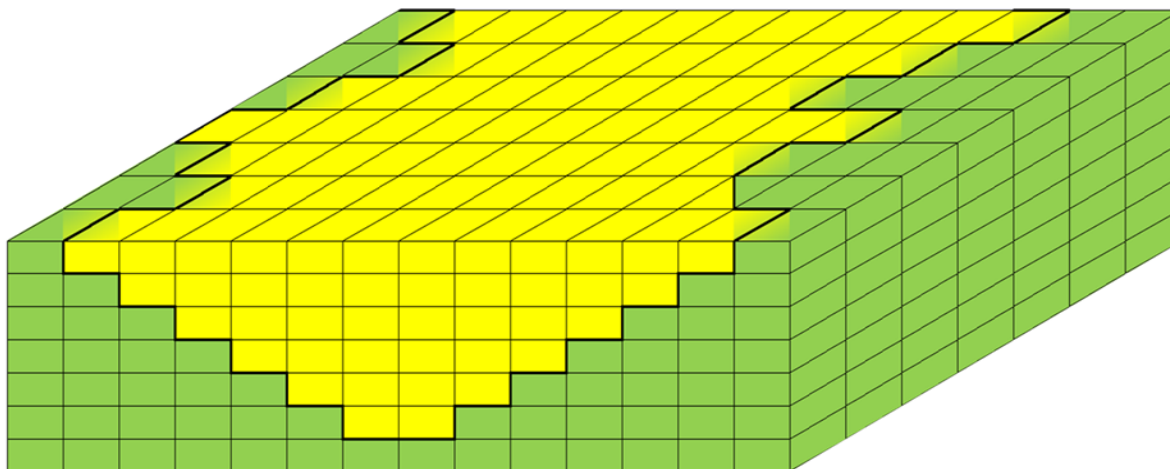


Figure 27 – MPS Model geo-body conceptual model

The fractions of the geo-body margins compared with the standard model ones could be modelled as shown here below Figure 28. It is not a single deterministic model, in fact the algorithm accounts for the different EoDs, channels width, length thickness and the layer number within the considered pseudozone. Finally, a more heterogeneous model, closer to the real sedimentological behavior will be generated.

The standard model made use of the EoD concept in Figure 26 where the facies fractions have a constant value from top to bottom.

On the MPS model, the top view of the channel body is defined on the sedimentological model (EoD), but the vertical evolution of the channel edge is not a constant vertical line, but changes as channel like orientation Figure 27. The EoD fraction on the edges of the channel section, depending on the width/thickness ratio, will most likely increase the shale facies content (green) and decrease the channel like facies content (yellow) Figure 28.

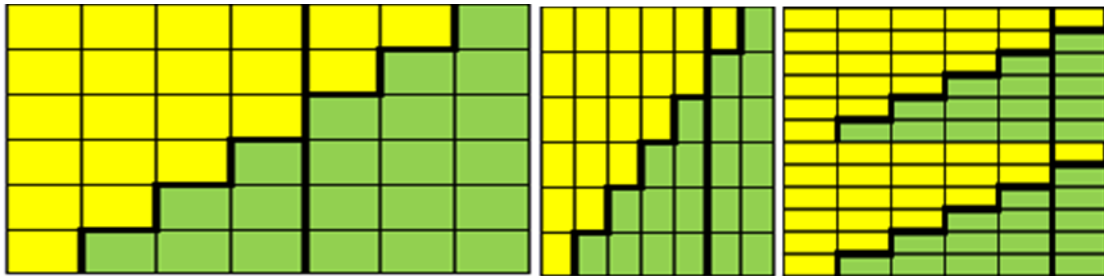


Figure 28 – MPS model channel margins in conceptual cross section

### 3.2 MPS application to an Angolan offshore field

The used input data set is the same one of the existing model (standard two-point modelling approach). The MPS static model workflow is similar to the one applied on the standard model work flow, considering that the main change is related with the geo-bodies definition, which now is performed in a probabilistic manner. In fact, the EoD are modelled by means of the MPS algorithm, using the training images and the EoD probability volumes as guiding tool during the facies distribution phase. In order to analyze the impact of the MPS facies simulation on the static volume in place, the petrophysical modelling settings have been kept unchanged with respect to the existing standard model as well as the modelling parameters. This approach allowed directly linking the model changes to the multiple point statistics facies simulation.

The workflow starts with the generation of EoD probability property from the existing EoD maps, and the generation of training images from the EoDs and the sedimentological model. The static model workflow (MPS facies modeling) is as follow:

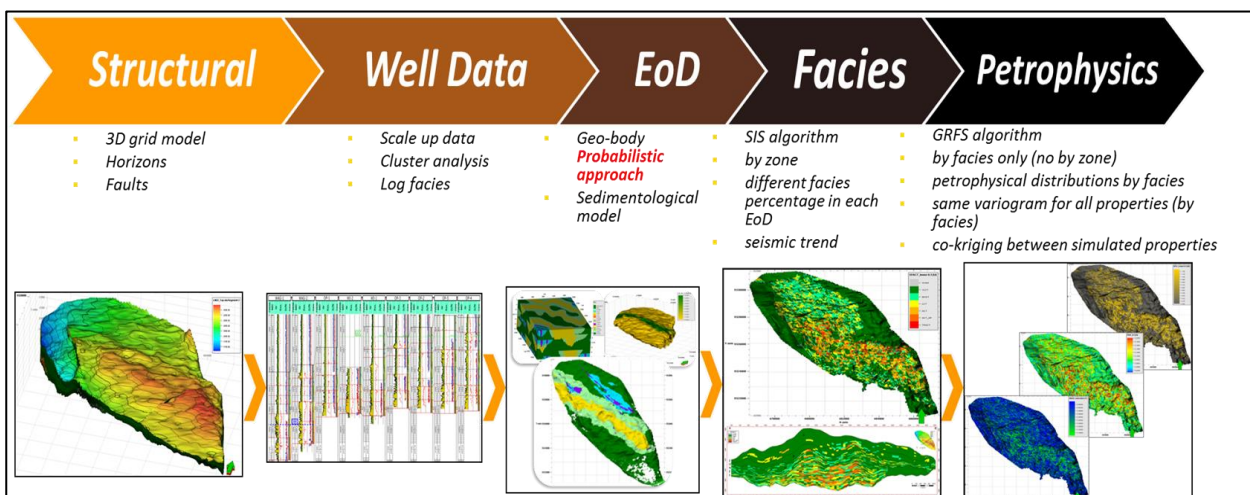


Figure 29 – Petrel static MPS modelling workflow

### 3.2.1 EoD Probability Volumes

From the existing EoD property in the standard model, for each EoD a probability map was generated. Taking into consideration the sedimentological model and analyzing the channel vertical sections, a sensitivity analysis was performed in order to remove the sharp edges of the EoD in the probability map, creating a more smoothed result.

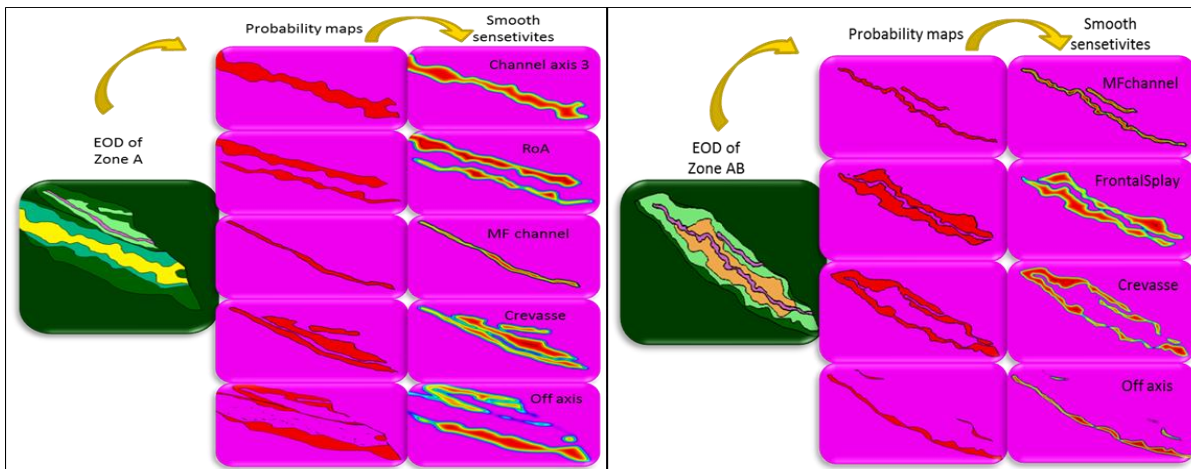


Figure 30 – Zone A and AB – EoD probability map

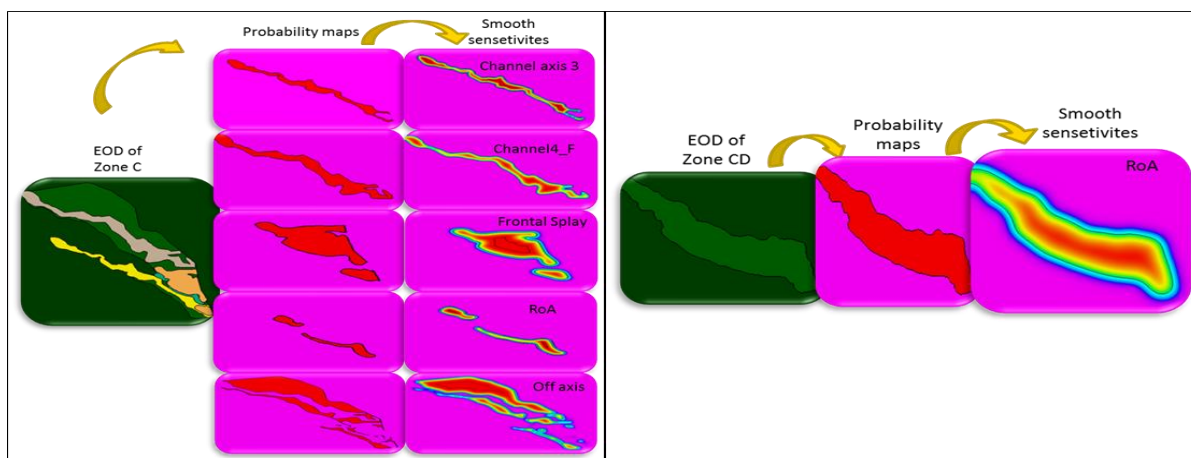


Figure 31 – Zone C and CD - EoD probability map

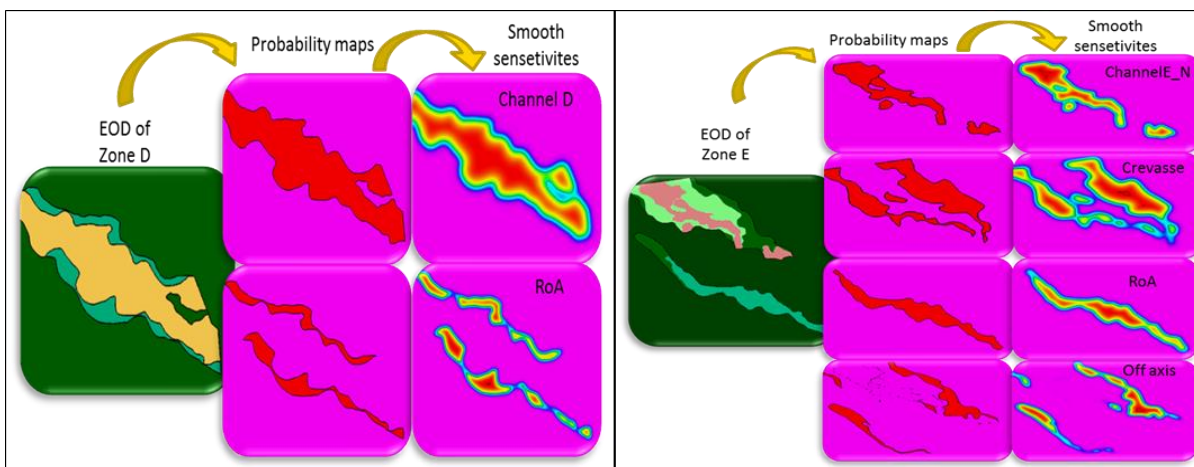


Figure 32 – Zone D and E - EoD probability map



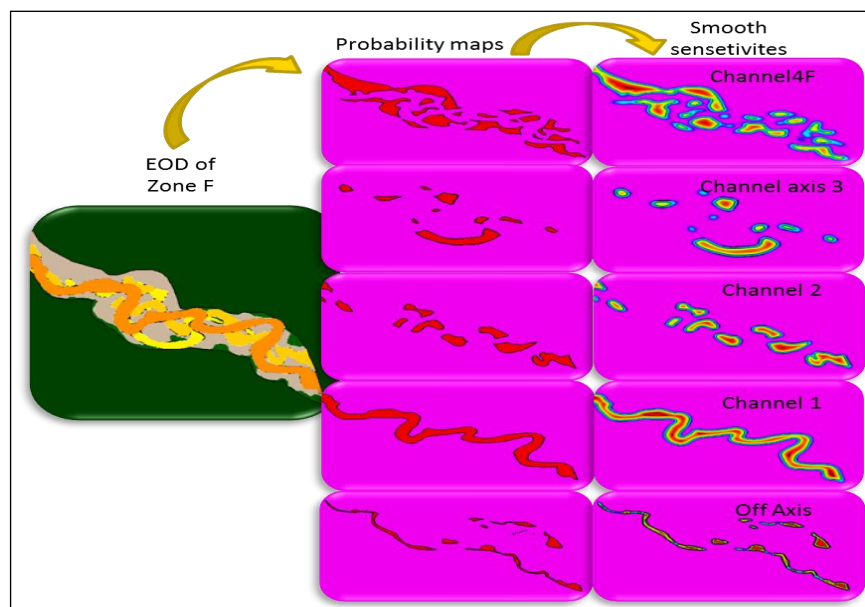


Figure 33 – Zone F - EoD probability map

Starting from the EoD probability maps, which now accounts for the smoothed transition of the heterogeneous and complex sedimentological settings, the same elements of deposition, present in different zones of the model were stacked together and a 3D property was created for each EoD.

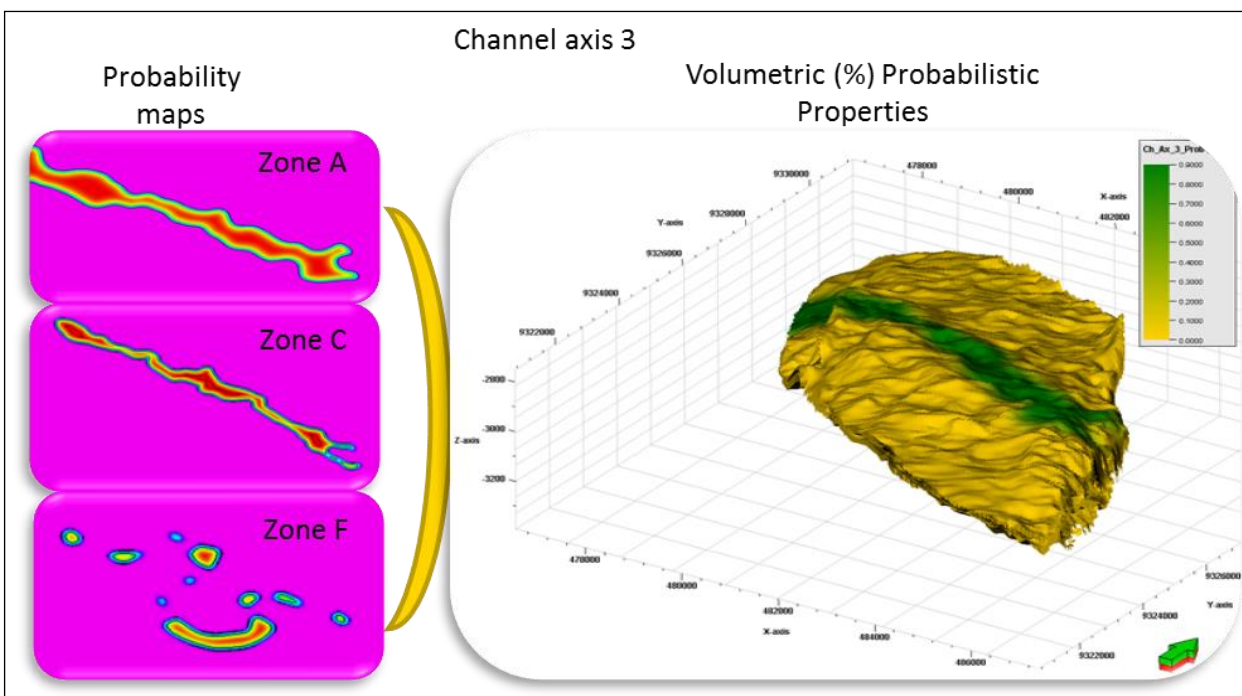


Figure 34 – Channel Axis 3 – EoD probability volume (3D property)

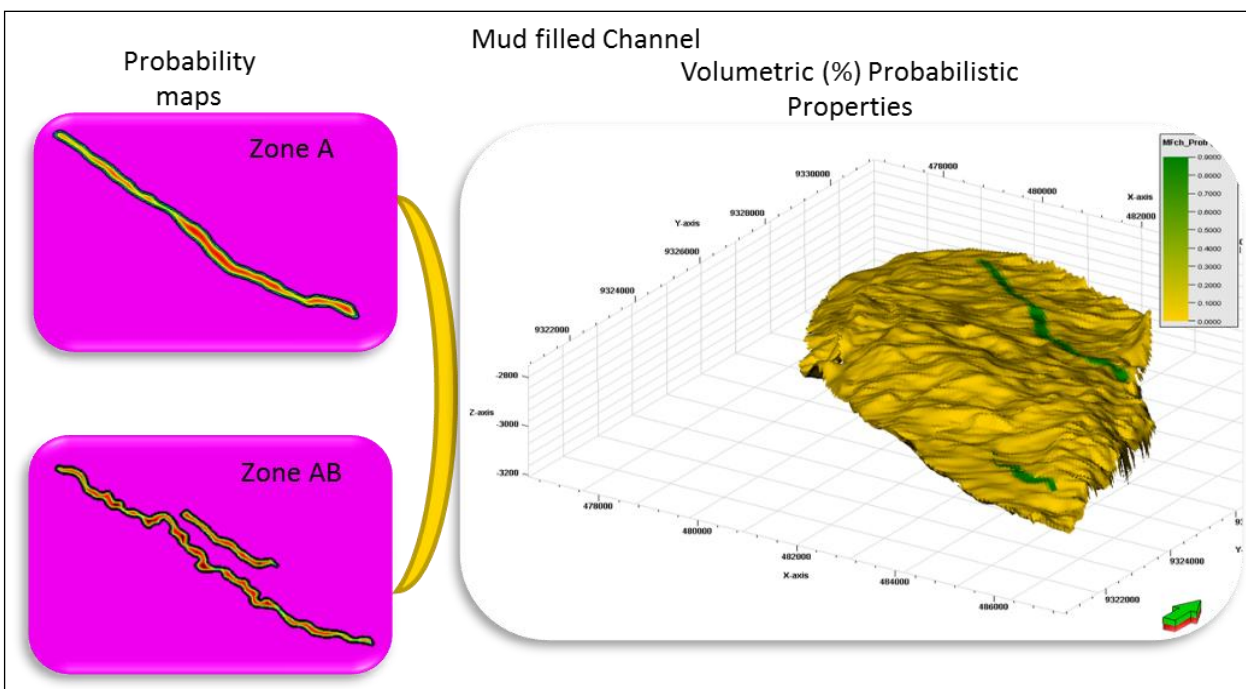


Figure 35 – Mud filled channel 3 – EoD probability volume (3D property)

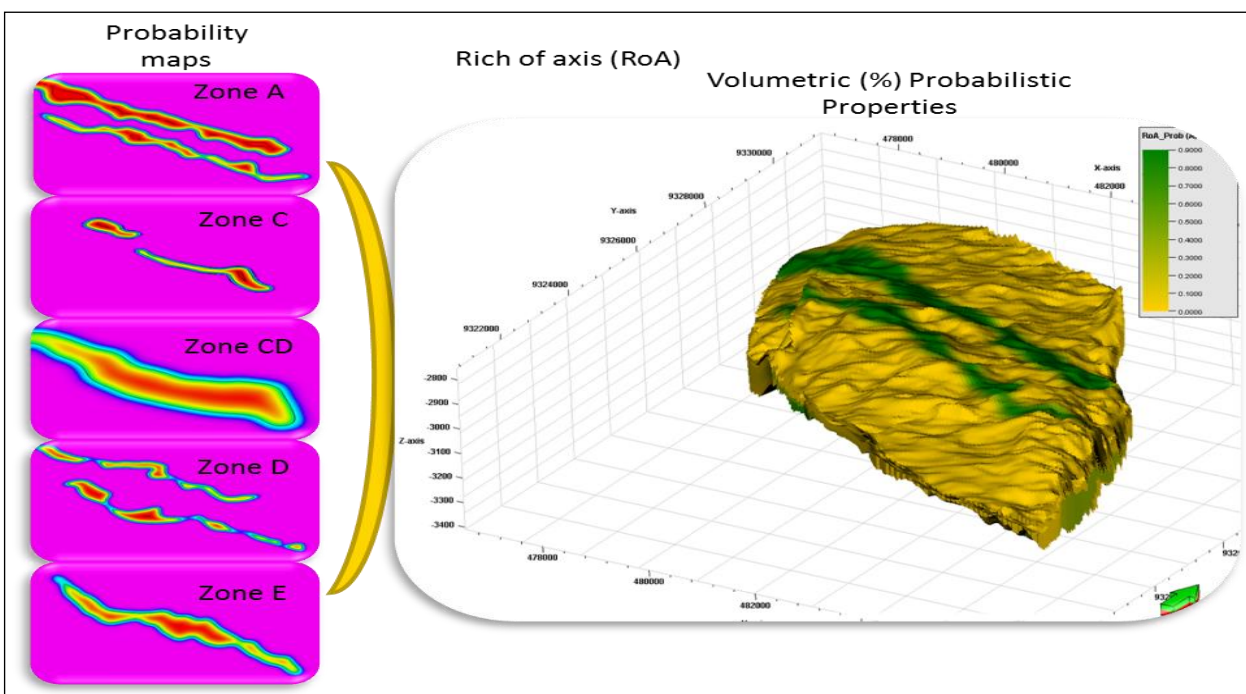


Figure 36 – Rich of Axis – EoD probability volume (3D property)

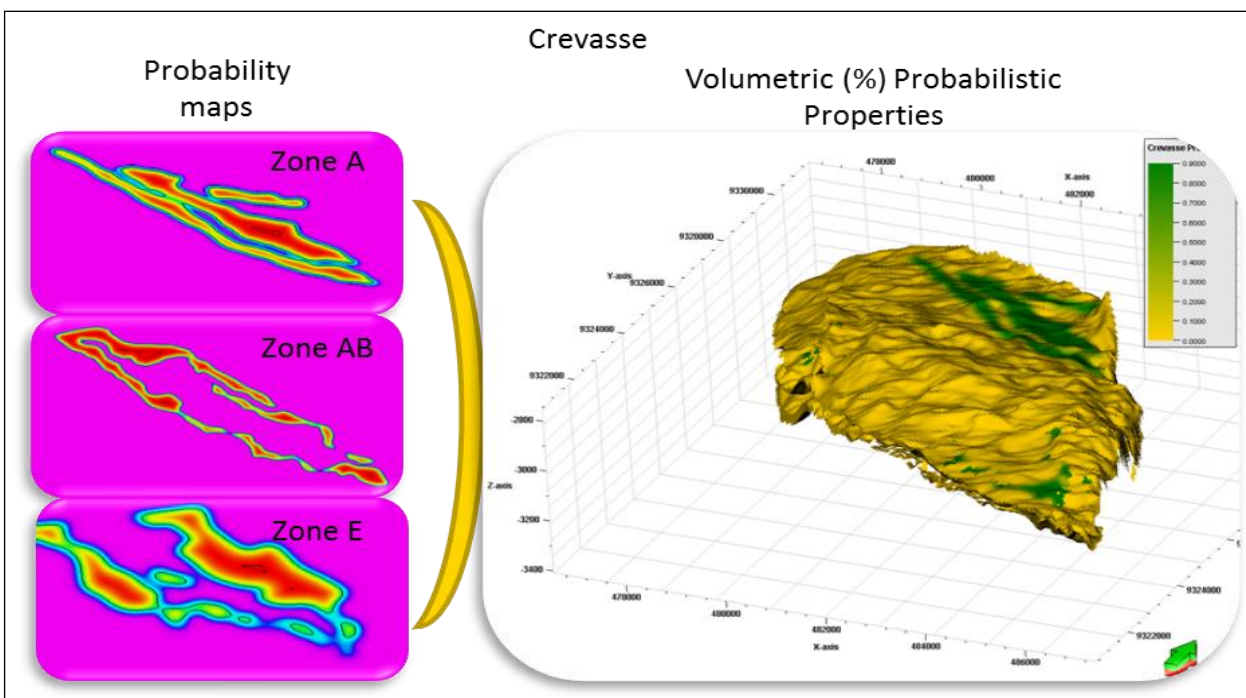


Figure 37 – Crevasse – EoD probability volume (3D property)

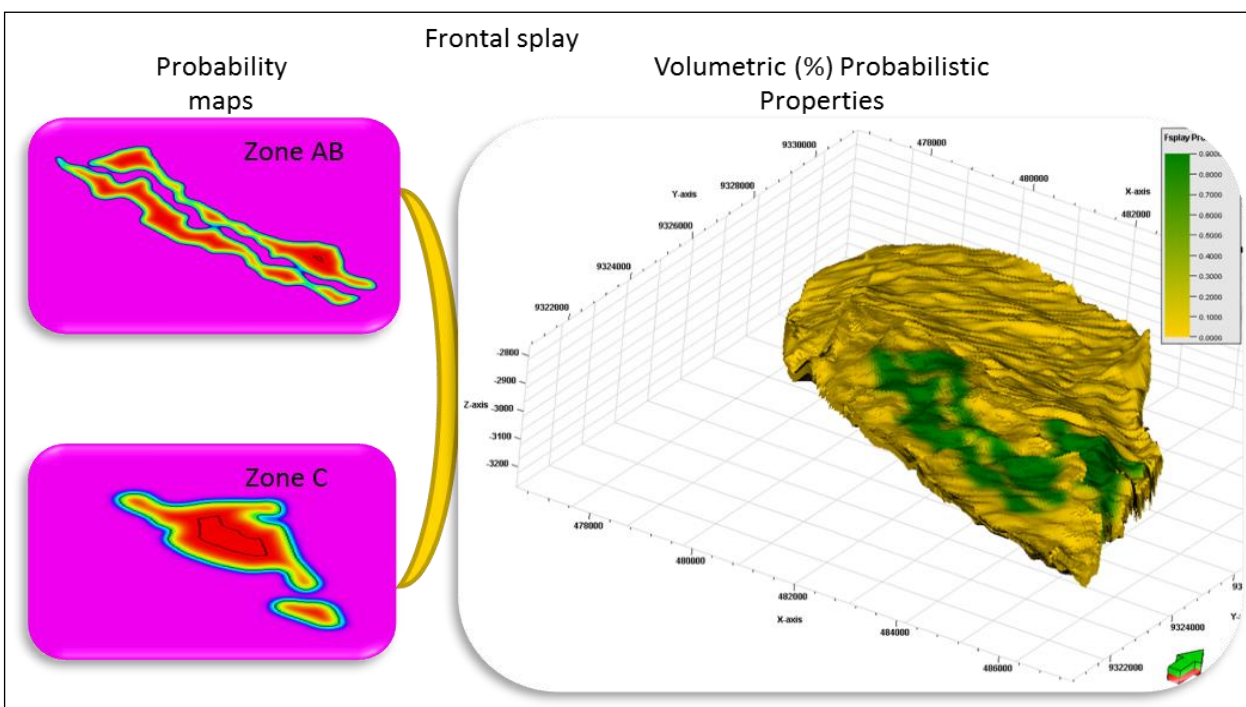


Figure 38 – Frontal Splay – EoD probability volume (3D property)



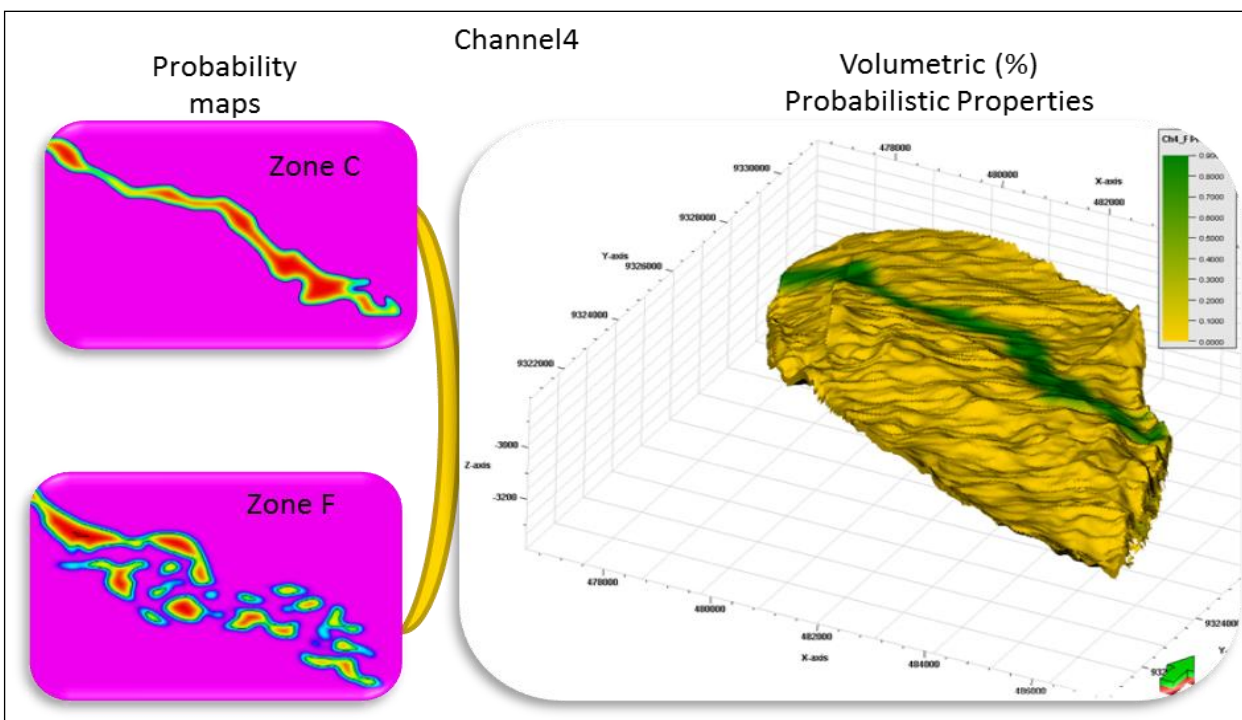


Figure 39 – Channel4 – EoD probability volume (3D property)

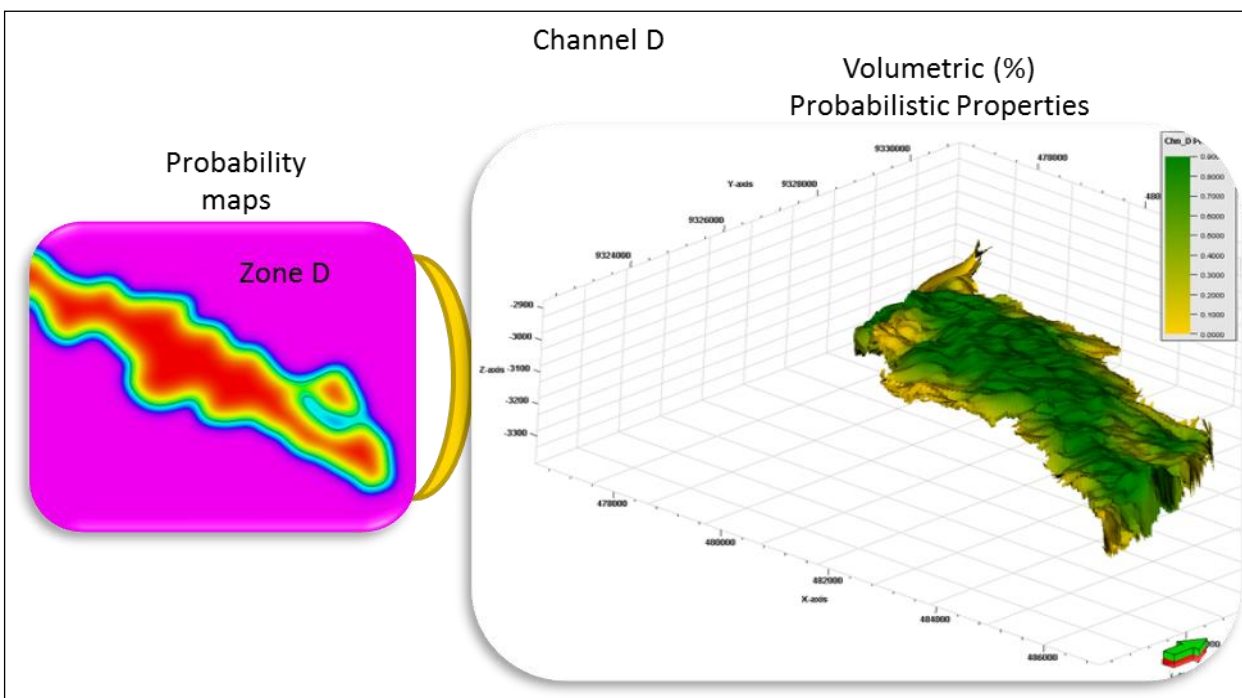


Figure 40 – Channel D – EoD probability volume (3D property)

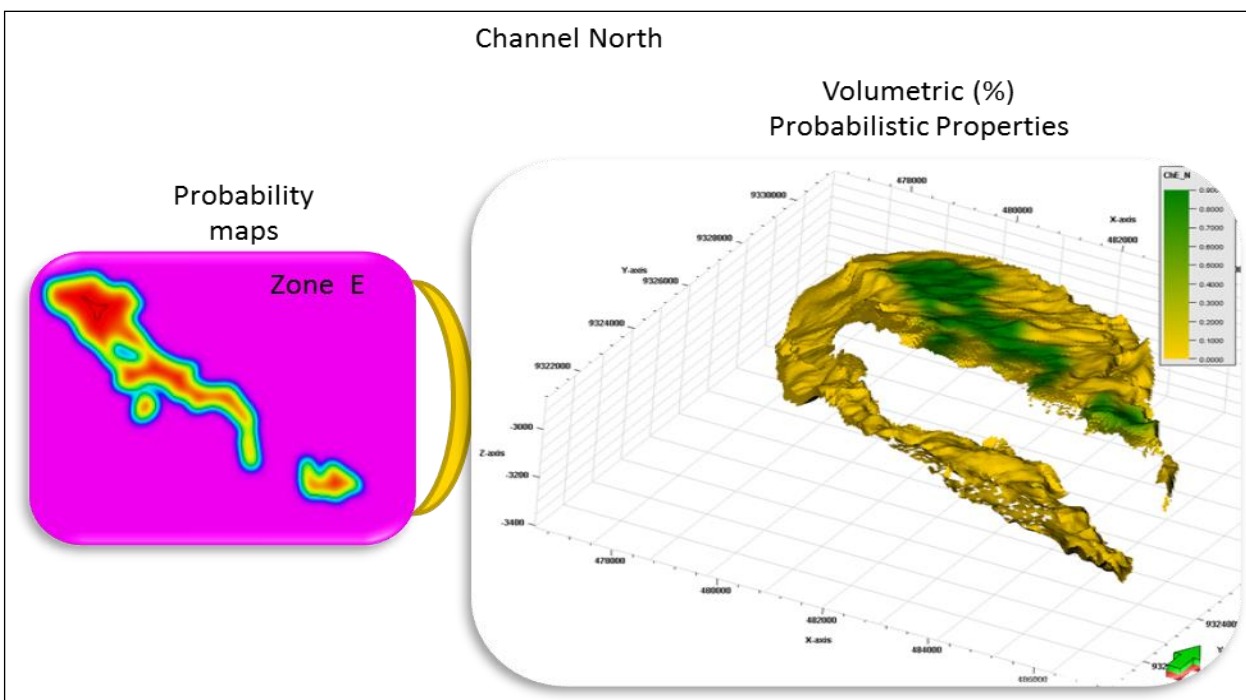


Figure 41 – Channel North – EoD probability volume (3D property)

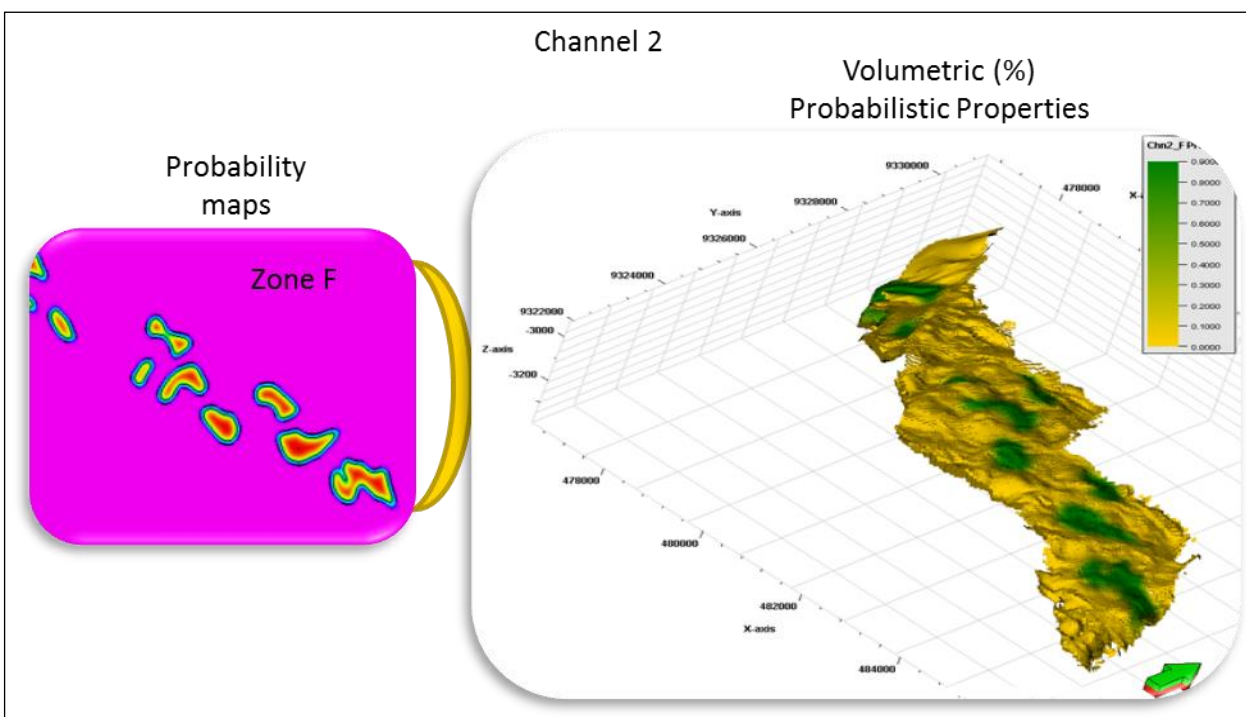


Figure 42 – Channel 2 – EoD probability volume (3D property)

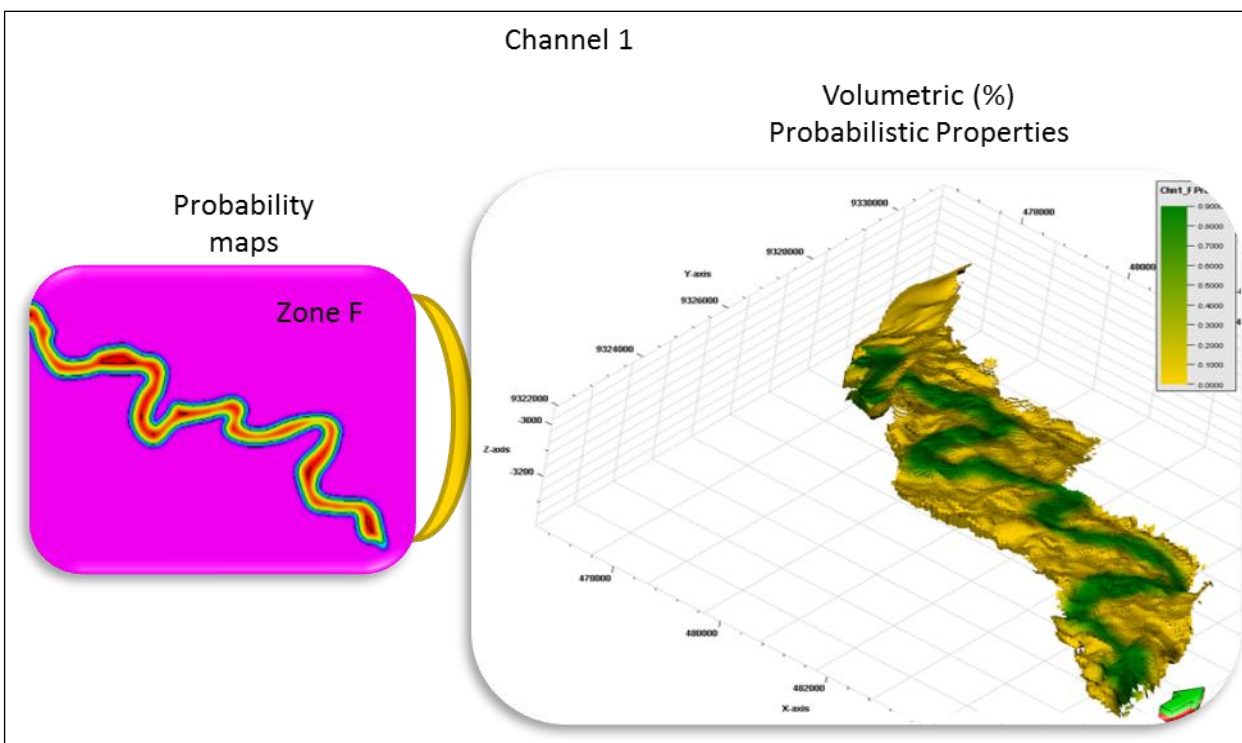


Figure 43 – Channel 1 – EoD probability volume (3D property)

Once defined the 3D probability volumes (3D properties) for each EoD, they will be used as a soft external constraint in MPS facies simulation, performed to simulate the EoD.

The 3D probability volume will work as a geometrical constraint, it will consider in a simplified way the non-stationary features of the data related with the environment of deposition (EoD), represented in the MPS model by the weight factor.

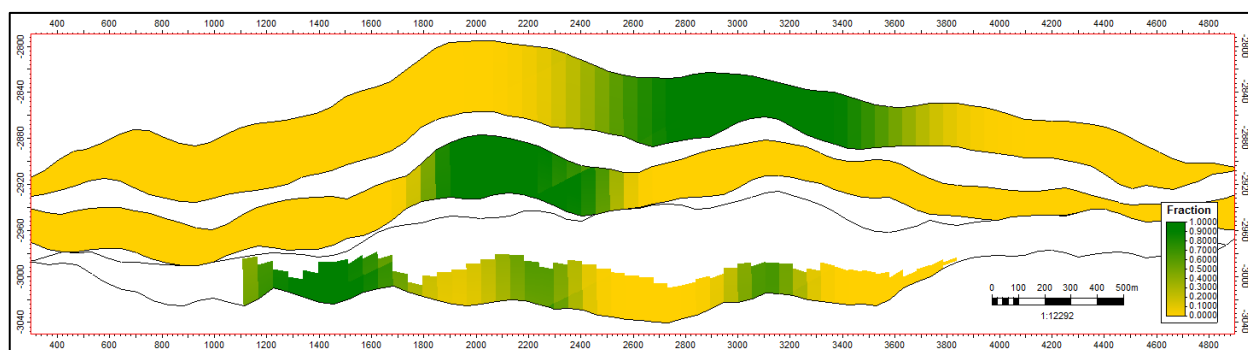


Figure 44 – smoothness principle applied on the MPS external constraint concept

Basically they contain the EoD probabilities in each cell of the simulation grid. An additional parameter, the relative weight of the 3D probabilities (within the range  $[0, 1]$ ), is used to balance the soft and hard-data derived facies probabilities. The greater the weight, the greater the influence of the soft probability cube compared to the training image derived facies probabilities. The default value is 0.5, which equals the influences. If the weight is 1, the facies probabilities inferred from the training image are ignored. If the weight is 0, the soft facies probabilities have no effect.



### 3.2.2 Training Image generation

A training image is a 2D image or regular 3D grid conceptual model, generated basing on the main 3D depositional model, which is able to represent heterogeneous and complex depositional features and honor the sedimentological model.

A training image will illustrate the patterns of the geo-bodies basing on their frequency and according with the geological shape. The spatial location of the body in the TI is irrelevant, what it is important is the shape and the frequency it will appear in the TI. They express a fractional relation between the simulated objects, reproducing in the meanwhile the geological and sedimentological models.

The TI generation workflow begins from the sedimentological interpretation: each geo-body has to be analyzed and carefully measured in order to be reproduced properly. The following input parameters have to be added to the TI modelling window: channel amplitude, wavelength, thickness, width, orientation, relative shape and fraction (which is basically connected to the frequency of the modelled geo-body in the TI). All these input parameters were derived from the standard model and the well logs. The TI 3D grid represents the sedimentological model for the referred zone and it contains information about the possible spatial configurations of the various geo-object and their spatial relationships (Figure 45).

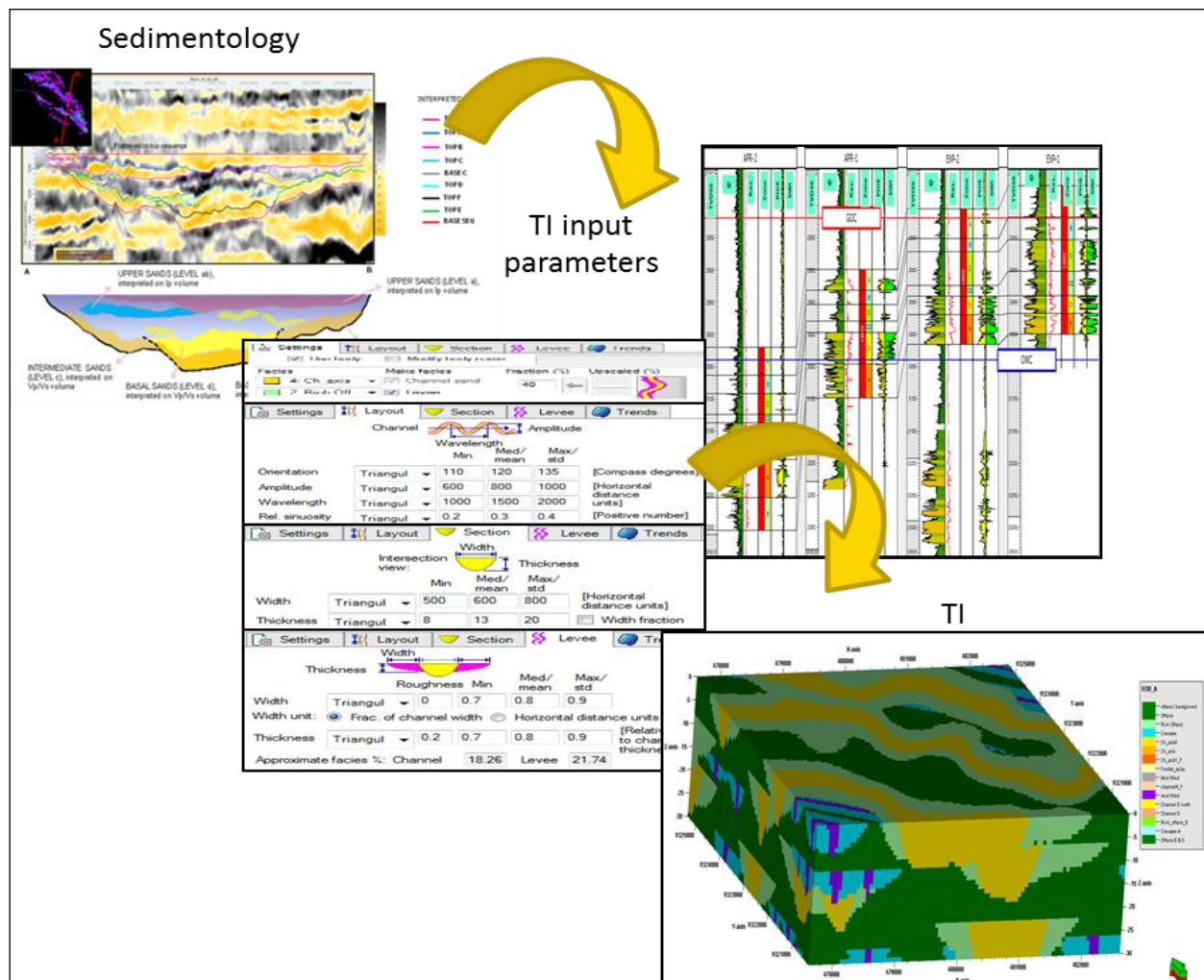


Figure 45 – Training Image work flow

The TI input data coming from the geo-body measurements and interpretation will not always give the desired outcome. In some cases, in order to carefully represent the sedimentological model, the relevant training image has an optimized input data set, due to scaling, heterogeneity and complexity of the geo-bodies setting.

The ratio between the training image grid and the model grid is a scale related issue and there is no a tool for calculating this. Therefore the recommendation is to use a maximum of 30% of the model grid volume, which should work efficiently.

The standard 3D model grid size is: (nI,nJ,nK) 121 x 284 x 96. As shown on the Figure 46, the TI 3D grid used is: (nI,nJ,nK) 100 x 100 x 30.

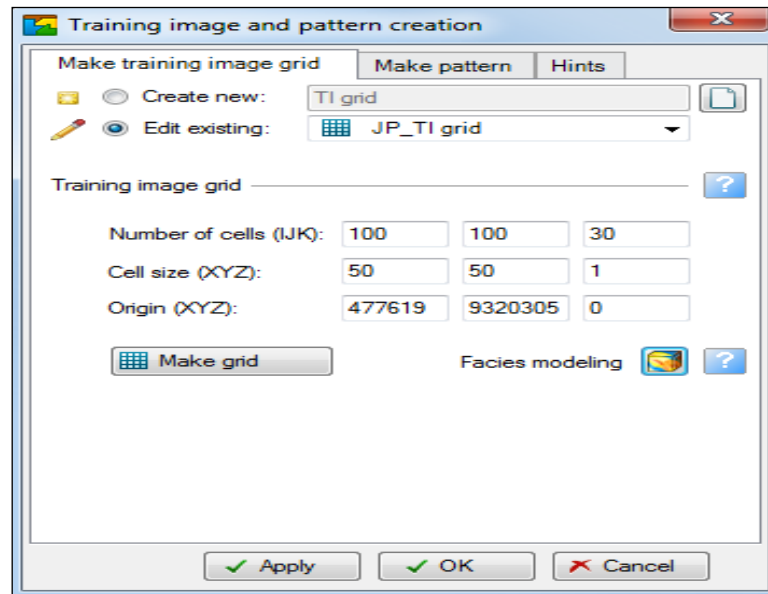


Figure 46 – Training Image grid input

Once the TI grid has been created, the geo-bodies modeling begins, creating the geo-bodies for each zone. By applying the object modeling (stochastic) algorithm, each geo-body is defined in terms of geometry, orientation, channel amplitude, channel wavelength, sinuosity, channel thickness, width and roughness.



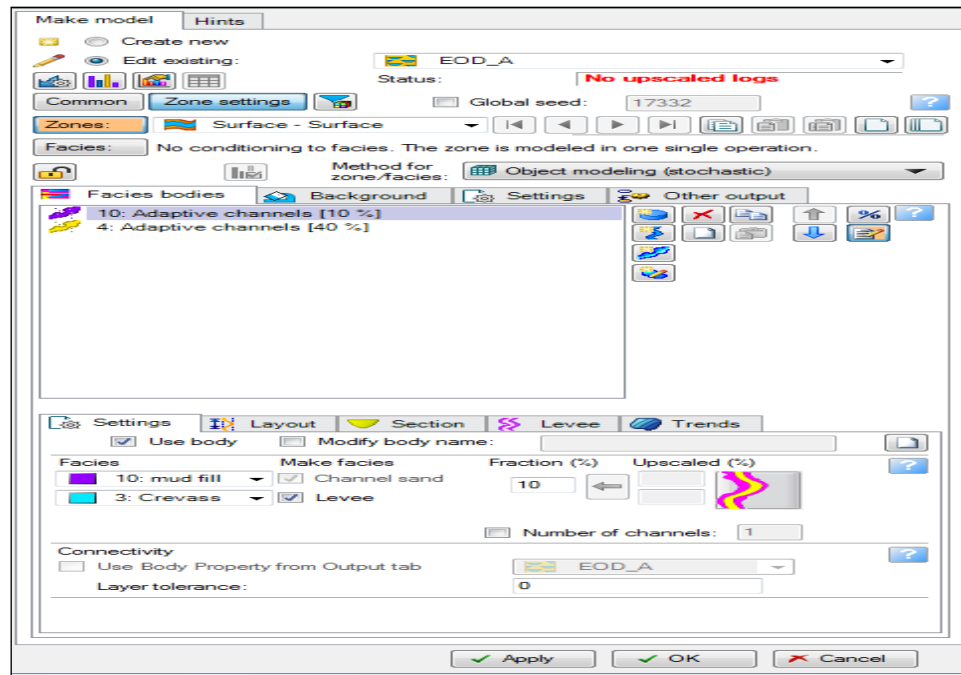


Figure 47 – Training Image facies modelling window

Basing on the input data (EoDs, sedimentological model and well logs), different simulations were run in order to find the best representation of the sedimentological features. For each zone, considering the specific EoDs, the geo-body or the geo-body combination (channel and levee) was analyzed, and a training image 3D grid was generated.

- Simulation one: in order to understand the TI impact on the MPS model, different MPS sensitivities for each zone (considering that each zone was modelled independently) were run, considering the changes on the Training Image input parameters and their impact on the final MPS simulation. Once the results of the MPS were in line with the EoDs and the sedimentological model, the TI was considered final and MPS simulations, including all the training images per zone were run. The set of TIs were therefore considered as conclusive.

Settings	Layout	Section	Levee	Trends	
<input checked="" type="checkbox"/> Use body <input type="checkbox"/> Modify body name:					
Facies: 4: Ch_axis <input checked="" type="checkbox"/> Channel sand <input type="checkbox"/> Levee <input type="checkbox"/> Mud fill <input type="checkbox"/> Crevasse					
Fraction (%) 40 Upscaled (%) 10					
Channel Amplitude Wavelength Min Med/mean Max/std					
Orientation	Triangul	110	120	135	[Compass degrees]
Amplitude	Triangul	600	800	1000	[Horizontal distance units]
Wavelength	Triangul	1000	1500	2000	
Rel. sinuosity	Triangul	0.2	0.3	0.4	[Positive number]
Intersection view: Width Thickness Min Med/mean Max/std					
Width	Triangul	500	600	800	[Horizontal distance units]
Thickness	Triangul	8	13	20	<input type="checkbox"/> Width fraction
Width Thickness Roughness Min Med/mean Max/std					
Width	Triangul	0	0.7	0.8	0.9
Width unit:	<input checked="" type="radio"/> Frac. of channel width <input type="radio"/> Horizontal distance units				
Thickness	Triangul	0.2	0.7	0.8	0.9
[Relative to channel thickness]					
Approximate facies %: Channel 18.26 Levee 21.74					

Figure 48 – Zone A- Channel axis 3 and mud filled channel inputs

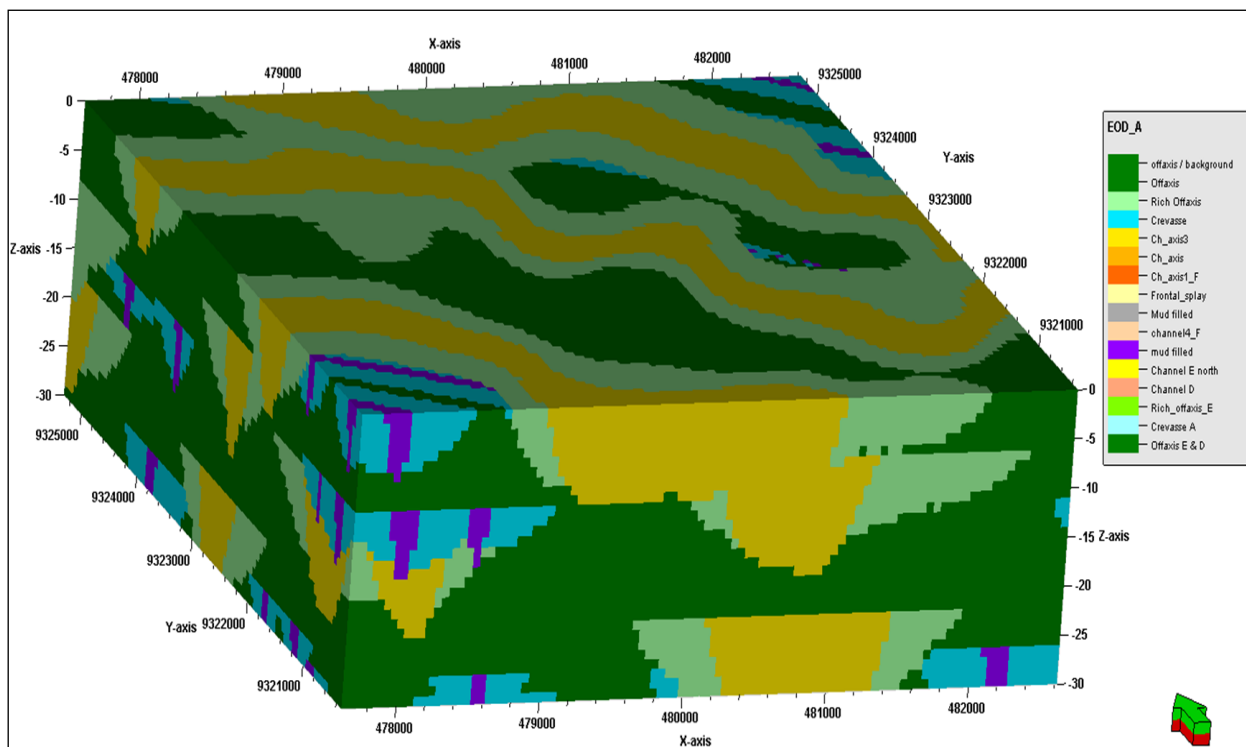


Figure 49 – Zone A Training Image 3D grid

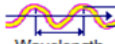
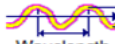
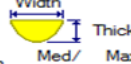
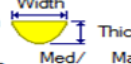
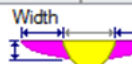
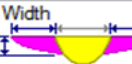
<p><b>Settings</b> <b>Layout</b> <b>Section</b> <b>Levee</b> <b>Trends</b></p> <p><input checked="" type="checkbox"/> Use body <input type="checkbox"/> Modify body name: _____</p> <p>Facies: 10: mud fill <input checked="" type="checkbox"/> Channel sand <input type="checkbox"/> Levee</p> <p>Fraction (%): 35</p> <p>Upscaled (%): _____</p>	<p><b>Settings</b> <b>Layout</b> <b>Section</b> <b>Levee</b> <b>Trends</b></p> <p><input checked="" type="checkbox"/> Use body <input type="checkbox"/> Modify body name: _____</p> <p>Facies: 10: mud fill <input checked="" type="checkbox"/> Channel sand <input type="checkbox"/> Levee</p> <p>Fraction (%): 35</p> <p>Upscaled (%): _____</p>
<p><b>Settings</b> <b>Layout</b> <b>Section</b> <b>Levee</b> <b>Trends</b></p> <p>Channel:  Amplitude</p> <p>Wavelength: Min 110, Med/mean 120, Max/std 135 [Compass degrees]</p> <p>Orientation: Triangul</p> <p>Amplitude: Triangul 600, 800, 1000 [Horizontal distance units]</p> <p>Wavelength: Triangul 1000, 1500, 2000 [Horizontal distance units]</p> <p>Rel. sinuosity: Triangul 0.2, 0.3, 0.4 [Positive number]</p>	<p><b>Settings</b> <b>Layout</b> <b>Section</b> <b>Levee</b> <b>Trends</b></p> <p>Channel:  Amplitude</p> <p>Wavelength: Min 110, Med/mean 120, Max/std 135 [Compass degrees]</p> <p>Orientation: Triangul</p> <p>Amplitude: Triangul 600, 800, 1000 [Horizontal distance units]</p> <p>Wavelength: Triangul 1000, 1500, 2000 [Horizontal distance units]</p> <p>Rel. sinuosity: Triangul 0.2, 0.3, 0.4 [Positive number]</p>
<p><b>Settings</b> <b>Layout</b> <b>Section</b> <b>Levee</b> <b>Trends</b></p> <p>Intersection view:  Thickness</p> <p>Width: Min 10, Med/mean 15, Max/std 30 [Horizontal distance units]</p> <p>Thickness: Triangul 3, 5, 7</p> <p><input type="checkbox"/> Width fraction</p>	<p><b>Settings</b> <b>Layout</b> <b>Section</b> <b>Levee</b> <b>Trends</b></p> <p>Intersection view:  Thickness</p> <p>Width: Min 5, Med/mean 15, Max/std 40 [Horizontal distance units]</p> <p>Thickness: Triangul 3, 5, 8</p> <p><input type="checkbox"/> Width fraction</p>
<p><b>Settings</b> <b>Layout</b> <b>Section</b> <b>Levee</b> <b>Trends</b></p> <p>Width:  Thickness</p> <p>Roughness: Min 0.1, Med/mean 2, Max/std 8, 10</p> <p>Width unit: <input checked="" type="radio"/> Frac. of channel width <input type="radio"/> Horizontal distance units</p> <p>Thickness: Triangul 0.1, 0.4, 0.8, 0.9 [Relative to channel thickness]</p> <p>Approximate facies %: Channel 2.55, Levee 32.45</p>	<p><b>Settings</b> <b>Layout</b> <b>Section</b> <b>Levee</b> <b>Trends</b></p> <p>Width:  Thickness</p> <p>Roughness: Min 0.2, Med/mean 2, Max/std 8, 10</p> <p>Width unit: <input checked="" type="radio"/> Frac. of channel width <input type="radio"/> Horizontal distance units</p> <p>Thickness: Triangul 0.2, 0.6, 0.8, 0.9 [Relative to channel thickness]</p> <p>Approximate facies %: Channel 2.55, Levee 32.45</p>

Figure 50 – Zone AB- Mud filled inputs

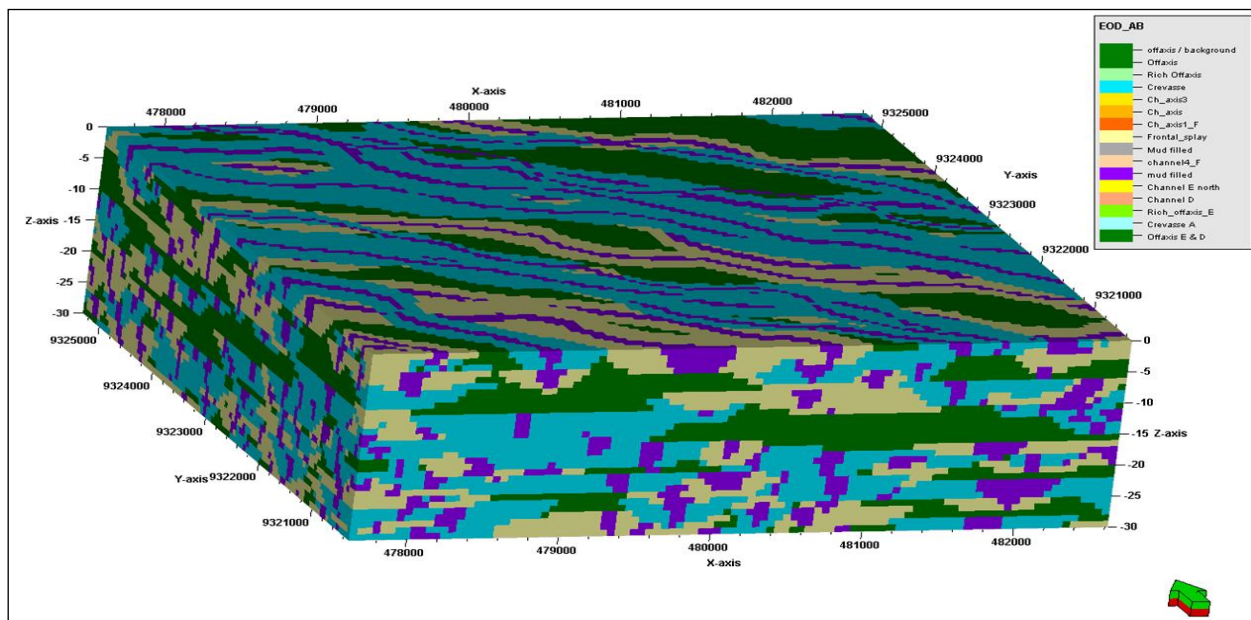


Figure 51 – Zone AB Training Image 3D grid



<div>Settings   Layout   Section   Trends</div> <div> <input checked="" type="checkbox"/> Use body   <input type="checkbox"/> Modify body name: </div> <div> Facies: 9: channel   Make facies: <input checked="" type="checkbox"/> Channel sand   Fraction (%): 8   Upscaled (%): </div> <div> Facies: 2: Rich Off   Make facies: <input type="checkbox"/> Levee </div>	<div>Settings   Layout   Section   Trends</div> <div> <input checked="" type="checkbox"/> Use body   <input type="checkbox"/> Modify body name: </div> <div> Facies: 4: Ch_axis   Make facies: <input checked="" type="checkbox"/> Channel sand   Fraction (%): 5   Upscaled (%): </div> <div> Facies: 1: Offaxis   Make facies: <input type="checkbox"/> Levee </div>																																																										
<div>Settings   Layout   Section   Trends</div> <div>Channel Amplitude</div> <div>Wavelength</div> <table border="1"> <thead> <tr> <th></th> <th>Min</th> <th>Med/mean</th> <th>Max/std</th> <th></th> </tr> </thead> <tbody> <tr> <td>Orientation</td> <td>Triangul</td> <td>110</td> <td>120</td> <td>130</td> <td>[Compass degrees]</td> </tr> <tr> <td>Amplitude</td> <td>Triangul</td> <td>600</td> <td>800</td> <td>1000</td> <td>[Horizontal distance units]</td> </tr> <tr> <td>Wavelength</td> <td>Triangul</td> <td>1000</td> <td>1500</td> <td>2000</td> <td>[Horizontal distance units]</td> </tr> <tr> <td>Rel. sinuosity</td> <td>Triangul</td> <td>0.1</td> <td>0.2</td> <td>0.3</td> <td>[Positive number]</td> </tr> </tbody> </table>		Min	Med/mean	Max/std		Orientation	Triangul	110	120	130	[Compass degrees]	Amplitude	Triangul	600	800	1000	[Horizontal distance units]	Wavelength	Triangul	1000	1500	2000	[Horizontal distance units]	Rel. sinuosity	Triangul	0.1	0.2	0.3	[Positive number]	<div>Settings   Layout   Section   Trends</div> <div>Channel Amplitude</div> <div>Wavelength</div> <table border="1"> <thead> <tr> <th></th> <th>Min</th> <th>Med/mean</th> <th>Max/std</th> <th></th> </tr> </thead> <tbody> <tr> <td>Orientation</td> <td>Triangul</td> <td>110</td> <td>120</td> <td>130</td> <td>[Compass degrees]</td> </tr> <tr> <td>Amplitude</td> <td>Triangul</td> <td>600</td> <td>800</td> <td>1000</td> <td>[Horizontal distance units]</td> </tr> <tr> <td>Wavelength</td> <td>Triangul</td> <td>1000</td> <td>1500</td> <td>2000</td> <td>[Horizontal distance units]</td> </tr> <tr> <td>Rel. sinuosity</td> <td>Triangul</td> <td>0.1</td> <td>0.2</td> <td>0.3</td> <td>[Positive number]</td> </tr> </tbody> </table>		Min	Med/mean	Max/std		Orientation	Triangul	110	120	130	[Compass degrees]	Amplitude	Triangul	600	800	1000	[Horizontal distance units]	Wavelength	Triangul	1000	1500	2000	[Horizontal distance units]	Rel. sinuosity	Triangul	0.1	0.2	0.3	[Positive number]
	Min	Med/mean	Max/std																																																								
Orientation	Triangul	110	120	130	[Compass degrees]																																																						
Amplitude	Triangul	600	800	1000	[Horizontal distance units]																																																						
Wavelength	Triangul	1000	1500	2000	[Horizontal distance units]																																																						
Rel. sinuosity	Triangul	0.1	0.2	0.3	[Positive number]																																																						
	Min	Med/mean	Max/std																																																								
Orientation	Triangul	110	120	130	[Compass degrees]																																																						
Amplitude	Triangul	600	800	1000	[Horizontal distance units]																																																						
Wavelength	Triangul	1000	1500	2000	[Horizontal distance units]																																																						
Rel. sinuosity	Triangul	0.1	0.2	0.3	[Positive number]																																																						
<div>Settings   Layout   Section   Trends</div> <div>Intersection view: Width Thickness</div> <table border="1"> <thead> <tr> <th></th> <th>Min</th> <th>Med/mean</th> <th>Max/std</th> <th></th> </tr> </thead> <tbody> <tr> <td>Width</td> <td>Triangul</td> <td>80</td> <td>130</td> <td>200</td> <td>[Horizontal distance units]</td> </tr> <tr> <td>Thickness</td> <td>Triangul</td> <td>5</td> <td>8</td> <td>12</td> <td><input type="checkbox"/> Width fraction</td> </tr> </tbody> </table>		Min	Med/mean	Max/std		Width	Triangul	80	130	200	[Horizontal distance units]	Thickness	Triangul	5	8	12	<input type="checkbox"/> Width fraction	<div>Settings   Layout   Section   Trends</div> <div>Intersection view: Width Thickness</div> <table border="1"> <thead> <tr> <th></th> <th>Min</th> <th>Med/mean</th> <th>Max/std</th> <th></th> </tr> </thead> <tbody> <tr> <td>Width</td> <td>Triangul</td> <td>70</td> <td>90</td> <td>120</td> <td>[Horizontal distance units]</td> </tr> <tr> <td>Thickness</td> <td>Triangul</td> <td>4</td> <td>7</td> <td>10</td> <td><input type="checkbox"/> Width fraction</td> </tr> </tbody> </table>		Min	Med/mean	Max/std		Width	Triangul	70	90	120	[Horizontal distance units]	Thickness	Triangul	4	7	10	<input type="checkbox"/> Width fraction																								
	Min	Med/mean	Max/std																																																								
Width	Triangul	80	130	200	[Horizontal distance units]																																																						
Thickness	Triangul	5	8	12	<input type="checkbox"/> Width fraction																																																						
	Min	Med/mean	Max/std																																																								
Width	Triangul	70	90	120	[Horizontal distance units]																																																						
Thickness	Triangul	4	7	10	<input type="checkbox"/> Width fraction																																																						

Figure 52 – Zone C- Channel 4 and Channel axis 3 inputs


<div>Settings   Layout   Section   Trends</div> <div> <input checked="" type="checkbox"/> Use body   <input type="checkbox"/> Modify body name: </div> <div> Facies: 2: Rich Off   Make facies: <input checked="" type="checkbox"/> Channel sand   Fraction (%): 1   Upscaled (%): </div> <div> Facies: 2: Rich Off   Make facies: <input type="checkbox"/> Levee </div> <div>Settings   Layout   Section   Trends</div> <div>Channel Amplitude</div> <div>Wavelength</div> <table border="1"> <thead> <tr> <th></th> <th>Drift [0-1]</th> <th>Min</th> <th>Med/mean</th> <th>Max/std</th> <th></th> </tr> </thead> <tbody> <tr> <td>Orientation</td> <td>Triangul</td> <td>0.2</td> <td>110</td> <td>120</td> <td>135</td> <td>[Compass degrees]</td> </tr> <tr> <td>Amplitude</td> <td>Triangul</td> <td>0.2</td> <td>600</td> <td>800</td> <td>1000</td> <td>[Horizontal distance units]</td> </tr> <tr> <td>Wavelength</td> <td>Triangul</td> <td>0.2</td> <td>1000</td> <td>1500</td> <td>2000</td> <td>[Horizontal distance units]</td> </tr> </tbody> </table> <p>If using flow lines in the 'Trend' tab, the orientation will not be used.</p>		Drift [0-1]	Min	Med/mean	Max/std		Orientation	Triangul	0.2	110	120	135	[Compass degrees]	Amplitude	Triangul	0.2	600	800	1000	[Horizontal distance units]	Wavelength	Triangul	0.2	1000	1500	2000	[Horizontal distance units]	<div>Settings   Geometry   Trends   Rules</div> <div> <input checked="" type="checkbox"/> Use body   <input type="checkbox"/> Modify body name: </div> <div> Facies: 7: Frontal_   Fraction (%): 5   Upscaled (%): </div>																						
	Drift [0-1]	Min	Med/mean	Max/std																																														
Orientation	Triangul	0.2	110	120	135	[Compass degrees]																																												
Amplitude	Triangul	0.2	600	800	1000	[Horizontal distance units]																																												
Wavelength	Triangul	0.2	1000	1500	2000	[Horizontal distance units]																																												
<div>Settings   Layout   Section   Trends</div> <div>Intersection view: Width Thickness</div> <table border="1"> <thead> <tr> <th></th> <th>Drift [0-1]</th> <th>Min</th> <th>Med/mean</th> <th>Max/std</th> <th></th> </tr> </thead> <tbody> <tr> <td>Width</td> <td>Triangul</td> <td>0.2</td> <td>20</td> <td>40</td> <td>60</td> <td>[Horizontal distance units]</td> </tr> <tr> <td>Thickness</td> <td>Triangul</td> <td>0.2</td> <td>3</td> <td>7</td> <td>10</td> <td><input type="checkbox"/> Width fraction</td> </tr> </tbody> </table>		Drift [0-1]	Min	Med/mean	Max/std		Width	Triangul	0.2	20	40	60	[Horizontal distance units]	Thickness	Triangul	0.2	3	7	10	<input type="checkbox"/> Width fraction	<div>Settings   Geometry   Trends   Rules</div> <div> Body shape: Half ellipse   Orientation:  Major width </div> <div> Radial profile: Rounded base   Minor width </div> <table border="1"> <thead> <tr> <th></th> <th>Min</th> <th>Med/mean</th> <th>Max/std</th> <th></th> </tr> </thead> <tbody> <tr> <td>Orientation</td> <td>Triangul</td> <td>110</td> <td>120</td> <td>135</td> <td>[Compass degrees]</td> </tr> <tr> <td>Minor width</td> <td>Triangul</td> <td>400</td> <td>700</td> <td>1200</td> <td>[Horiz. distance units]</td> </tr> <tr> <td>Maj/Min ratio</td> <td>Triangul</td> <td>0.8</td> <td>1</td> <td>1.4</td> <td></td> </tr> <tr> <td>Thickness</td> <td>Triangul</td> <td>12</td> <td>17</td> <td>20</td> <td><input type="checkbox"/> Fraction of width [Fraction of length]</td> </tr> </tbody> </table>		Min	Med/mean	Max/std		Orientation	Triangul	110	120	135	[Compass degrees]	Minor width	Triangul	400	700	1200	[Horiz. distance units]	Maj/Min ratio	Triangul	0.8	1	1.4		Thickness	Triangul	12	17	20	<input type="checkbox"/> Fraction of width [Fraction of length]
	Drift [0-1]	Min	Med/mean	Max/std																																														
Width	Triangul	0.2	20	40	60	[Horizontal distance units]																																												
Thickness	Triangul	0.2	3	7	10	<input type="checkbox"/> Width fraction																																												
	Min	Med/mean	Max/std																																															
Orientation	Triangul	110	120	135	[Compass degrees]																																													
Minor width	Triangul	400	700	1200	[Horiz. distance units]																																													
Maj/Min ratio	Triangul	0.8	1	1.4																																														
Thickness	Triangul	12	17	20	<input type="checkbox"/> Fraction of width [Fraction of length]																																													

Figure 53 – Zone C- Rich off Axis and Frontal Splay inputs

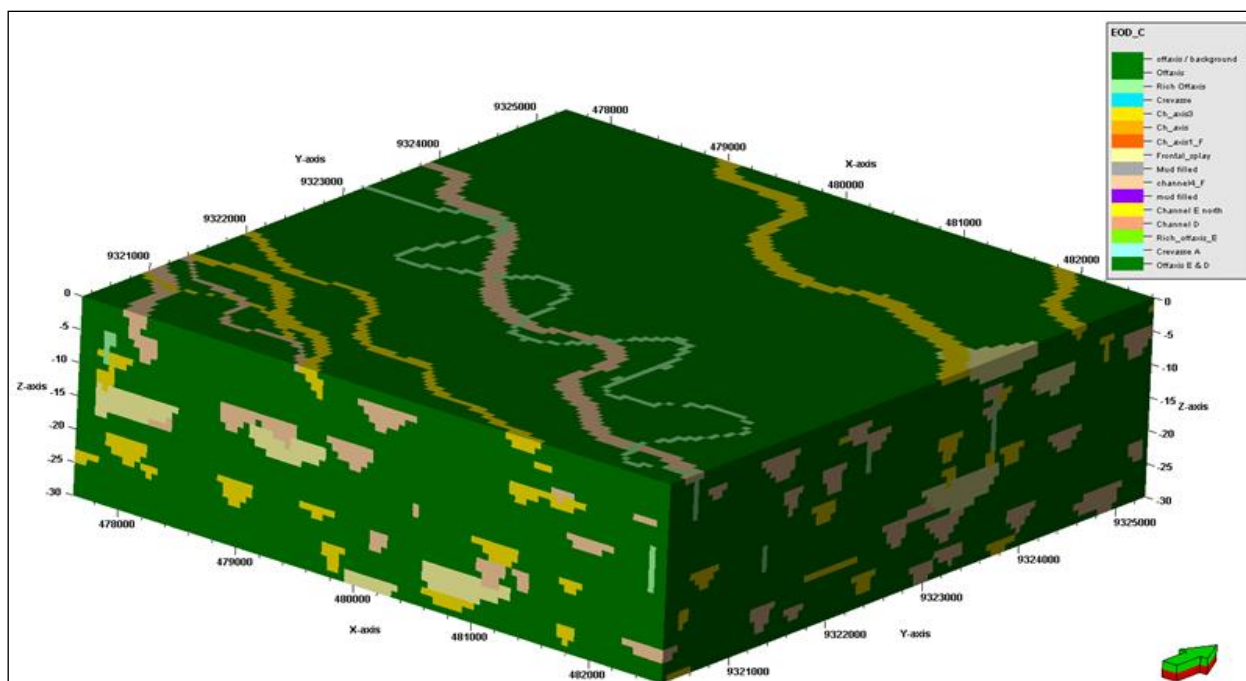


Figure 54 – Zone C Training Image 3D grid

Settings Layout Section Trends

☒ Use body ☐ Modify body name:

Facies Make facies Fraction (%) Upscaled (%)

☒ 2: Rich Off ☒ Channel sand 30

☐ 2: Rich Off ☐ Levee

Settings Layout Section Trends

Channel Amplitude

Wavelength

	Min	Med/ mean	Max/ std		
Orientation	Triangul	110	120	130	[Compass degrees]
Amplitude	Triangul	1000	1500	2000	[Horizontal distance units]
Wavelength	Triangul	2000	3000	4000	[Horizontal distance units]
Rel. sinuosity	Triangul	0.1	0.2	0.3	[Positive number]

Settings Layout Section Trends

Intersection view: Thickness

	Min	Med/ mean	Max/ std		
Width	Triangul	600	700	800	[Horizontal distance units]
Thickness	Triangul	0.5	3	5	<input type="checkbox"/> Width fraction

Figure 55 – Zone CD Rich off Axis inputs



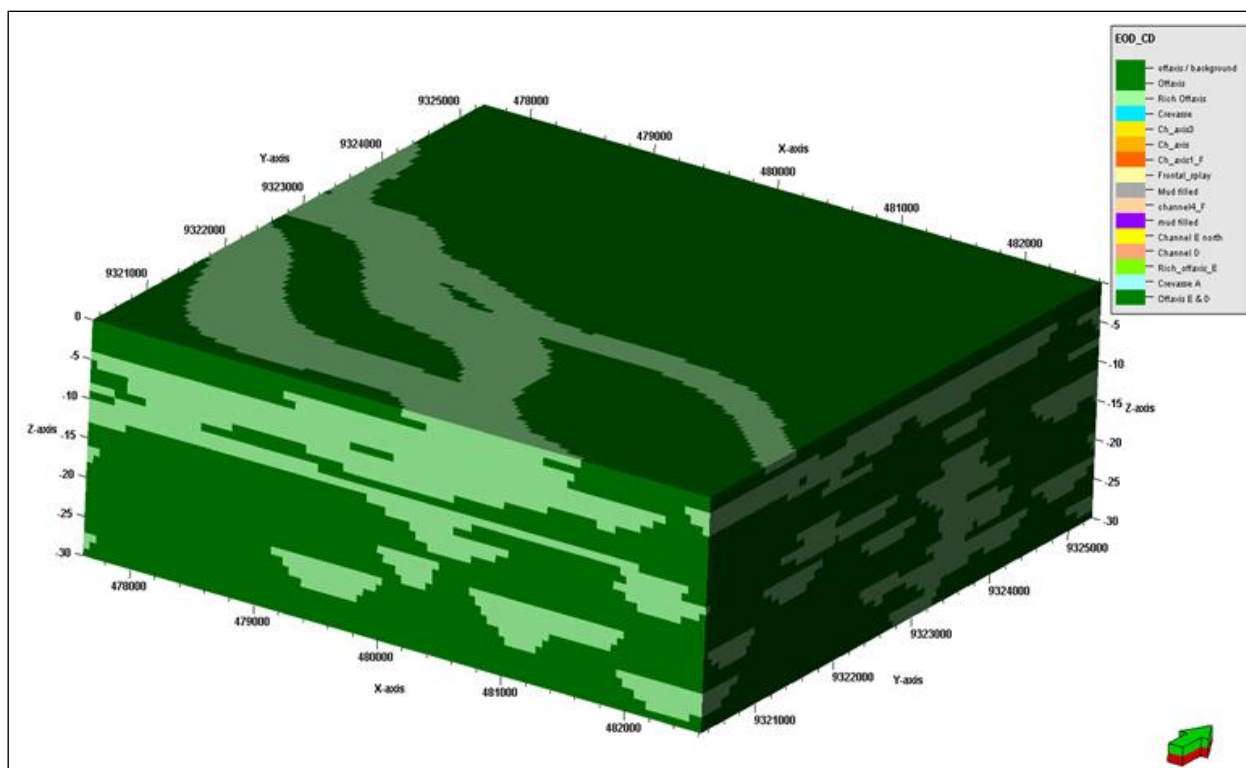


Figure 56 – Zone CD Training Image 3D grid

Settings Layout Section Levee Trends

☒ Use body ☐ Modify body name:

Facies Make facies Fraction (%) Upscaled (%)

12: Chann ☒ Channel sand 80

2: Rich Off ☒ Levee

Settings Layout Section Levee Trends

Channel Wavelength Amplitude

Wavelength Min Med/mean Max/std

Orientation Triangul 110 120 130 [Compass degrees]

Amplitude Triangul 600 800 1000 [Horizontal distance units]

Wavelength Triangul 1000 1500 2000 [Horizontal distance units]

Rel. sinuosity Triangul 0.2 0.3 0.4 [Positive number]

Settings Layout Section Levee Trends

Intersection view: Width Thickness

Width Min Med/mean Max/std

Thickness Triangul 3 7 10 [Horizontal distance units]

Width Triangul 1000 1200 1500 [Horizontal distance units]

Thickness Triangul 0.1 0.2 0.4 0.9 [Relative to channel thickness]

Width unit: ☒ Frac. of channel width ☐ Horizontal distance units

Thickness Triangul 0.1 0.2 0.8 0.9 [Relative to channel thickness]

Approximate facies %: Channel 51.36 Levee 28.64

Figure 57 – Zone D Channel D input

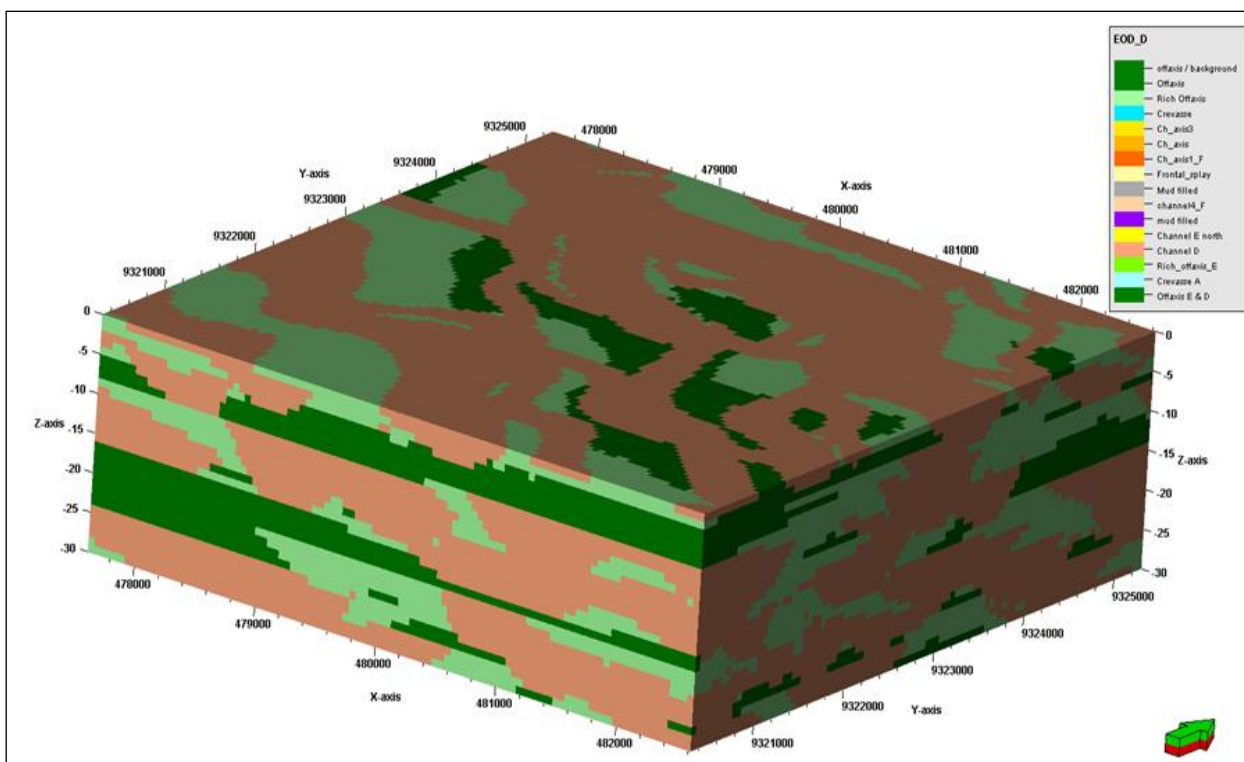


Figure 58 – Zone D Training Image 3D grid

Settings

Layout

Section

Levee

Trends

☒ Use body
 ☐ Modify body name:

Facies

Make facies

Fraction (%)

Upscaled (%)

11: Chann

☒ Channel sand

30

3: Crevass

☒ Levee

Settings

Layout

Section

Levee

Trends

Channel

Amplitude

Wavelength

Orientation

Triangul

0.2

110

120

135

[Compass degrees]

Amplitude

Triangul

0.2

600

800

1000

[Horizontal distance units]

Wavelength

Triangul

0.2

2000

4000

6000

If using flow lines in the 'Trend tab', the orientation will not be used.

Settings

Layout

Section

Levee

Trends

Intersection view:

Width

Thickness

Drift [0-1]

Min

Med/mean

Max/std

[Horizontal distance units]

Width

Triangul

0.2

300

400

600

Thickness

Triangul

0.2

2

5

10

☐ Width fraction

Settings

Layout

Section

Levee

Trends

Thickness

Width

Drift

Min

Med/mean

Max/std

[Relative to channel thickness]

Width

Triangul

0.2

0.7

0.9

1.2

Width unit:

☒ Frac. of channel width

☐ Horizontal distance units

Thickness

Triangul

0.2

0.6

0.7

0.9

Approximate facies %: Channel 13.92 Levee 16.08

Settings

Layout

Section

Levee

Trends

Intersection view:

Width

Thickness

Drift [0-1]

Min

Med/mean

Max/std

[Horizontal distance units]

Width

Triangul

0.2

400

600

800

Thickness

Triangul

0.2

3

5

10

☐ Width fraction

Figure 59 – Zone E Channel E North and Rich off axis input

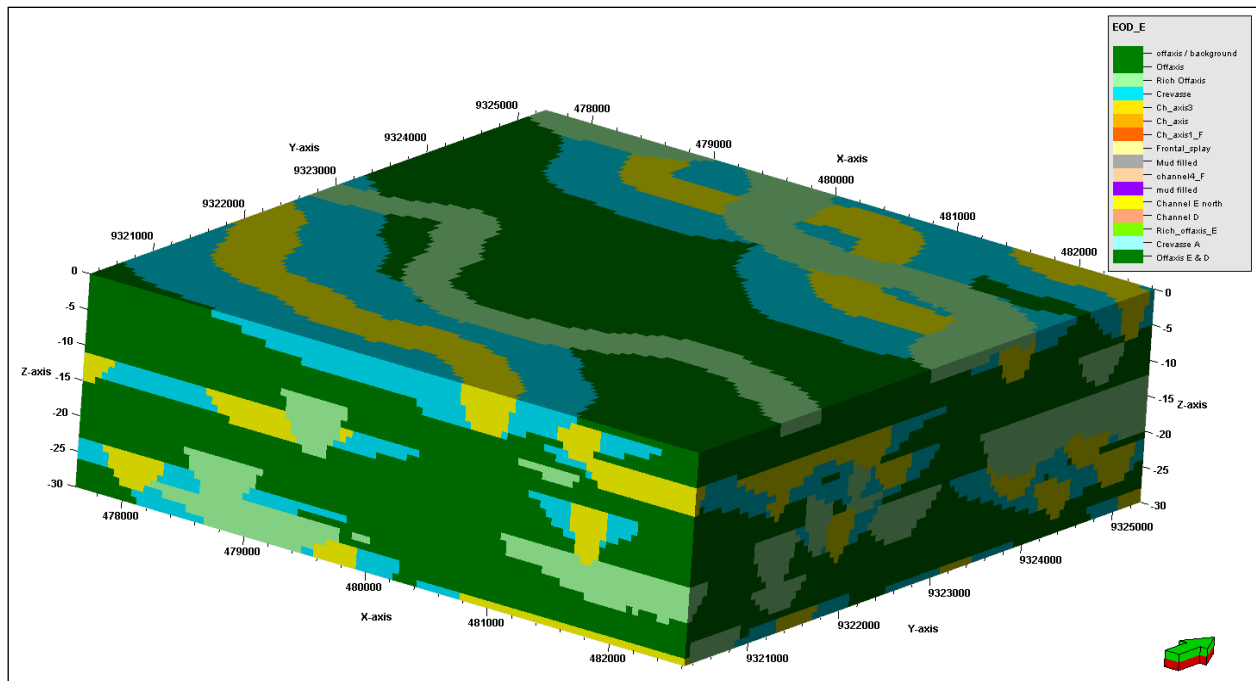


Figure 60 – Zone E Training Image 3D grid

Settings	Layout	Section	Trends
<input checked="" type="checkbox"/> Use body <input type="checkbox"/> Modify body name:			
Facies: 9: channel <input checked="" type="checkbox"/> Make facies: Channel sand Fraction (%) 40 Upscaled (%)			
Facies: 2: Rich Off <input type="checkbox"/> Make facies: Levee			
Channel: Wavelength Min Med/mean Max/std			
Orientation: Triangul 110 120 135 [Compass degrees]			
Amplitude: Triangul 600 800 1000 [Horizontal distance units]			
Wavelength: Triangul 1000 1500 2000			
Rel. sinuosity: Triangul 0.2 0.3 0.4 [Positive number]			
Width: Min Med/mean Max/std			
Thickness: Min Med/mean Max/std			
Width fraction: <input type="checkbox"/>			

Figure 61 – Zone F Channel 4 and Channel axis 3 inputs



Figure 10 displays four screenshots of the software interface, showing the configuration of a channel cross-section. The top row shows the 'Facies' panel with '5: Ch\_axis' and '2: Rich Off' selected, and 'Channel sand' checked. The 'Fraction (%)' is set to 15. The bottom row shows the 'Channel' panel with 'Amplitude' and 'Wavelength' set to 1000, and 'Orientation' set to 'Triangul'. The 'Intersection view' shows a cross-section of the channel with 'Width' and 'Thickness' set to 200 and 5 respectively. The 'Trends' panel shows 'Drift [0-1]' set to 0.2, 'Min' set to 110, 'Med/mean' set to 120, and 'Max/std' set to 135.

Figure 62 – Zone F Channel 2 and Channel 1 input

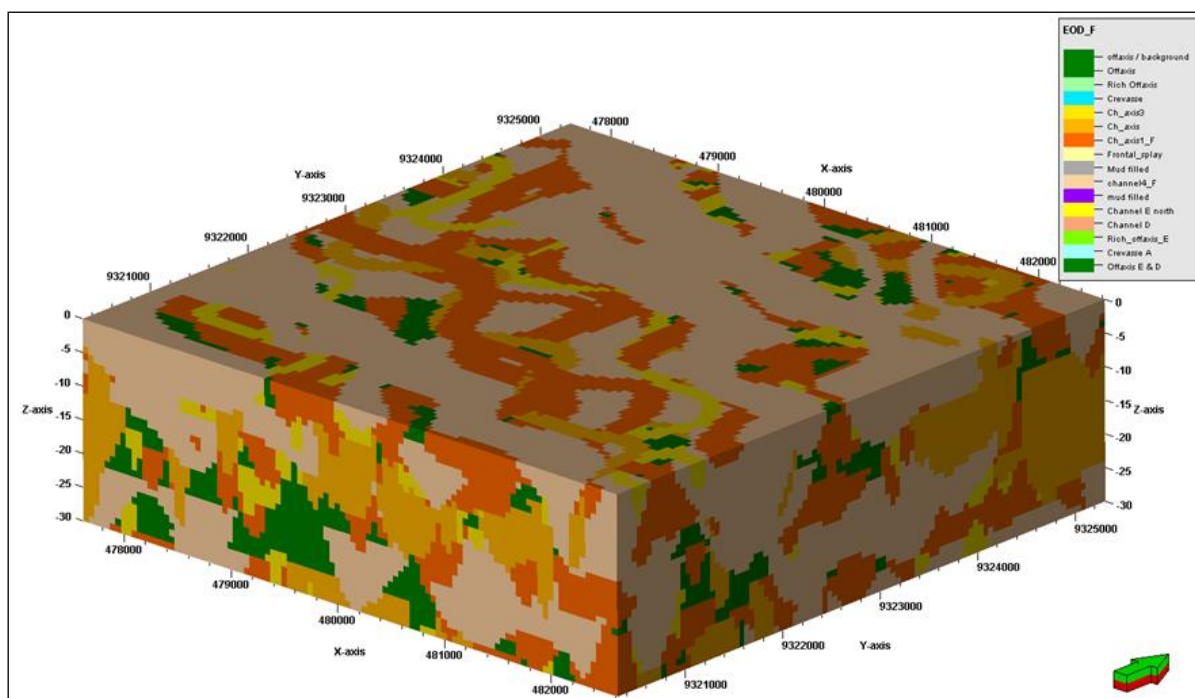


Figure 63 – Zone F Training Image 3D grid

- Simulation two: by analyzing the amplitude maps, some possible improvements could be made to optimize the EoD representation on zone C and zone D:

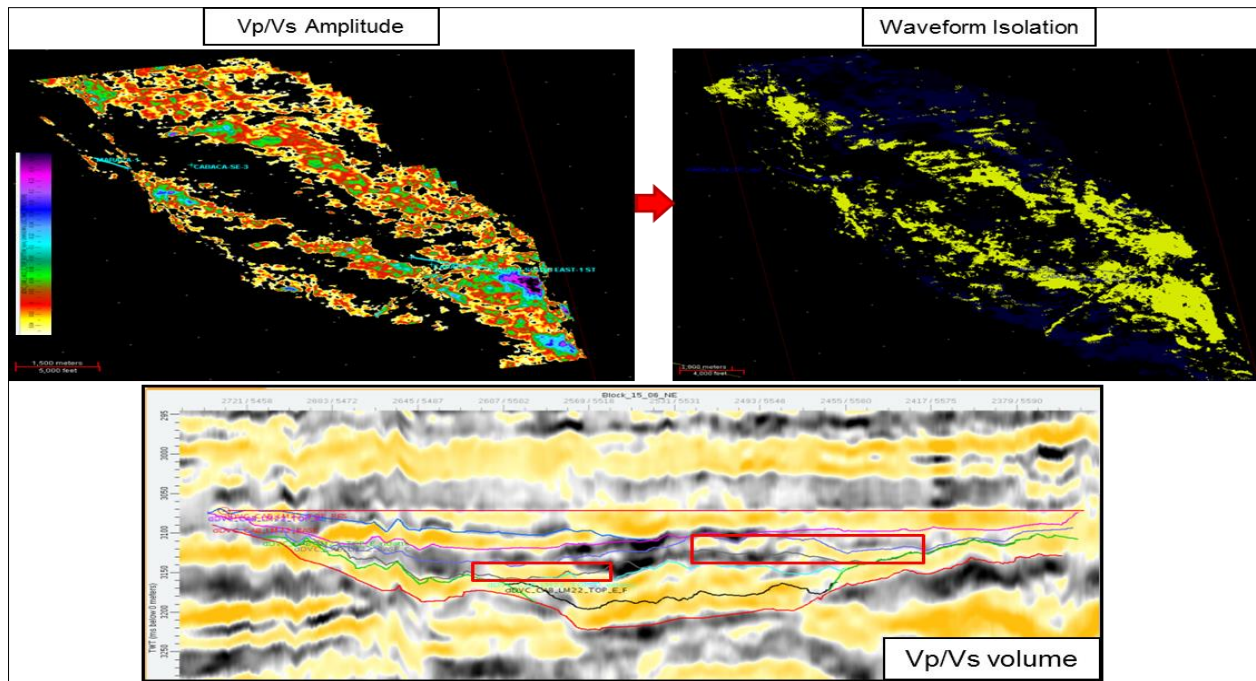


Figure 64 – Zone C, facies interpretation – Seismic

- Zone C: in Figure 64 the channel boundaries are not as clear as the EoD maps used on the standard model and on the TI simulation one. A levee was added to the two main channels on these zones;
- Zone D: changes were made in the TI input parameters optimizing the EoD boundaries and increasing the levee fraction on the training image.

Settings	Layout	Section	Levee	Trends
<input checked="" type="checkbox"/> Use body <input type="checkbox"/> Modify body name:				
Facies: 9: channel <input checked="" type="checkbox"/> Channel sand 12 <input type="checkbox"/> Upscaled (%) 3: Crevass <input checked="" type="checkbox"/> Levee				
Channel Wavelength: Min 110, Med/mean 120, Max/std 130 [Compass degrees] Orientation: Triangul Amplitude: Triangul 600, 800, 1000 [Horizontal distance units] Wavelength: Triangul 1000, 1500, 2000 Rel. sinuosity: Triangul 0.1, 0.2, 0.3 [Positive number]				
Intersection view: Width 60, 130, 200 [Horizontal distance units] Thickness: Triangul 1, 5, 10 Width fraction: <input type="checkbox"/>				
Thickness Roughness: Min 0.2, 0.5, 0.8, 0.9 Width unit: <input checked="" type="radio"/> Frac. of channel width <input type="radio"/> Horizontal distance units Thickness: Triangul 0.2, 0.7, 0.8, 0.9 [Relative to channel thickness] Approximate facies %: Channel 5.48, Levee 6.52				

Settings	Layout	Section	Levee	Trends
<input checked="" type="checkbox"/> Use body <input type="checkbox"/> Modify body name:				
Facies: 4: Ch_axis <input checked="" type="checkbox"/> Channel sand 10 <input type="checkbox"/> Upscaled (%) 3: Crevass <input checked="" type="checkbox"/> Levee				
Channel Wavelength: Min 110, Med/mean 120, Max/std 130 [Compass degrees] Orientation: Triangul Amplitude: Triangul 600, 800, 1000 [Horizontal distance units] Wavelength: Triangul 1000, 1500, 2000 Rel. sinuosity: Triangul 0.08, 0.1, 0.2 [Positive number]				
Intersection view: Width 70, 100, 150 [Horizontal distance units] Thickness: Triangul 4, 5, 10 Width fraction: <input type="checkbox"/>				
Thickness Roughness: Min 0.2, 0.7, 0.8, 0.9 Width unit: <input checked="" type="radio"/> Frac. of channel width <input type="radio"/> Horizontal distance units Thickness: Triangul 0.2, 0.5, 0.7, 0.9 [Relative to channel thickness] Approximate facies %: Channel 4.96, Levee 5.04				

Figure 65 – Zone C- Channel 4 and Channel axis 3 inputs (second simulation)



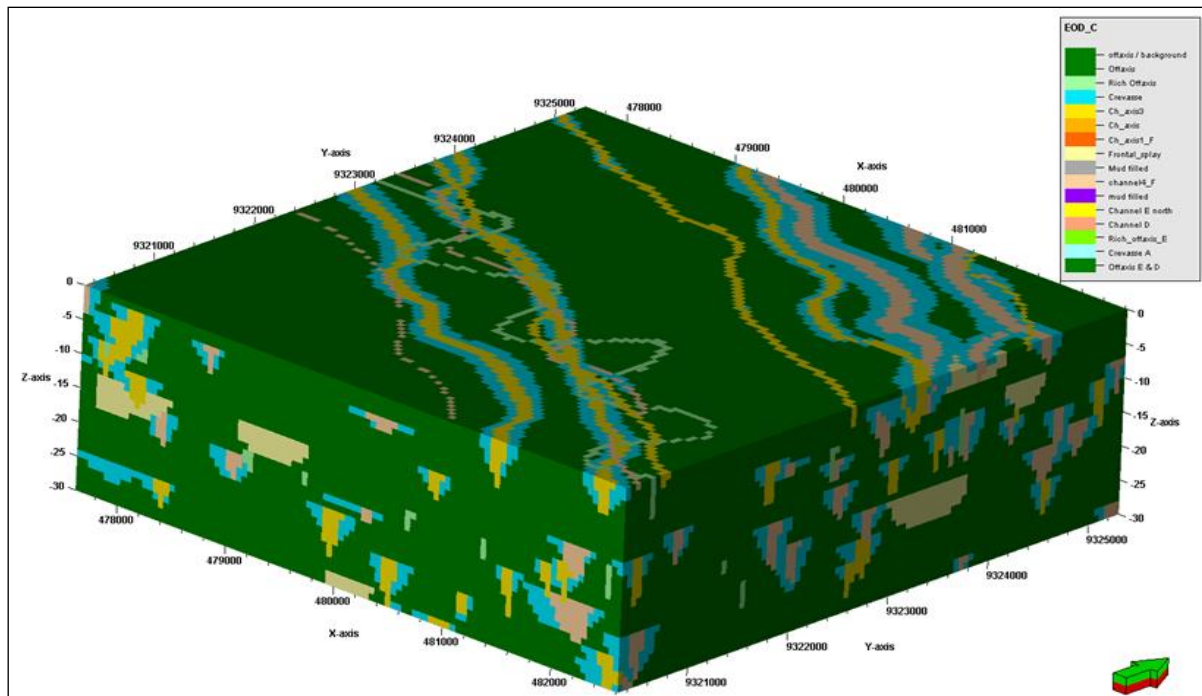


Figure 66 – Zone C Training Image 3D grid (second simulation)

Settings Layout Section Levee Trends

☒ Use body ☐ Modify body name:

Facies Make facies Fraction (%) Upscaled (%)

12: Chann ☒ Channel sand 70

2: Rich Off ☒ Levee

---

Settings Layout Section Levee Trends

Channel Amplitude

Wavelength Min Med/mean Max/std

Orientation Triangul 110 120 130 [Compass degrees]

Amplitude Triangul 600 800 1000 [Horizontal distance units]

Wavelength Triangul 1000 1500 2000

Rel. sinuosity Triangul 0.2 0.3 0.4 [Positive number]

---

Settings Layout Section Levee Trends

Intersection view: Width Thickness

Min Med/mean Max/std

Width Triangul 600 900 1200 [Horizontal distance units]

Thickness Triangul 3 6 10 ☐ Width fraction

---

Settings Layout Section Levee Trends

Width Thickness Roughness Min Med/mean Max/std

Width Triangul 0.2 0.3 0.6 0.8

Width unit: ☒ Frac. of channel width ☐ Horizontal distance units

Thickness Triangul 0.2 0.3 0.8 0.9 [Relative to channel thickness]

Approximate facies %: Channel 37.38 Levee 32.62

Figure 67 – Zone D- Channel D inputs (second simulation)

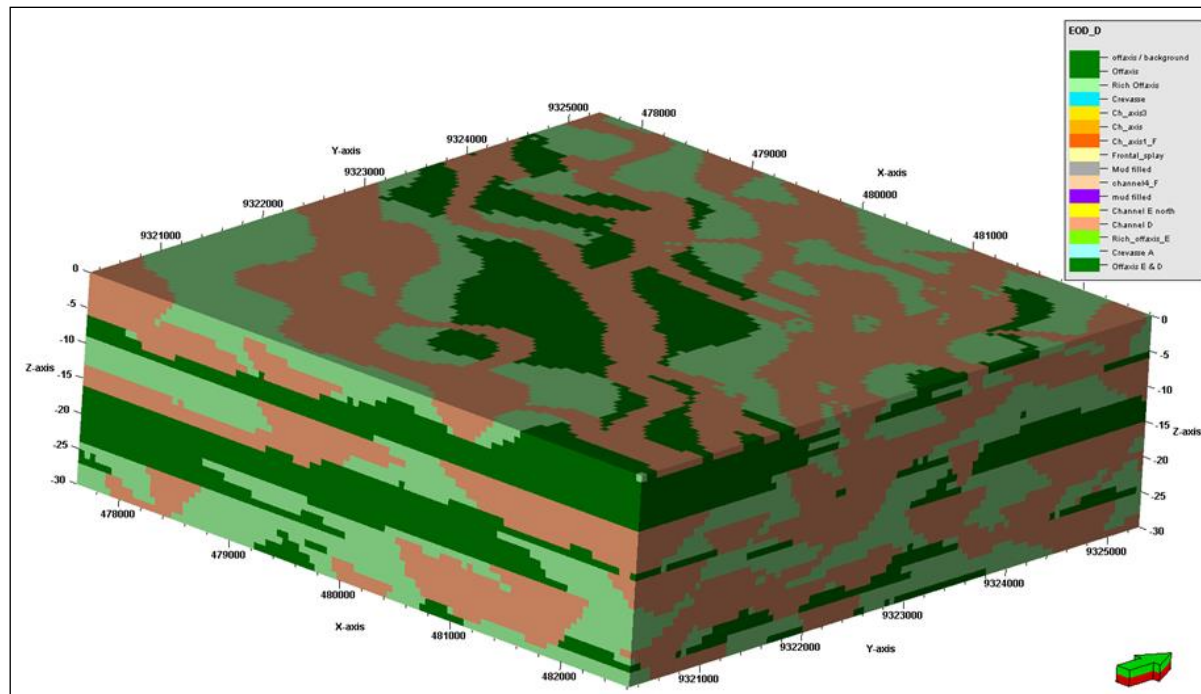


Figure 68 – Zone D Training Image 3D grid (second simulation)

Various sensitivities were realized until the TIs were representing the most likely model, honoring the well log correlation, the seismic data (amplitude maps), the sedimentological model and the EoD in each zone.

On the TIs 3D grid the channels amalgamation on each zone can be appreciated, respecting the fining upward trend on the sand content and the geo-bodies channel geometry definition, in line with the sedimentological model.

### 3.2.3 MPS Geo-body Facies (EoD) model

Once up-scaled the facies (EoD) log in the 3D grid, the EoD simulation has been performed by means of the MPS simulation algorithm. The process has been run by zone, since the TI has been defined by zone as well. On the data selection pane, the training images have been loaded considering that the facies fraction on the Training Image output was approximated to the facies fractions of the reference standard model and considering that the main impact on the training image facies fraction output is the EoD fraction input in the Training Image.

In the external constraint window, it is possible to add a probability property which acts as a guiding tool for the property distribution. The weight correction between the simulated facies and the secondary trend ranges from 0 to 1. Considering that the TI is the main input for the MPS facies distribution, different sensitivities have been made using different weight correction factors.

Data selection External constraints Expert Hints

Training image

Training image property:  Grid:

☐ Same zone as primary property

Facies / target fractions

Global fractions:

Use	Facies	Training image facies	Fractions
<input type="checkbox"/>	0: Offaxis / background		
<input checked="" type="checkbox"/>	1: Offaxis	1: Offaxis	50.73
<input type="checkbox"/>	2: Rich Offaxis	2: Rich Offaxis	20.54
<input checked="" type="checkbox"/>	3: Crevasse	3: Crevasse	8.02
<input checked="" type="checkbox"/>	4: Ch_axis3	4: Ch_axis3	18.34
<input type="checkbox"/>	5: Ch_axis		
<input type="checkbox"/>	6: Ch_axis1_F		
<input type="checkbox"/>	7: Frontal_splay		
<input type="checkbox"/>	8: Mud filled		
<input type="checkbox"/>	9: channel4_F		
<input checked="" type="checkbox"/>	10: mud filled	10: mud filled	2.37
<input type="checkbox"/>	11: Channel E north		
<input type="checkbox"/>	12: Channel D		
<input type="checkbox"/>	13: Rich_offaxis_E		
<input type="checkbox"/>	14: ...		
Total %			100.00

Data selection External constraints Expert Hints

Training image

Training image property:  Grid:

☐ Same zone as primary property

Facies / target fractions

Global fractions:

Use	Facies	Training image facies	Fractions
<input checked="" type="checkbox"/>	0: offaxis / background	0: offaxis / background	30.57
<input type="checkbox"/>	1: Offaxis		
<input type="checkbox"/>	2: Rich Offaxis		
<input checked="" type="checkbox"/>	3: Crevasse	3: Crevasse	28.21
<input type="checkbox"/>	4: Ch_axis3		
<input type="checkbox"/>	5: Ch_axis		
<input type="checkbox"/>	6: Ch_axis1_F		
<input checked="" type="checkbox"/>	7: Frontal_splay	7: Frontal_splay	26.92
<input type="checkbox"/>	8: Mud filled		
<input type="checkbox"/>	9: channel4_F		
<input checked="" type="checkbox"/>	10: mud filled	10: mud filled	14.30
<input type="checkbox"/>	11: Channel E north		
<input type="checkbox"/>	12: Channel D		
<input type="checkbox"/>	13: Rich_offaxis_E		
<input type="checkbox"/>	14: ...		
Total %			100.00

Data selection External constraints Expert Hints

Proportion / probability constraints

☐ Vertical proportion functions ☒ Inverse x-axis

☐ Proportion maps

☐ Proportion region properties

☒ Probability properties Weight:

Facies	Probability properties
1: 0: Offaxis	<input type="checkbox"/> <input type="text" value="Fra OffAxis_Pr ... AB,C,D,E,F"/>
2: 2: Rich Offaxis	<input checked="" type="checkbox"/> <input type="text" value="Fra RoA_Prob (A,C,D,D,E)"/>
3: 3: Crevasse	<input checked="" type="checkbox"/> <input type="text" value="Fra Crevasse Prob (AB,E)"/>
4: 4: Ch_axis3	<input checked="" type="checkbox"/> <input type="text" value="Fra Ch_Ax_3_Prob (A,C,F)"/>
5: 10: mud filled	<input checked="" type="checkbox"/> <input type="text" value="Fra MFch_Prob (A,AB)"/>

Data selection External constraints Expert Hints

Proportion / probability constraints

☐ Vertical proportion functions ☒ Inverse x-axis

☐ Proportion maps

☐ Proportion region properties

☒ Probability properties Weight:

Facies	Probability properties
1: 0: offaxis / background	<input type="checkbox"/> <input type="text" value="Fra OffAxis_Pr ... (AB,E)"/>
2: 3: Crevasse	<input checked="" type="checkbox"/> <input type="text" value="Fra Crevasse ... (AB,E)"/>
3: 7: Frontal_splay	<input checked="" type="checkbox"/> <input type="text" value="Fra Fspaly ... (AB,C)"/>
4: 10: mud filled	<input checked="" type="checkbox"/> <input type="text" value="Fra MFch ... A,AB)"/>

Table 8 – Pseudozones A and AB - MPS Facies Model

Data selection External constraints Expert Hints

Training image  
Training image property:  Grid:   
☐ Same zone as primary property Zones: Apply to all zones

Facies / target fractions  
Global fractions:

Use	Facies	Training image facies	Fractions
<input checked="" type="checkbox"/>	0: offaxis / background	0: offaxis / background	81.04
<input type="checkbox"/>	1: Offaxis		
<input checked="" type="checkbox"/>	2: Rich Offaxis	2: Rich Offaxis	0.94
<input type="checkbox"/>	3: Crevasse		
<input checked="" type="checkbox"/>	4: Ch_axis3	4: Ch_axis3	4.96
<input type="checkbox"/>	5: Ch_axis		
<input type="checkbox"/>	6: Ch_axis1_F		
<input checked="" type="checkbox"/>	7: Frontal_splay	7: Frontal_splay	4.84
<input type="checkbox"/>	8: Mud filled		
<input checked="" type="checkbox"/>	9: channel4_F	9: channel4_F	8.21
<input type="checkbox"/>	10: mud filled		
<input type="checkbox"/>	11: Channel E north		
<input type="checkbox"/>	12: Channel D		
<input type="checkbox"/>	13: Rich_offaxis_E		

Total % 99.99

Data selection External constraints Expert Hints

Proportion / probability constraints  
☐ Vertical proportion functions ☒ Inverse x-axis  
☐ Proportion maps  
☐ Proportion region properties  
☒ Probability properties Weight:

Facies	Probability properties
1: 0: offaxis / background	<input type="checkbox"/> <input type="text" value="=&gt; Fra RoA_Pr ... D,D,E"/>
2: 2: Rich Offaxis	<input checked="" type="checkbox"/> <input type="text" value="=&gt; Fra Ch_Ax ... (A,C,F)"/>
3: 4: Ch_axis3	<input checked="" type="checkbox"/> <input type="text" value="=&gt; Fra Fspaly ... (AB,C)"/>
4: 7: Frontal_splay	<input checked="" type="checkbox"/> <input type="text" value="=&gt; Fra Ch4_F Prob (C,F)"/>
5: 9: channel4_F	<input checked="" type="checkbox"/>

Data selection External constraints Expert Hints

Training image  
Training image property:  Grid:   
☐ Same zone as primary property Zones: Apply to all zones

Facies / target fractions  
Global fractions:

Use	Facies	Training image facies	Fractions
<input checked="" type="checkbox"/>	0: offaxis / background	0: offaxis / background	70.18
<input type="checkbox"/>	1: Offaxis		
<input checked="" type="checkbox"/>	2: Rich Offaxis	2: Rich Offaxis	29.82
<input type="checkbox"/>	3: Crevasse		
<input type="checkbox"/>	4: Ch_axis3		
<input type="checkbox"/>	5: Ch_axis		
<input type="checkbox"/>	6: Ch_axis1_F		
<input type="checkbox"/>	7: Frontal_splay		
<input type="checkbox"/>	8: Mud filled		
<input type="checkbox"/>	9: channel4_F		
<input type="checkbox"/>	10: mud filled		
<input type="checkbox"/>	11: Channel E north		
<input type="checkbox"/>	12: Channel D		
<input type="checkbox"/>	13: Rich_offaxis_E		

Total % 100.00

Data selection External constraints Expert Hints

Proportion / probability constraints  
☐ Vertical proportion functions ☒ Inverse x-axis  
☐ Proportion maps  
☐ Proportion region properties  
☒ Probability properties Weight:

Facies	Probability properties
1: 0: offaxis / background	<input type="checkbox"/> <input type="text" value="=&gt; Fra RoA_Pr ... D,D,E"/>
2: 2: Rich Offaxis	<input checked="" type="checkbox"/> <input type="text" value="=&gt; Fra RoA_Pr ... D,D,E"/>

Table 9 – Pseudozones C and CD - MPS Facies Model



The screenshot displays the MPS Facies Model software interface, showing the configuration for training images and probability constraints for Pseudozones D and E.

**Training image selection:**

- Training image property:** EOD\_D (Left) and EOD\_E (Right)
- Grid:** JP\_T1 grid
- Global fractions:** From training image property

**Facies / target fractions table:**

Use	Facies	Training image facies	Fractions
1	0: offaxis / background	0: offaxis / background	19.06
2	1: Offaxis		
3	2: Rich Offaxis	2: Rich Offaxis	27.21
4	3: Crevasse		
5	4: Ch_axis3		
6	5: Ch_axis		
7	6: Ch_axis1_F		
8	7: Frontal_splay		
9	8: Mud filled		
10	9: channel4_F		
11	10: mud filled		
12	11: Channel E north		
13	12: Channel D	12: Channel D	53.73
14	13: Rich offaxis E		
Total %			100.00

**Proportion / probability constraints:**

- ☐ Vertical proportion functions
- ☒ Inverse x-axis
- ☐ Proportion maps
- ☐ Proportion region properties
- ☒ Probability properties (Weight: 0.301)

**Facies and Probability properties table:**

Facies	Probability properties
0: offaxis / background	
2: Rich Offaxis	Fra RoA_Pr ... D,D,E
12: Channel D	Fra Chn_D Prob

Table 10 – Pseudozones D and E - MPS Facies Model

The screenshot displays the MPS Facies Model software interface, showing the configuration for training image selection and probability constraints for Pseudozone F.

**Training image selection:**

- Training image property:** EOD\_F
- Grid:** JP\_T1 grid
- Global fractions:** From training image property

**Facies / target fractions table:**

Use	Facies	Training image facies	Fractions
1	0: offaxis / background	0: offaxis / background	12.49
2	1: Offaxis		
3	2: Rich Offaxis		
4	3: Crevasse		
5	4: Ch_axis3	4: Ch_axis3	6.41
6	5: Ch_axis	5: Ch_axis	15.10
7	6: Ch_axis1_F	6: Ch_axis1_F	26.04
8	7: Frontal_splay		
9	8: Mud filled		
10	9: channel4_F	9: channel4_F	39.96
11	10: mud filled		
12	11: Channel E north		
13	12: Channel D		
14	13: Rich offaxis E		
Total %			100.00

**Proportion / probability constraints:**

- ☐ Vertical proportion functions
- ☒ Inverse x-axis
- ☐ Proportion maps
- ☐ Proportion region properties
- ☒ Probability properties (Weight: 0.301)

**Facies and Probability properties table:**

Facies	Probability properties
0: offaxis / background	
4: Ch_axis3	Fra Ch_Ax_ ... (A,C,F)
5: Ch_axis	Fra Chn2_F Prob
6: Ch_axis1_F	Fra Chn1_F Prob
9: channel4_F	Fra Ch4_F Prob (C,F)

Table 11 – Pseudozones F - MPS Facies Model



From different input settings arrangement a few simulations were run and correlated with the pre-existing standard model:

- Simulation 1: make use of the first training image simulation and a weight correction of 0.5;
- Simulation 2: using the same TI as simulation one, but reducing the weight correction impact to 0.3, which means giving more emphases to the Training Image;
- Simulation 3: make use of the second training image simulation, which emphasizes the optimization of pseudozone C and pseudozone D and with a weight correction of 0.3;
- Simulation 4: maintaining the second training image simulation and changing the weight correction from 0.3 to 0.2, increasing the Training Image influence on the final EoD distribution.

As listed here above, two types of sensitivities were run: one aimed to test the effect of the Training Images on the final EoD model, and another one aimed to test the effect of the weight factor with the EoD probability volume. The results of these sensitivities follow below.

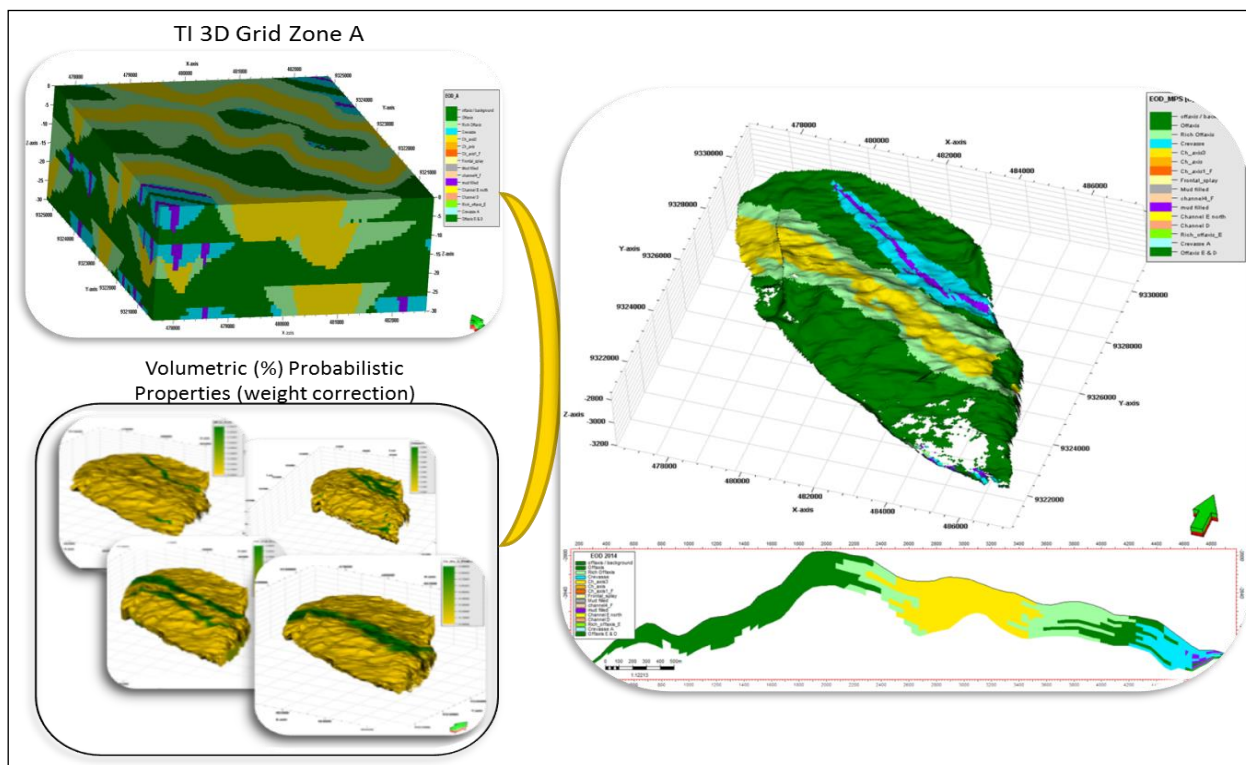


Figure 69 – MPS Facies modelling concept

- Simulation 1: training image simulation one and weight correction = 0.5

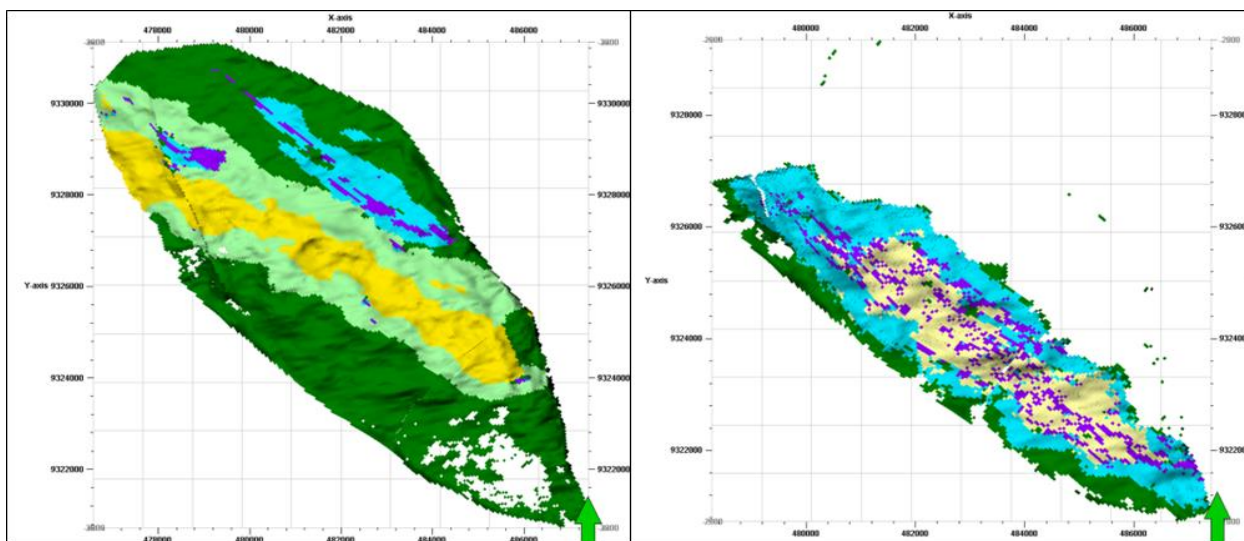


Figure 70 – Pseudozones A and AB – MPS model (simulation 1)

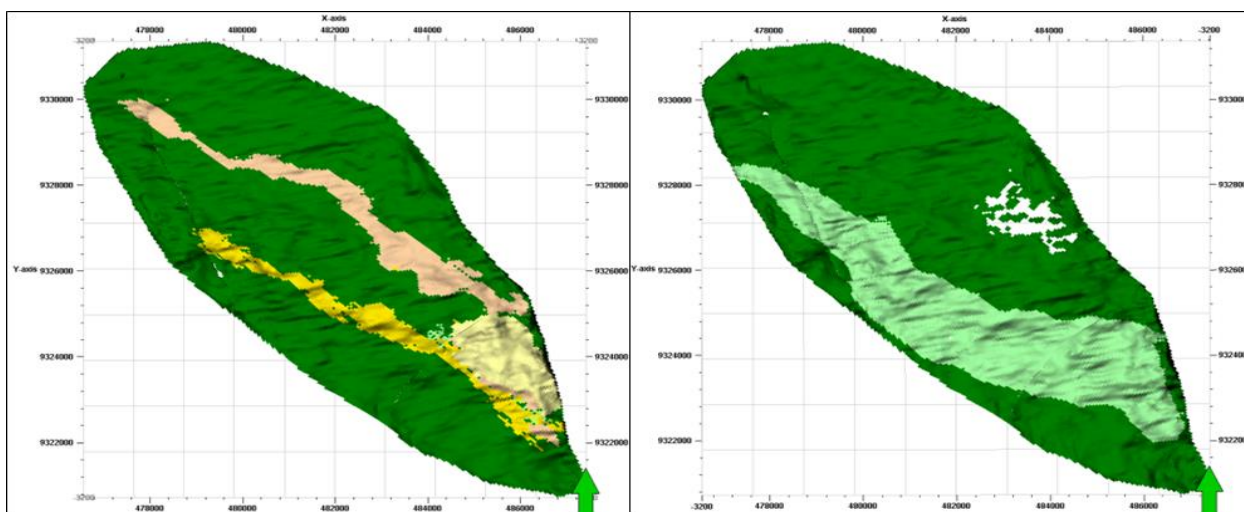


Figure 71 – Zone C and CD – MPS model (simulation 1)

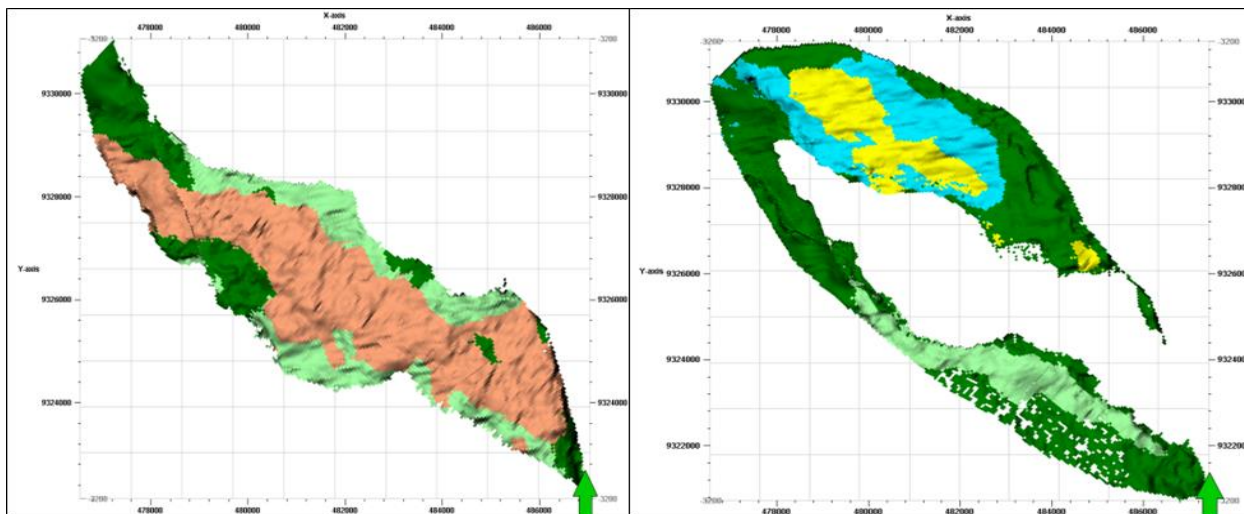


Figure 72 – Pseudozones D and E – MPS model (simulation 1)

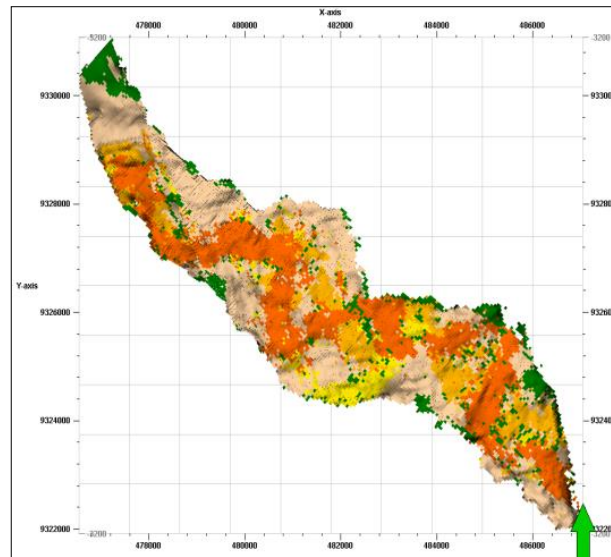


Figure 73 – Pseudozone F – MPS model (simulation 1)

- Simulation 2: training image as simulation one and weight correction of 0,3.

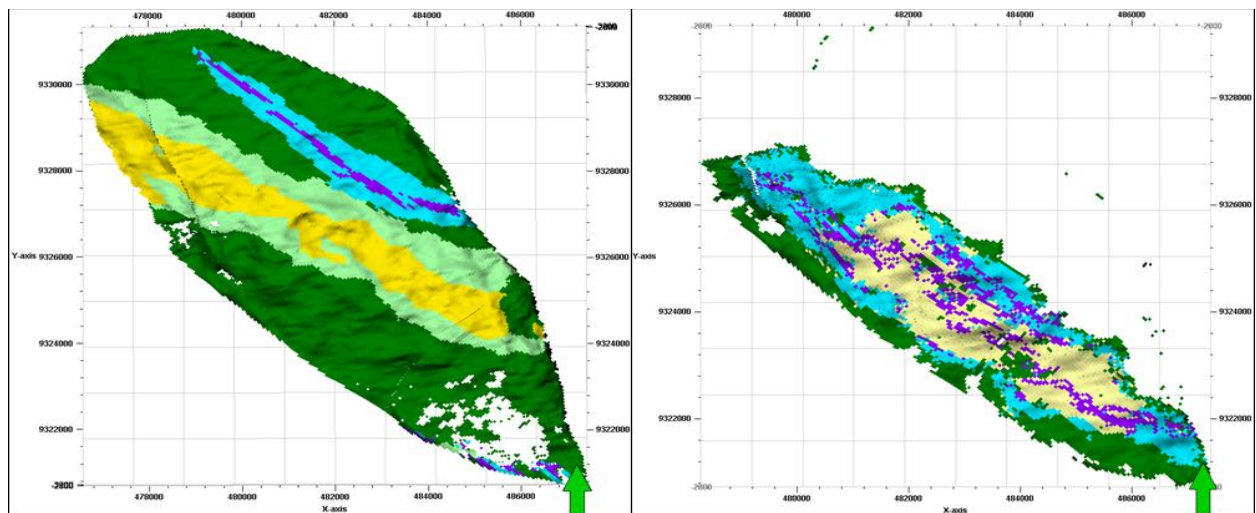


Figure 74 – Pseudozones A and AB – MPS model (simulation 2)



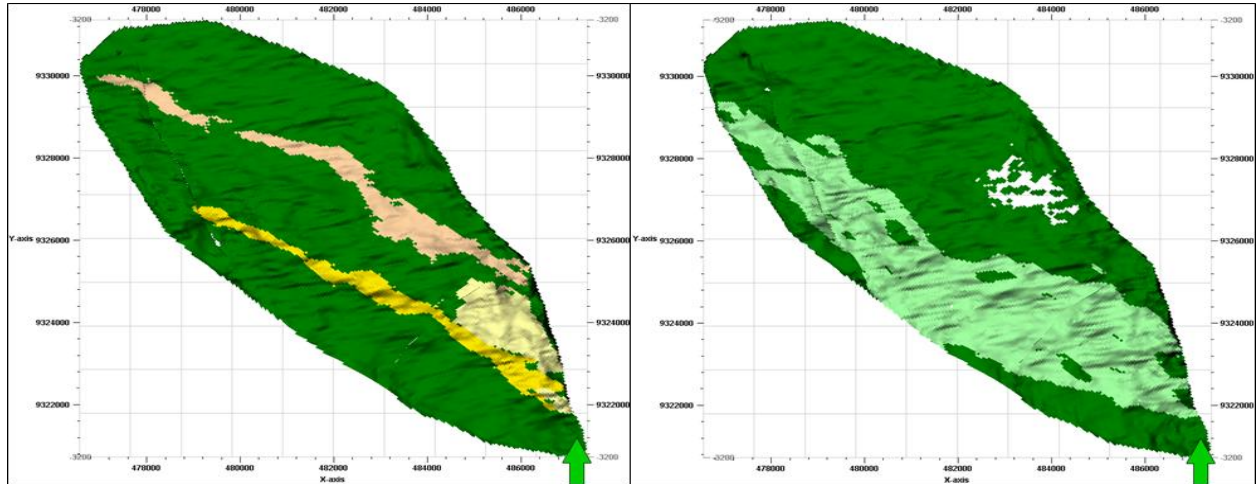


Figure 75 – Pseudozones C and CD – MPS model (simulation 2)

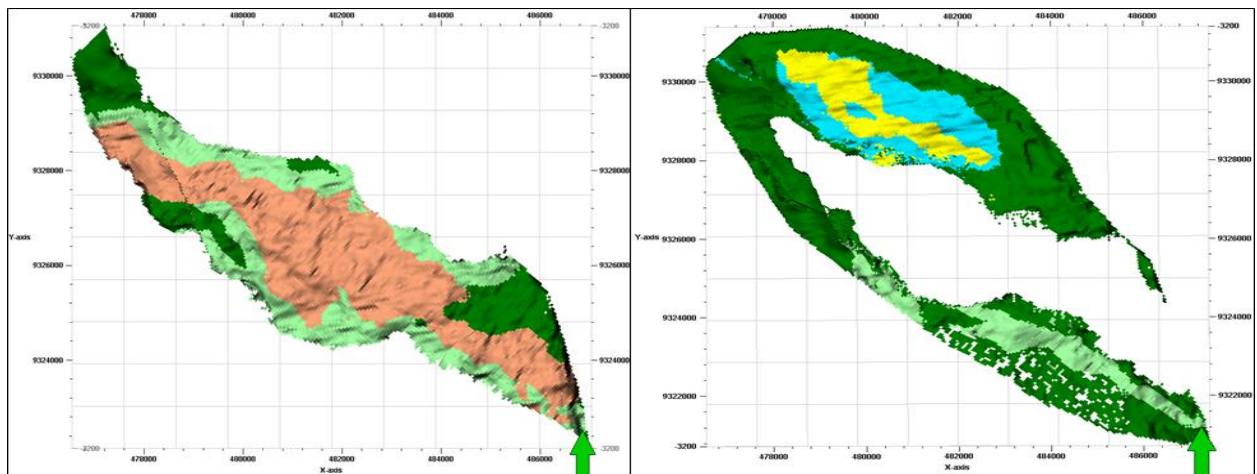


Figure 76 – Pseudozones D and E – MPS model (simulation 2)

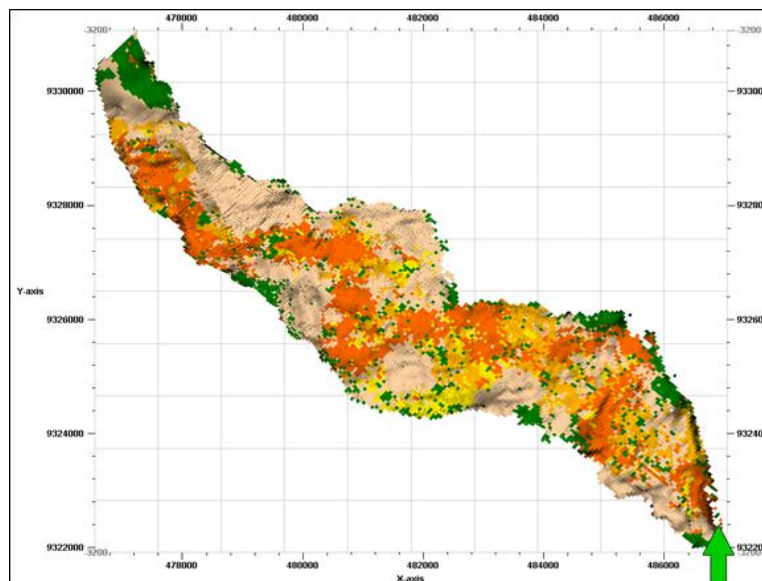


Figure 77 – Pseudozones F – MPS model (simulation 2)



By decreasing the weight correction factor from 0.5 (simulation 1) to 0.3 (simulation 2), the channel geometry changes: the definition of the shape reduces as well as the channel continuity (see Figure 75, zone C, where the channel 4 is illustrated).

Passing from a deterministic interpretation to a stochastic EoD simulation, the main improvement is related to geometry of the modelled objects. They reflect their real geological shape, allowing a better reconstruction of the depositional history, which strongly impacts on the dynamic behavior.

Here below this phenomenon can be appreciated in zone A, D and F, in line with the seismic analysis (Figure 78 and Figure 79).

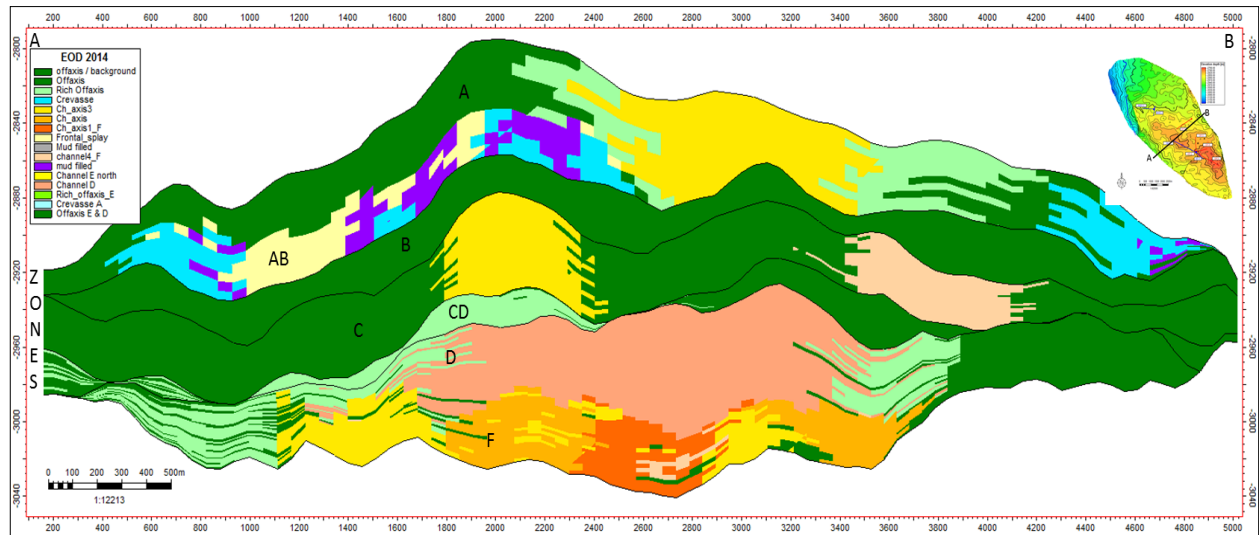


Figure 78 – Cross section – MPS model

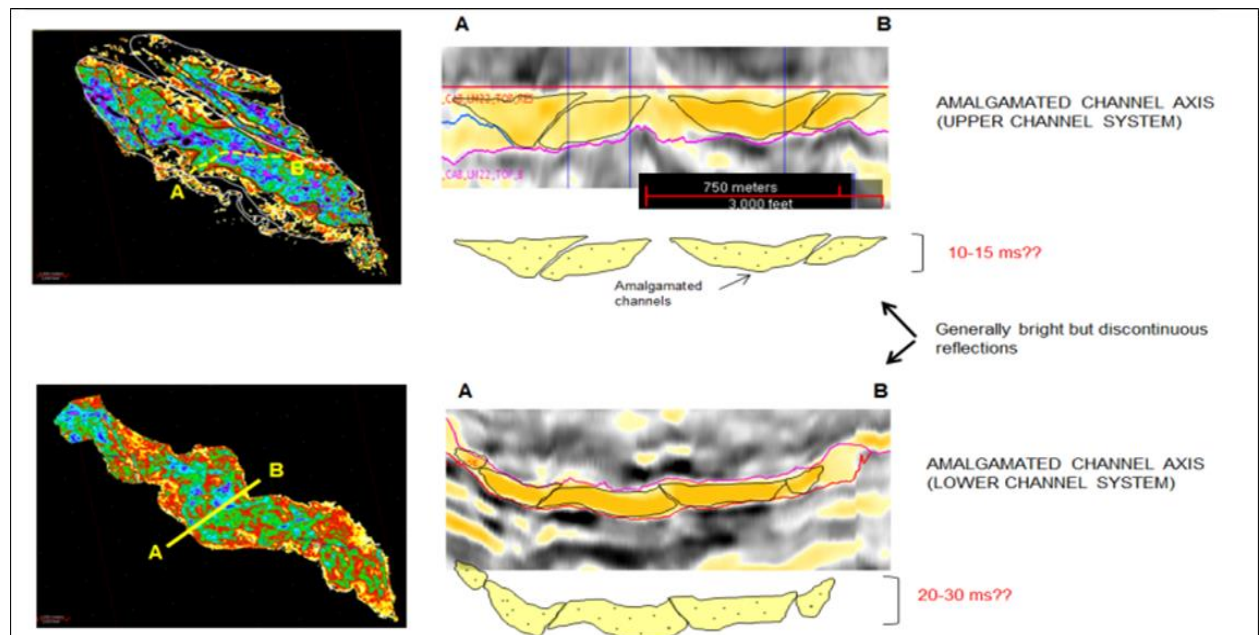


Figure 79 – Pseudozone A and F, Facies Interpretation - Seismic

- Simulation 3: based on the first results, an optimization on the training images of zone C and zone D was carried out (supported by the amplitude maps). A weight factor = 0.3 was considered. In particular, the main changes are listed here below:

Zone C: introduction of levee (crevasse) to the two isolated channels (EOD), supported by seismic interpretation (Vp/Vs volume).

Zone D: optimization of the TI (Figure 67), by reviewing the facies fraction of the different elements of deposition.

Geobodies		Facies	Fractions
Pseudozone C	offaxis	VLCT	83
		MXDT	16
		LCT	1
	Rich off Axis	VLCT	81
		MXDT	11.4
		LCT	6.94
		HCT_HP	0.66
	Crevasse	VLCT	70
		LCT	22
		HCT	8
	Channel 4	VLCT	82.5
		MXDT	10.23
		LCT	5
		HCT	6.27
	Channel axis 3	VLCT	49.74
		MXDT	11.06
		LCT	33.64
		HCT	2.3
		HCT_HP	10.33
	Frontal splay	TRCT	2.46
		VLCT	26.27
		MXDT	33.67
		LCT	13.53
		HCT	13.87
		HCT_HP	12.66

Table 12- Zone C MPS Facies Fraction

**Data selection** **External constraints** **Expert** **Hints**

Training image  
Training image property:  Grid:   
☐ Same zone as primary property

Facies / target fractions  
Global fractions:

	Use	Facies	Training image facies	Fractions
1	<input checked="" type="checkbox"/>	0: offaxis / background	0: offaxis / background	71.49
2	<input type="checkbox"/>	1: Offaxis		
3	<input checked="" type="checkbox"/>	2: Rich Offaxis	2: Rich Offaxis	1.03
4	<input checked="" type="checkbox"/>	3: Crevasse	3: Crevasse	11.08
5	<input checked="" type="checkbox"/>	4: Ch_axis3	4: Ch_axis3	5.39
6	<input type="checkbox"/>	5: Ch_axis		
7	<input type="checkbox"/>	6: Ch_axis1_F		
8	<input checked="" type="checkbox"/>	7: Frontal_splay	7: Frontal_splay	5.40
9	<input type="checkbox"/>	8: Mud filled		
10	<input checked="" type="checkbox"/>	9: channel4_F	9: channel4_F	5.61
11	<input type="checkbox"/>	10: mud filled		
12	<input type="checkbox"/>	11: Channel E north		
13	<input type="checkbox"/>	12: Channel D		

Total % 100.00

**Data selection** **External constraints** **Expert** **Hints**

Proportion / probability constraints  
☐ Vertical proportion functions ☒ Inverse x-axis  
☐ Proportion maps  
☐ Proportion region properties  
☒ Probability properties Weight:

	Facies	Probability properties
1	0: offaxis / background	<input type="checkbox"/> <input type="button" value="Frac RoA_Prob (A,C,CD,D,E)"/>
2	2: Rich Offaxis	<input checked="" type="checkbox"/> <input type="button" value="Frac Ch_Ax_3_Prob (A,C,F)"/>
3	3: Crevasse	<input checked="" type="checkbox"/> <input type="button" value="Frac Fsplay Prob (AB,C)"/>
4	4: Ch_axis3	<input checked="" type="checkbox"/> <input type="button" value="Frac Ch4_F_Prob (C,F)"/>
5	7: Frontal_splay	
6	9: channel4_F	

Table 13 – Pseudozones C - MPS Facies Model (simulation 3)

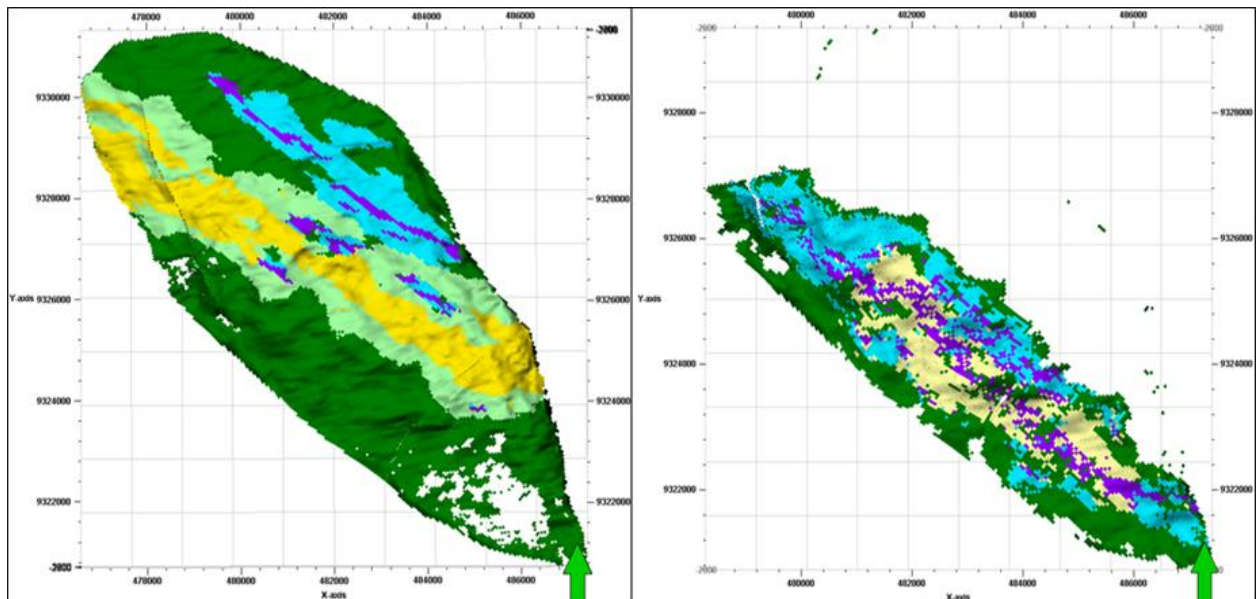


Figure 80 – Pseudozones A and AB – MPS model (simulation 3)

In simulation 3, Pseudozone C is in line with the seismic analysis represented on Figure 64, with the introduction of a levee for the two main channels.

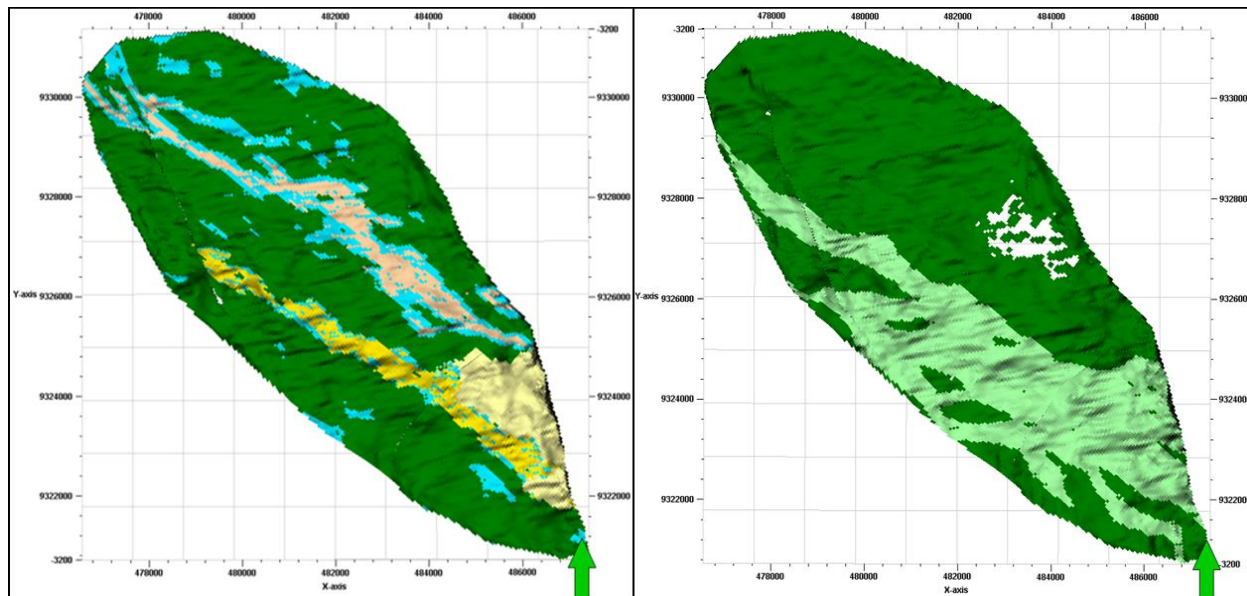


Figure 81 – Zone C and CD – MPS model (simulation 3)

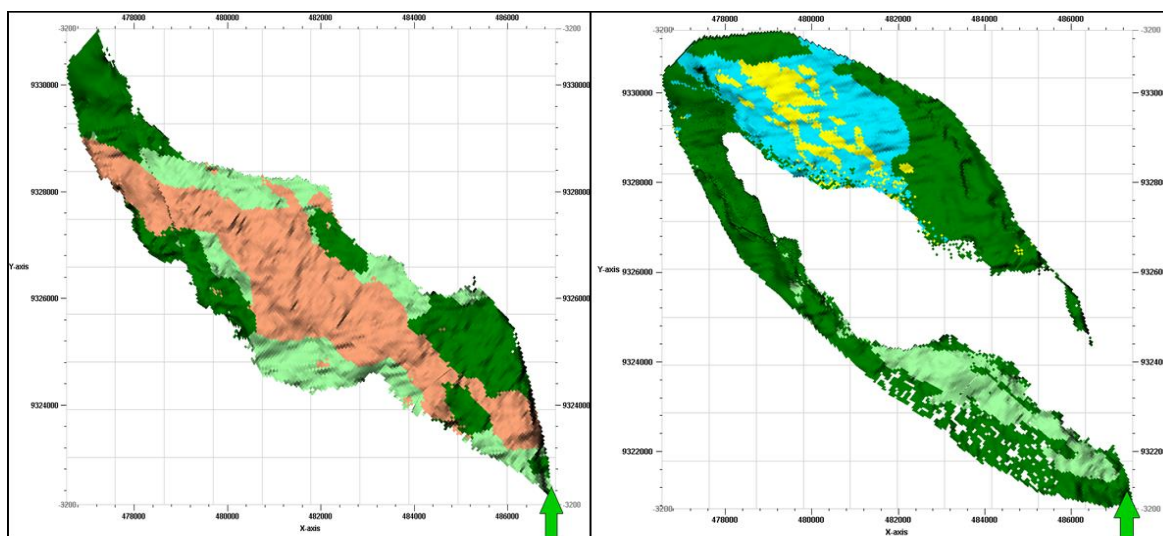


Figure 82 – Pseudozones D and E – MPS model (simulation 3)



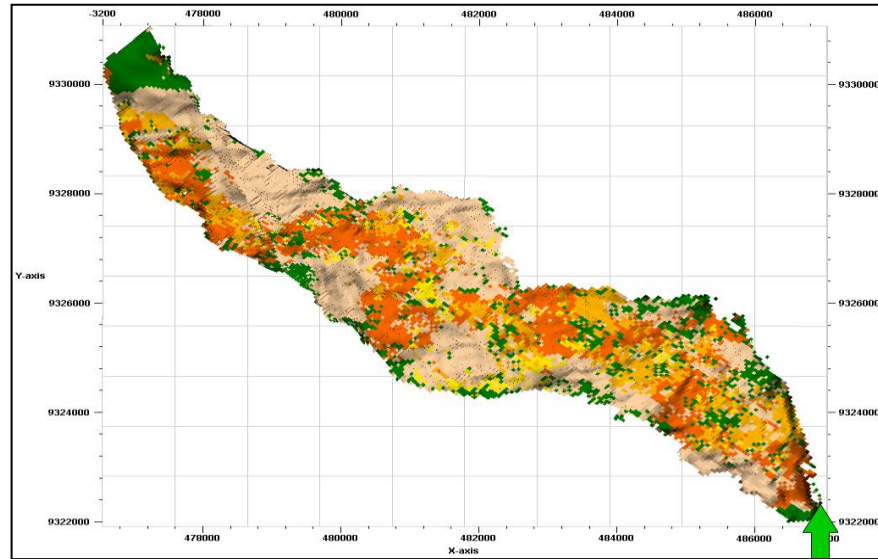


Figure 83 – Pseudozone F – MPS model simulation 3)

- Simulation 4: using the same training image of the simulation 3 and decreasing the weight factor from 0.3 to 0.2. Leading to the following changes:

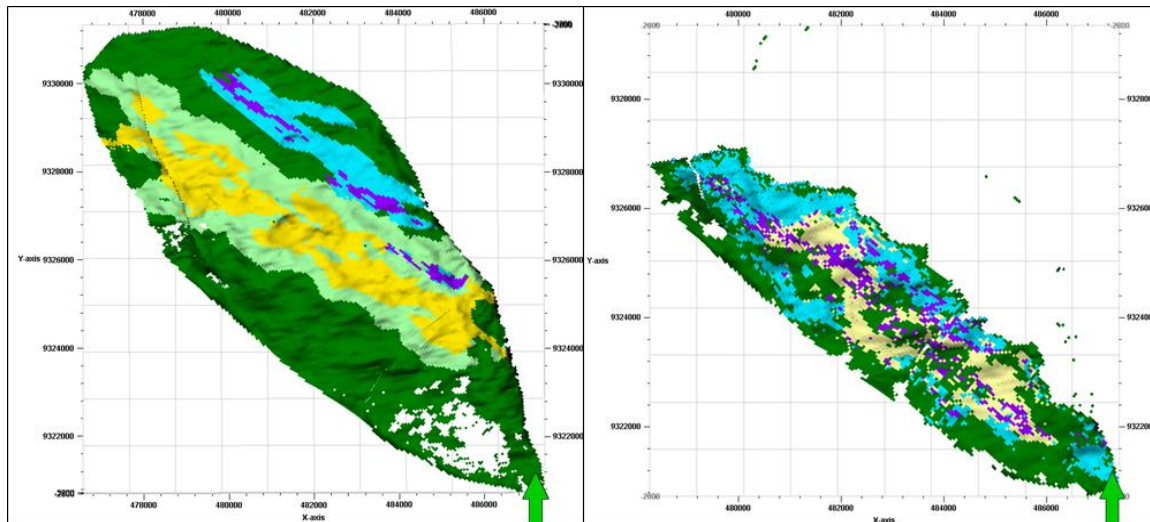


Figure 84 – Pseudozones A and AB – MPS model (simulation 4)

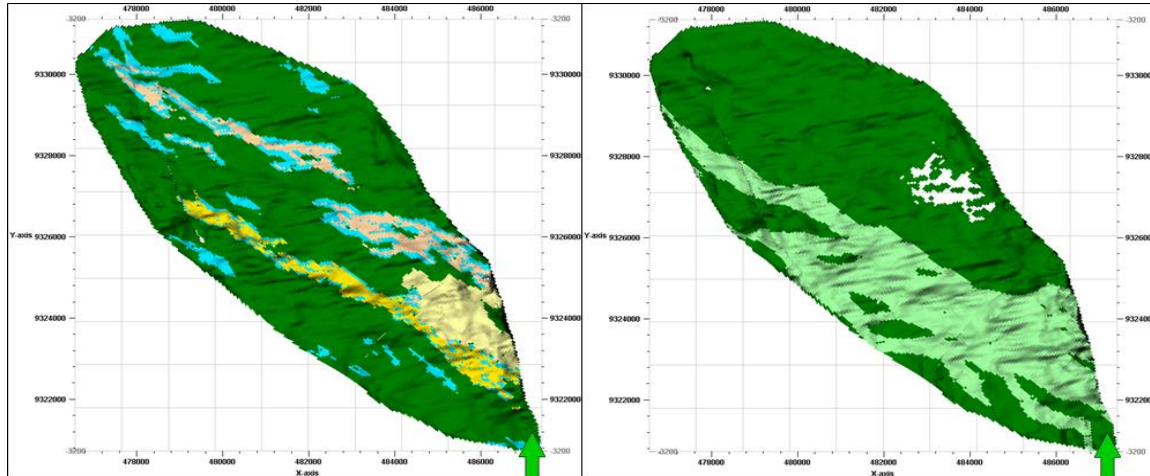


Figure 85 – Pseudozones C and CD – MPS model (simulation 4)

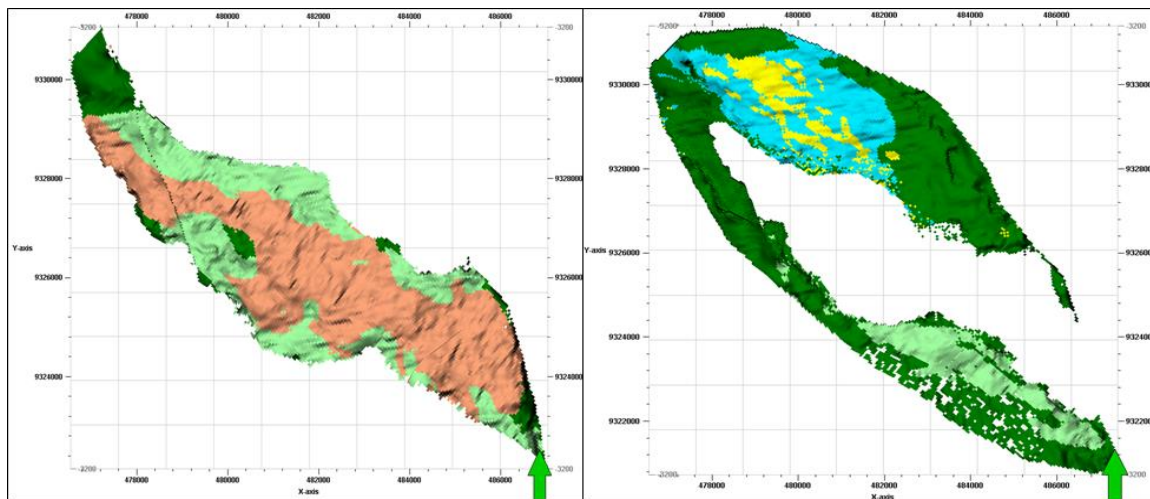


Figure 86 – Pseudozones D and E – MPS model (simulation 4)

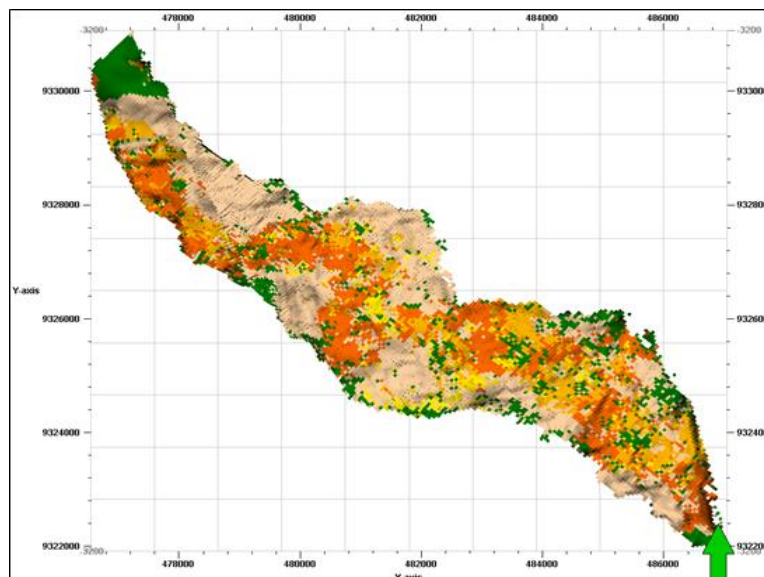


Figure 87 – Pseudozones F – MPS model (simulation 4)

Looking at the simulations above, a reduction of the weight factor leads to an increase of the Training Image effect on the EoD distribution. Moreover it impacts on the channels continuity, as shown in Figure 84, Figure 85, Figure 86 and Figure 87. Looking at the four MPS facies simulations performed above, the stationary data features were compromised, mainly the channels axis continuity.

From the four different simulations performed, simulation 3 captures all the desired geological and sedimentological settings, analyzed on the log facies, amplitude maps and sedimentological model (Figure 88).

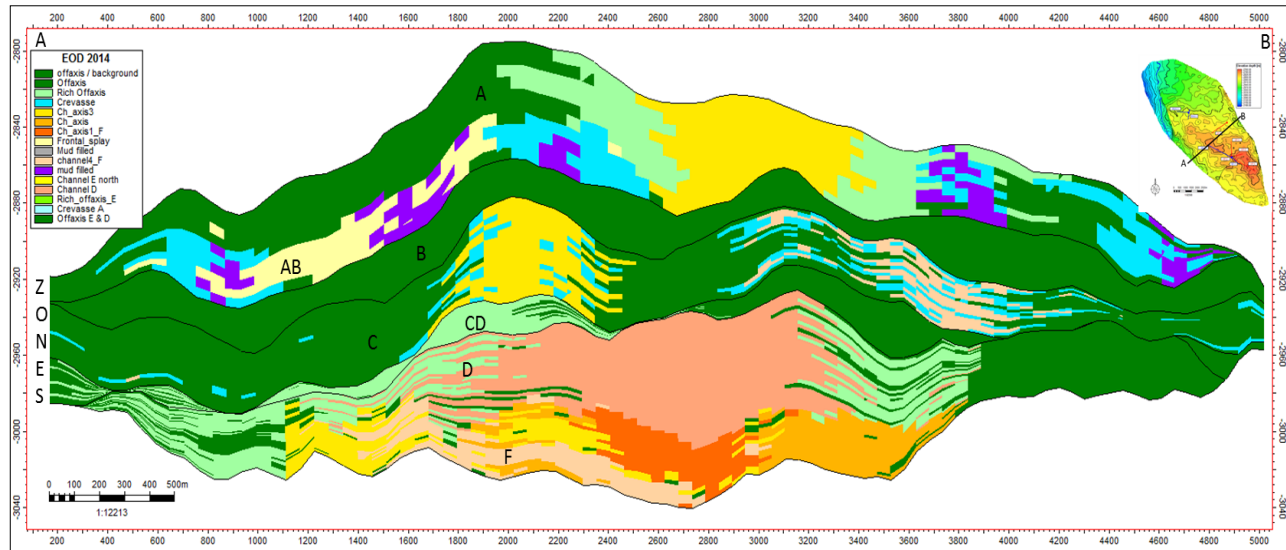


Figure 88 – Cross section – MPS model (simulation 3)

A significant change can be appreciated on the vertical cross section, where the relative geo-body geometry changes progressively to channel like boundary respecting the superposition law as well (see the basal sand level) (Figure 78 and Figure 88).

The results of the MPS modelling in Figure 89 and Figure 90 were achieved after different sensitivities, performed basing on the balance between the Training Images and the external constraints. The heterogeneous channels complex system was gradually represented through the simulations, where the geo-bodies channel shape was achieved.

The model changes in each pseudozone, clearly underline the impact of the multiple point statistics approach, reproducing:

- The geo-body channel like geometry;
- The amalgamated basal channels, as per the sedimentological model;
- The channel erosion, based on the sequence stratigraphy and superposition law.

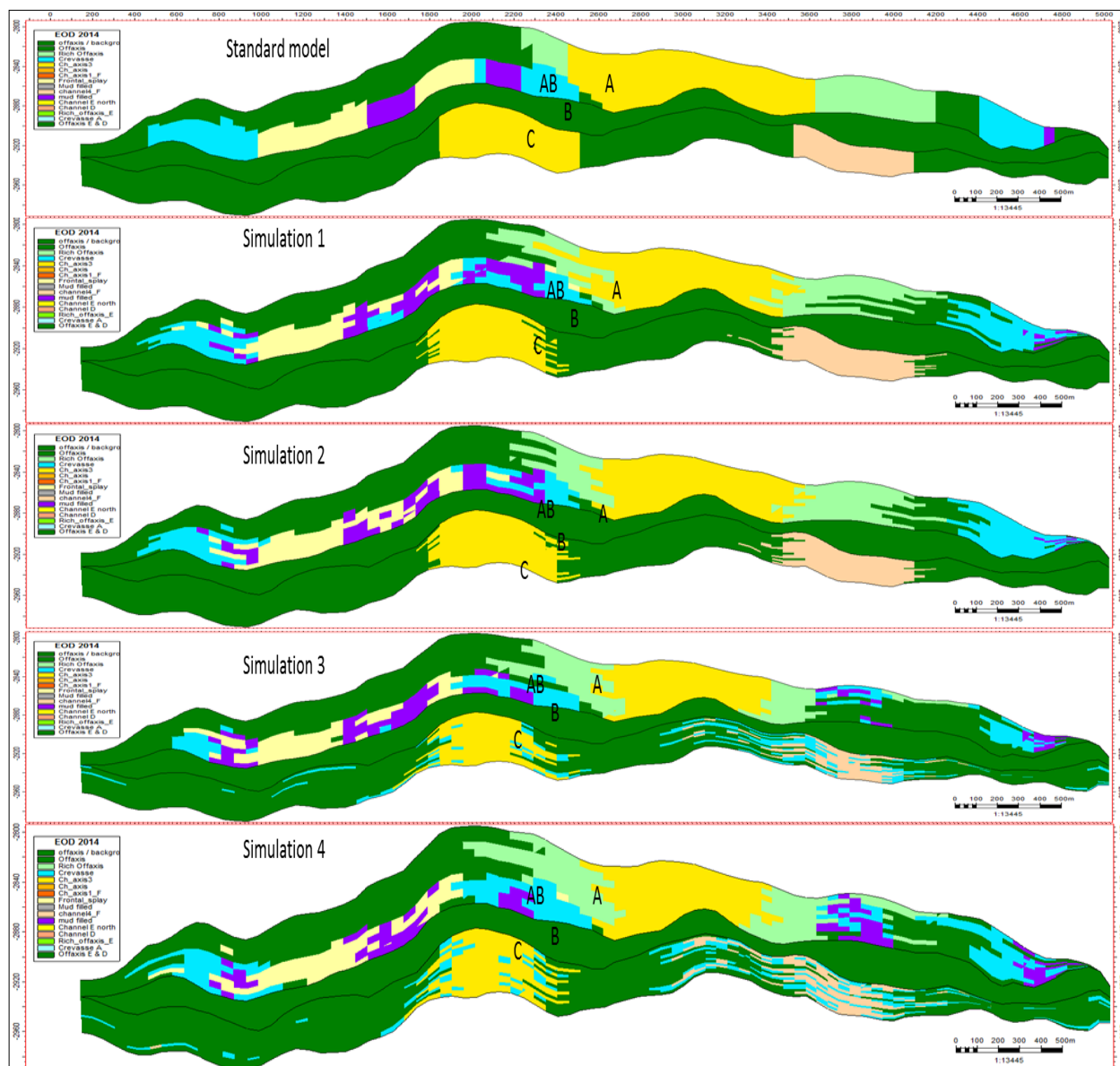


Figure 89 – Pseudozones A and AB and C Cross section – simulation progress



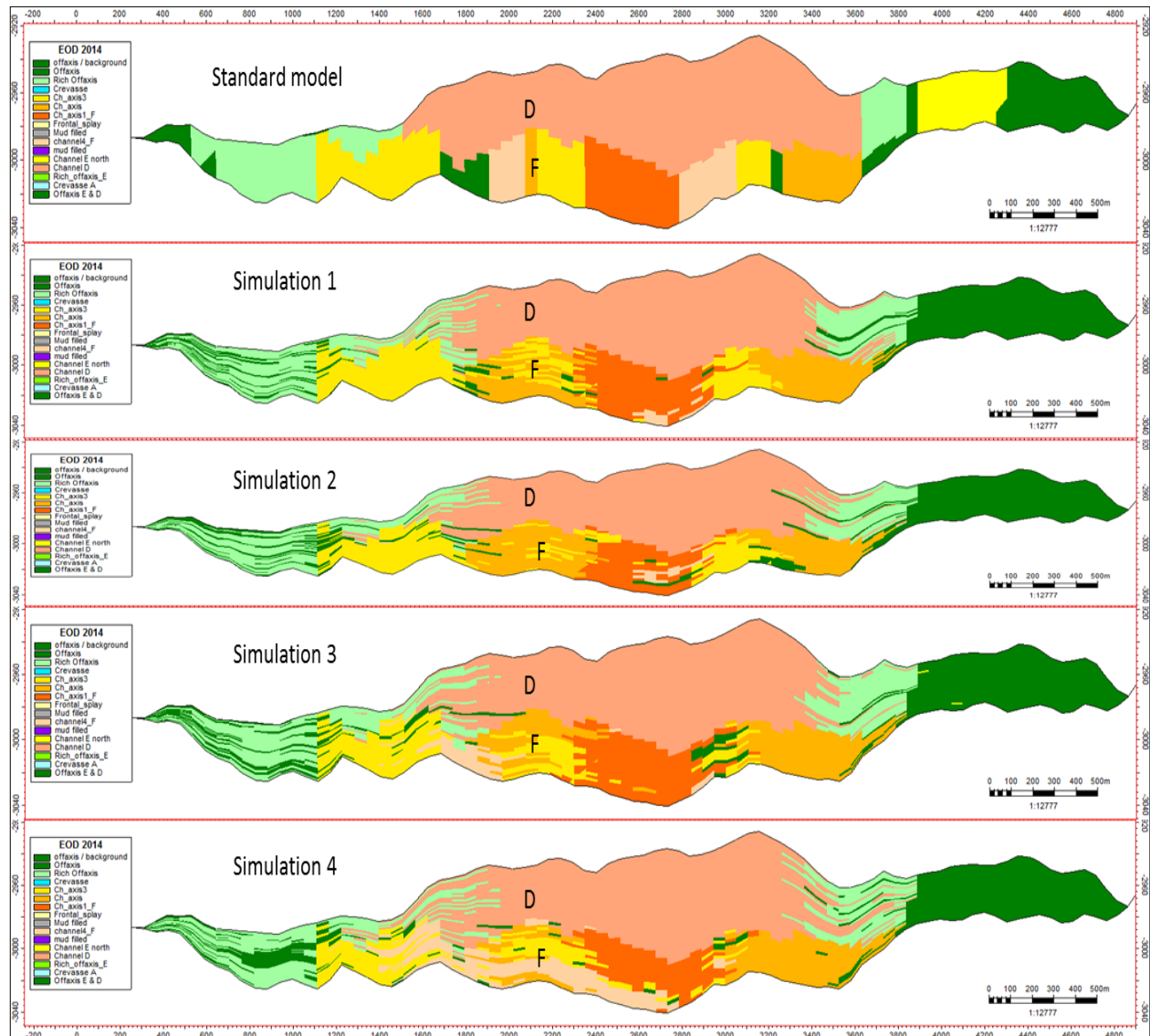


Figure 90 – Pseudozones D and F Cross section – simulation progress

During the MPS EoD (facies) modeling, the different distributions in each zone were analyzed, having the standard model facies fractions as reference.

Considering the Training Image used in the MPS and the sedimentological understanding of the channel shapes, an average gradual decrease of the channel (EoDs) facies fractions within each zone and a relative increase in the off-axis facies fraction were experienced, in line with expectations Figure 28.

In the Pseudozone C, the Offaxis facies fraction has been reduced, due to the new crevasse facies introduction. It was added as levee to the pre-existing channels (channel 4 and channel axis 3), basing on the analysis of the Vp/Vs amplitude maps (Figure 64).

The final facies fractions for each pseudozone in the reference model (standard model) and in the four MPS facies simulation models performed are reported below (Table 14).

Standard model			Simulation 1			Simulation 2			Simulation 3			Simulation 4		
Code	Name	%	Code	Name	%	Code	Name	%	Code	Name	%	Code	Name	%
0	offaxis / background	16.46	1	Offaxis	50.92	1	Offaxis	50.65	0	offaxis / background	49.75	0	offaxis / background	49.78
1	Offaxis	26.50	2	Rich Offaxis	20.64	2	Rich Offaxis	20.90	1	Offaxis	0.06	1	Offaxis	0.06
2	Rich Offaxis	22.62	3	Crevasse	7.69	3	Crevasse	7.53	2	Rich Offaxis	21.02	2	Rich Offaxis	21.20
3	Crevasse	9.89	4	Ch_axis3	19.15	4	Ch_axis3	19.18	3	Crevasse	7.73	3	Crevasse	7.63
4	Ch_axis3	22.34	10	mud filled	1.59	10	mud filled	1.74	4	Ch_axis3	18.83	4	Ch_axis3	18.67
10	mud filled	2.19							10	mud filled	2.62	10	mud filled	2.65
AB														
Code	Name	%	Code	Name	%	Code	Name	%	Code	Name	%	Code	Name	%
0	offaxis / background	6.17	0	offaxis / background	29.49	0	offaxis / background	29.73	0	offaxis / background	43.19	0	offaxis / background	43.17
1	Offaxis	15.47	3	Crevasse	28.13	3	Crevasse	28.10	3	Crevasse	24.69	3	Crevasse	24.92
3	Crevasse	38.86	7	Frontal_splay	27.50	7	Frontal_splay	27.60	7	Frontal_splay	20.50	7	Frontal_splay	20.53
7	Frontal_splay	29.88	10	mud filled	14.88	10	mud filled	14.57	10	mud filled	11.61	10	mud filled	11.37
10	mud filled	9.62												
C														
Code	Name	%	Code	Name	%	Code	Name	%	Code	Name	%	Code	Name	%
0	offaxis / background	54.38	0	offaxis / background	80.05	0	offaxis / background	80.14	0	offaxis / background	71.53	0	offaxis / background	71.69
1	Offaxis	23.35	1	Offaxis	0.02	1	Offaxis	0.02	1	Offaxis	0.02	1	Offaxis	0.02
2	Rich Offaxis	1.00	2	Rich Offaxis	0.07	2	Rich Offaxis	0.04	2	Rich Offaxis	0.11	2	Rich Offaxis	0.08
4	Ch_axis3	5.89	4	Ch_axis3	5.83	4	Ch_axis3	5.67	3	Crevasse	11.33	3	Crevasse	11.35
7	Frontal_splay	5.53	7	Frontal_splay	5.59	7	Frontal_splay	5.44	4	Ch_axis3	5.62	4	Ch_axis3	5.57
9	channel4_F	9.86	9	channel4_F	8.44	9	channel4_F	8.70	7	Frontal_splay	6.08	7	Frontal_splay	5.63
									9	channel4_F	5.31	9	channel4_F	5.66
CD														
Code	Name	%	Code	Name	%	Code	Name	%	Code	Name	%	Code	Name	%
0	offaxis / background	53.04	0	offaxis / background	69.29	0	offaxis / background	69.31	0	offaxis / background	69.31	0	offaxis / background	69.31
1	Offaxis	7.87	1	Offaxis	0.01	1	Offaxis	0.01	1	Offaxis	0.01	1	Offaxis	0.01
2	Rich Offaxis	39.09	2	Rich Offaxis	30.70	2	Rich Offaxis	30.68	2	Rich Offaxis	30.68	2	Rich Offaxis	30.68
D														
Code	Name	%	Code	Name	%	Code	Name	%	Code	Name	%	Code	Name	%
0	offaxis / background	4.02	0	offaxis / background	18.97	0	offaxis / background	18.97	0	offaxis / background	19.09	0	offaxis / background	19.06
1	Offaxis	1.30	2	Rich Offaxis	27.21	2	Rich Offaxis	27.23	2	Rich Offaxis	28.53	2	Rich Offaxis	28.27
2	Rich Offaxis	19.21	12	Channel D	53.82	12	Channel D	53.80	12	Channel D	52.37	12	Channel D	52.67
12	Channel D	75.47												
E														
Code	Name	%	Code	Name	%	Code	Name	%	Code	Name	%	Code	Name	%
0	offaxis / background	28.14	0	offaxis / background	55.47	0	offaxis / background	55.02	0	offaxis / background	51.26	0	offaxis / background	50.81
1	Offaxis	15.64	1	Offaxis	0.00	1	Offaxis	0.00	1	Offaxis	0.00	1	Offaxis	0.00
2	Rich Offaxis	17.79	2	Rich Offaxis	14.90	2	Rich Offaxis	14.80	2	Rich Offaxis	15.02	2	Rich Offaxis	14.92
3	Crevasse	19.22	3	Crevasse	16.73	3	Crevasse	16.84	3	Crevasse	23.58	3	Crevasse	23.96
6	Ch_axis1_F	0.04	11	Channel E north	12.90	11	Channel E north	13.34	11	Channel E north	10.13	11	Channel E north	10.30
11	Channel E north	19.17												
F														
Code	Name	%	Code	Name	%	Code	Name	%	Code	Name	%	Code	Name	%
0	offaxis / background	4.03	0	offaxis / background	12.02	0	offaxis / background	11.97	0	offaxis / background	13.98	0	offaxis / background	13.66
1	Offaxis	4.57	4	Ch_axis3	6.00	4	Ch_axis3	6.20	4	Ch_axis3	4.12	4	Ch_axis3	4.62
4	Ch_axis3	5.70	5	Ch_axis	16.02	5	Ch_axis	16.02	5	Ch_axis	16.65	5	Ch_axis	16.20
5	Ch_axis	15.34	6	Ch_axis1_F	26.73	6	Ch_axis1_F	26.55	6	Ch_axis1_F	25.93	6	Ch_axis1_F	26.29
6	Ch_axis1_F	29.91	9	channel4_F	39.24	9	channel4_F	39.26	9	channel4_F	39.31	9	channel4_F	39.24
9	channel4_F	40.44												

Table 14- Geo-bodies Facies Fraction per zone for all simulations



### 3.2.4 SIS Facies distribution property model

The lithological facies distribution was realized applying the Sequential Indicator Simulation (SIS) algorithm. For the off-axis/background facies a constant value (VLCT) was assigned. And for the other facies derived from the cluster analysis Figure 9, the same parameters and process as per the standard model were applied.

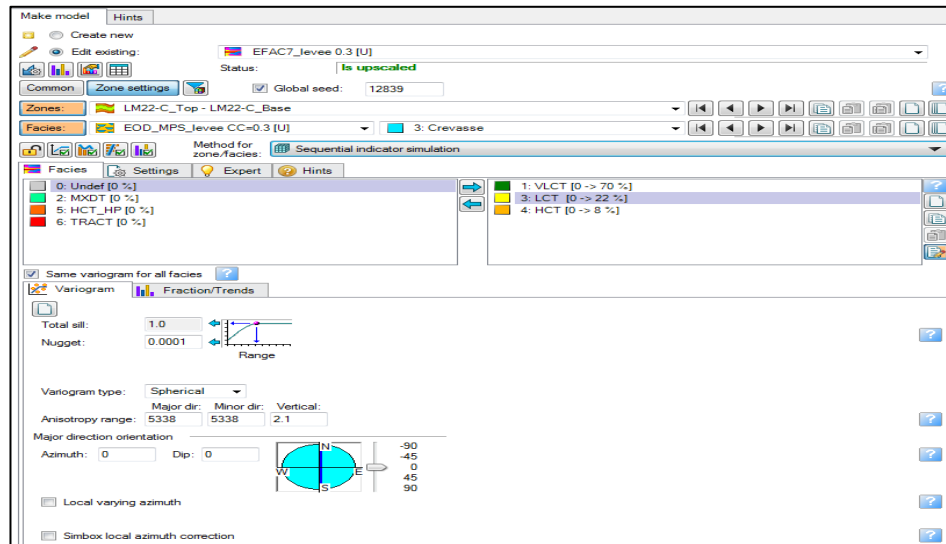


Figure 91 – Facies model settings

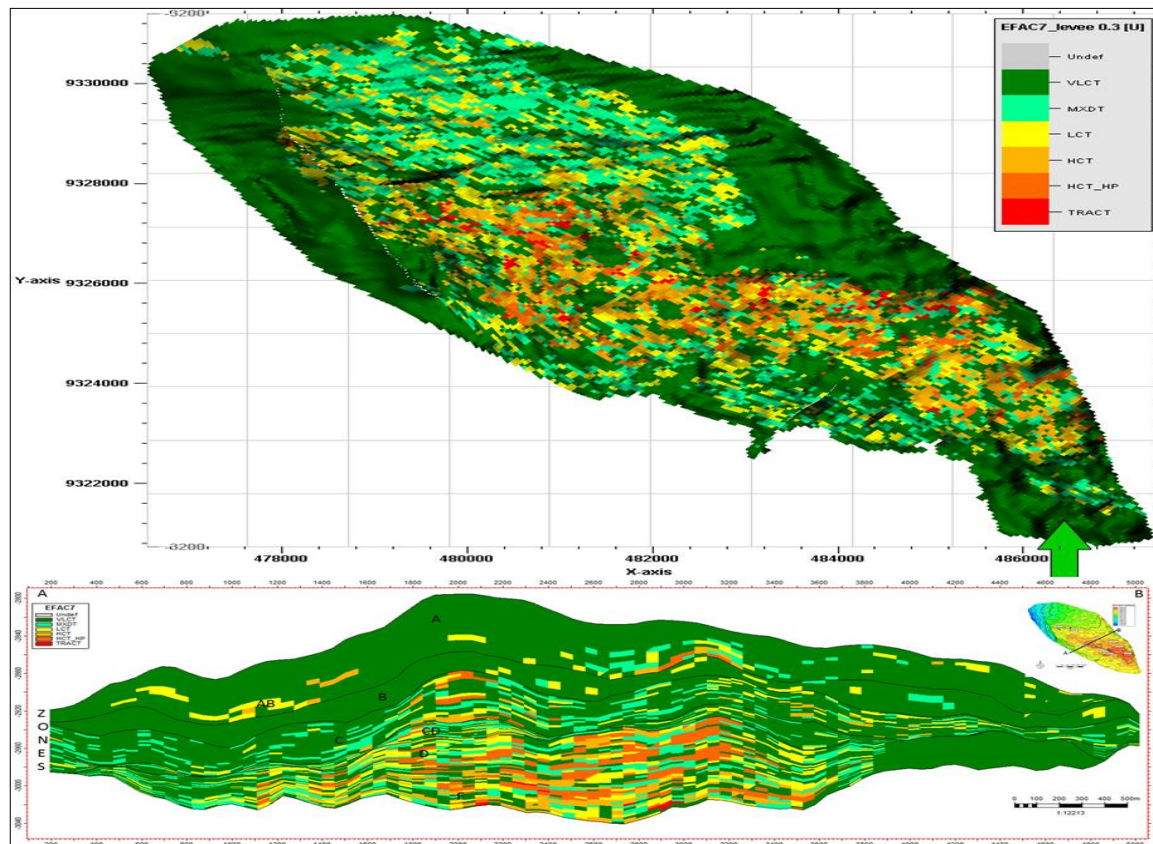


Figure 92 – Facies distribution result

### 3.2.5 SGS Petrophysical properties model

The Sequential Gaussian Simulation (SGS) petrophysical modeling, which involved NTG, Porosity and Water Saturation, followed the same process (by facies) and parameters as the standard model.

NTG was modeled considering the facies distribution that is represented above (Figure 92). It was performed by means of the Gaussian random function simulation algorithm (GRFS) for VLCT, MXDT and LCT, while for HCT, HCT\_HP and TRACTION a constant value of one was assigned.

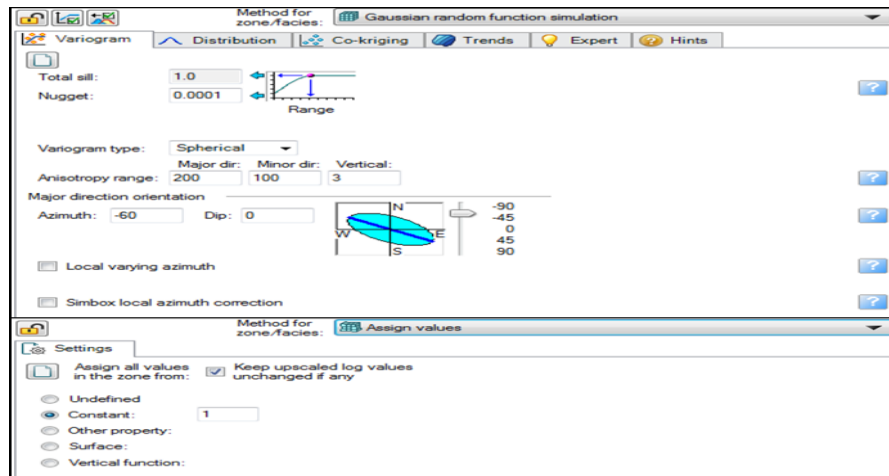


Figure 93 – NTG Properties distribution settings

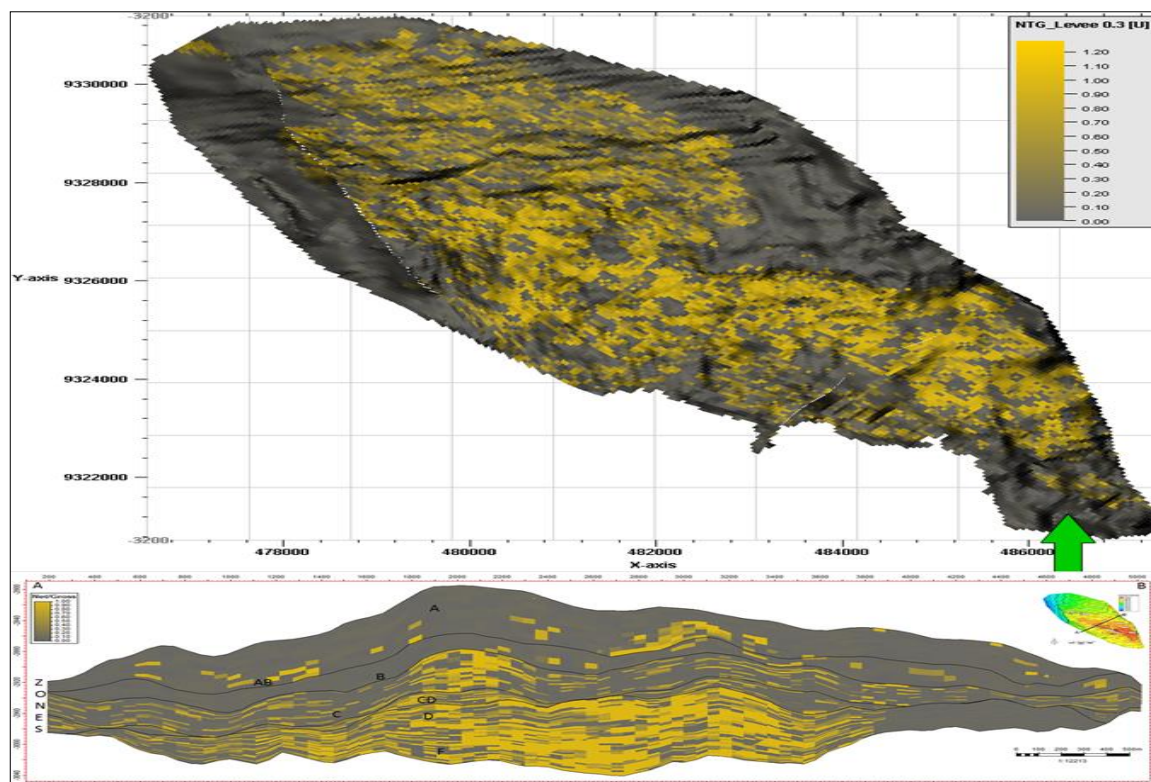


Figure 94 – NTG distribution



Porosity, the second element on the petrophysical modeling workflow, was modeled by means of the GRFS algorithm. The NTG volume modeled above was used as collocated co-Kriging property (Figure 94).

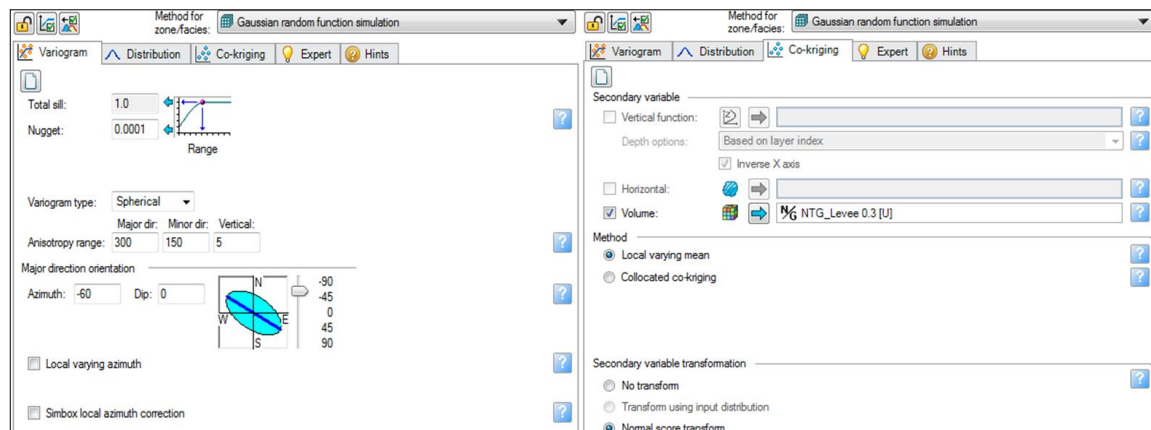


Figure 95 – Porosity Properties distribution settings

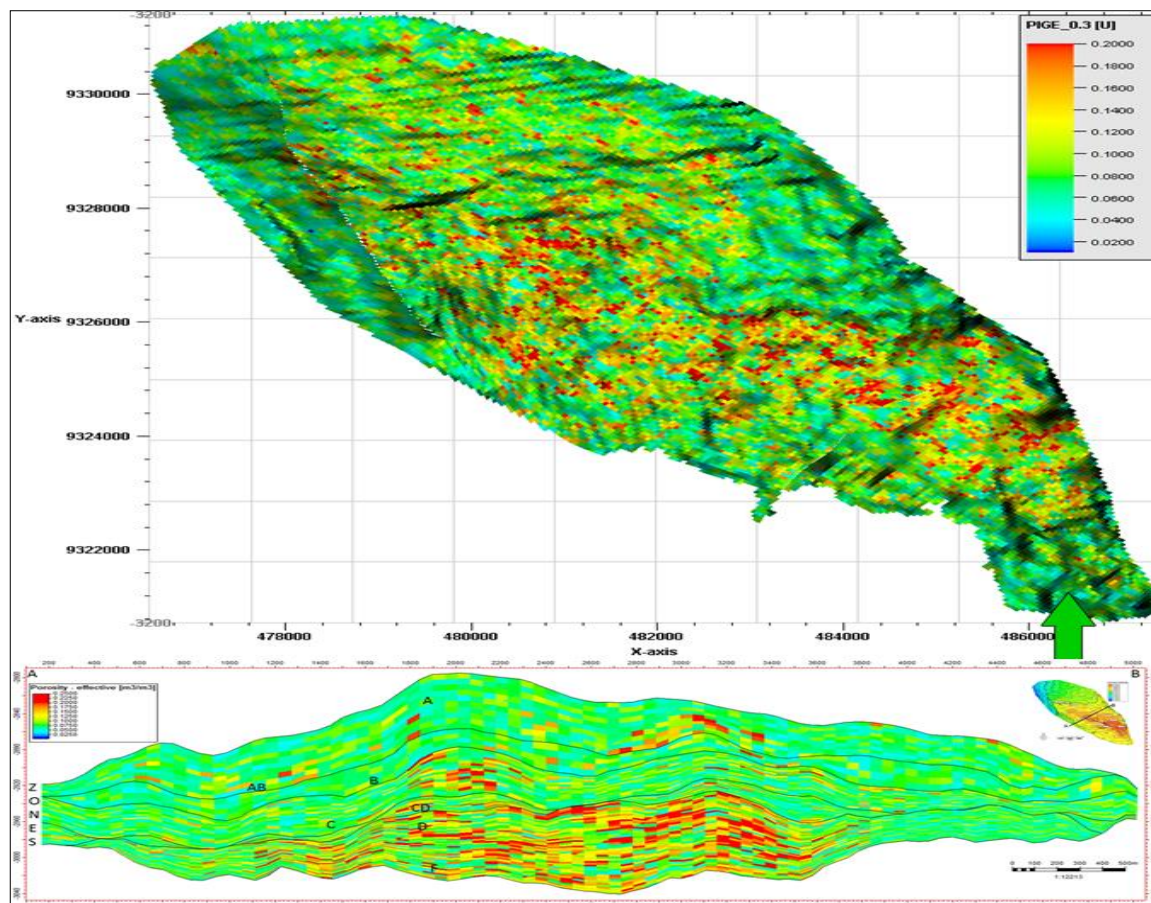


Figure 96 – Porosity distribution

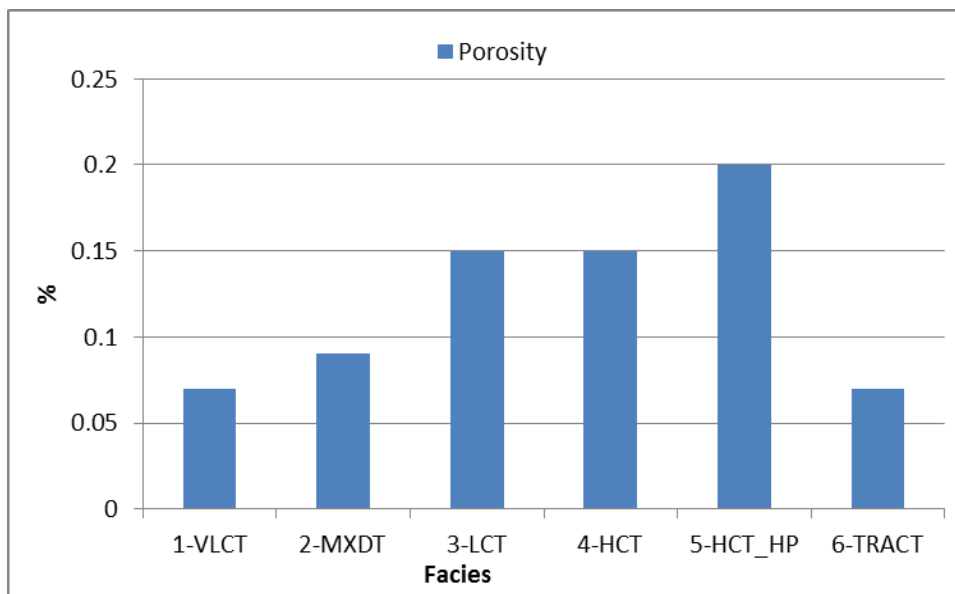


Figure 97 – Porosity model distribution per facies

The Water saturation distribution was performed by means of the GRFS algorithm, having as collocated co-Kriging property the Porosity (Figure 96).

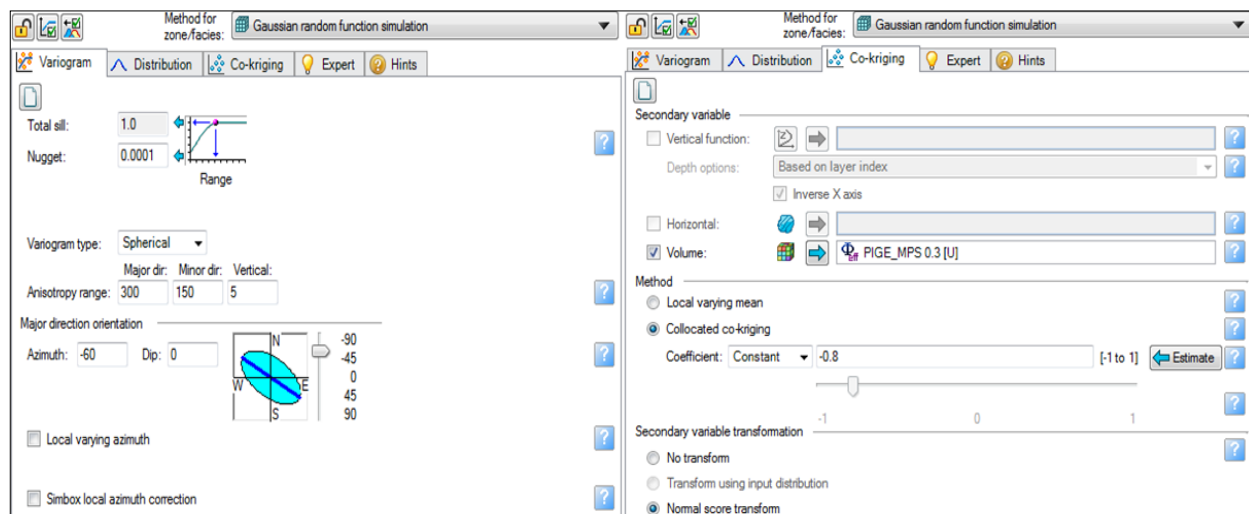


Figure 98 – Porosity Properties distribution settings

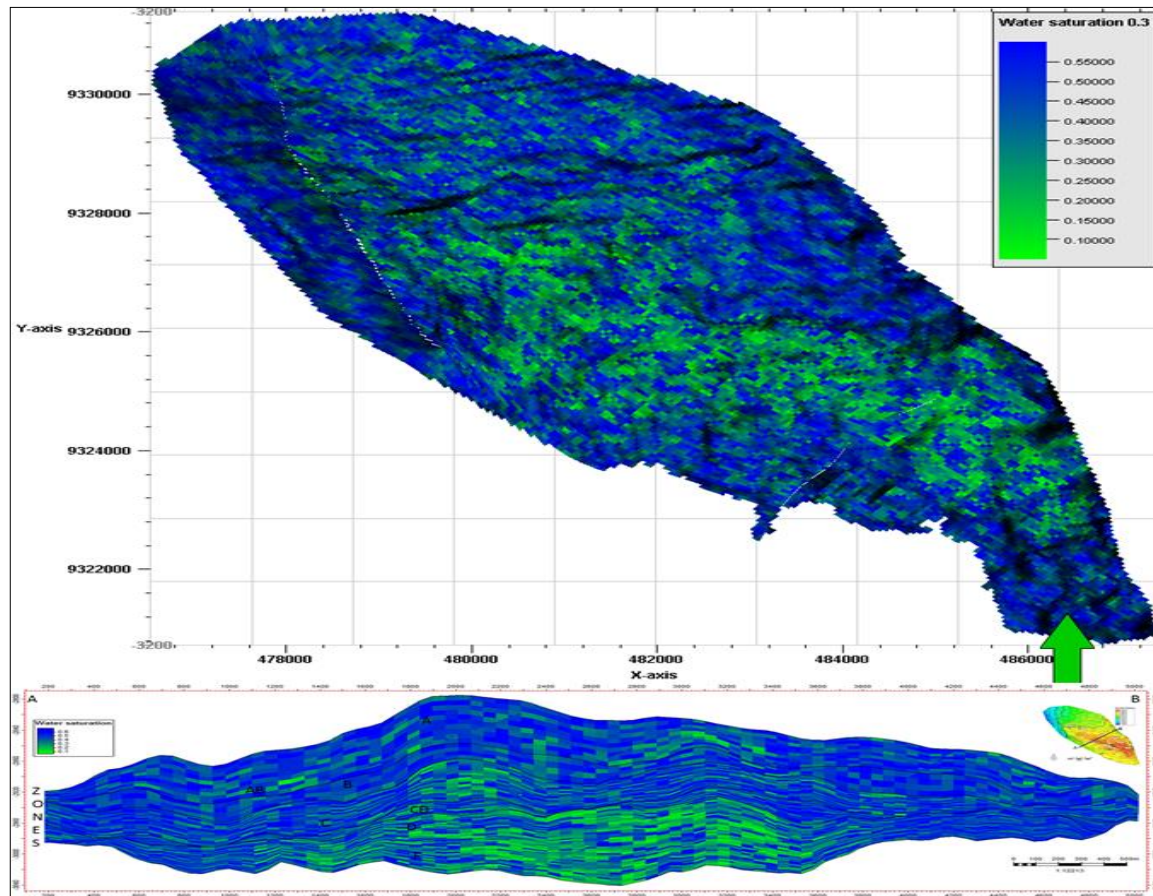


Figure 99 – Water Saturation distribution

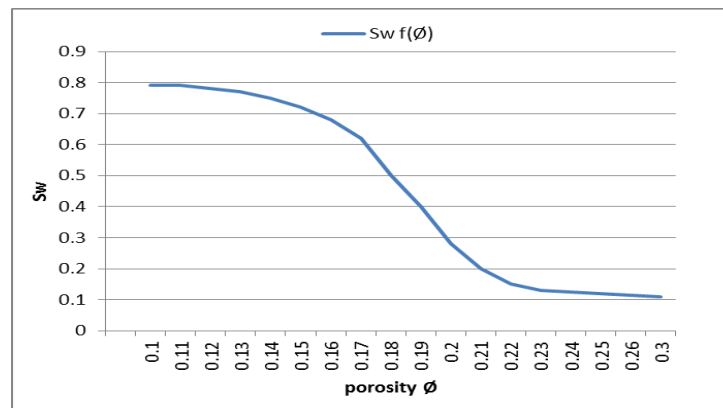


Figure 100 – Water saturation changes as a function of the porosity

The water saturation changes as a function of the porosity (Figure 100), when the porosity increases the water saturation decreases.

On the water saturation histogram (Figure 101), the  $Sw$  classes of the standard model are related with the ones coming from the four simulations performed following the principle shown in Figure 100.



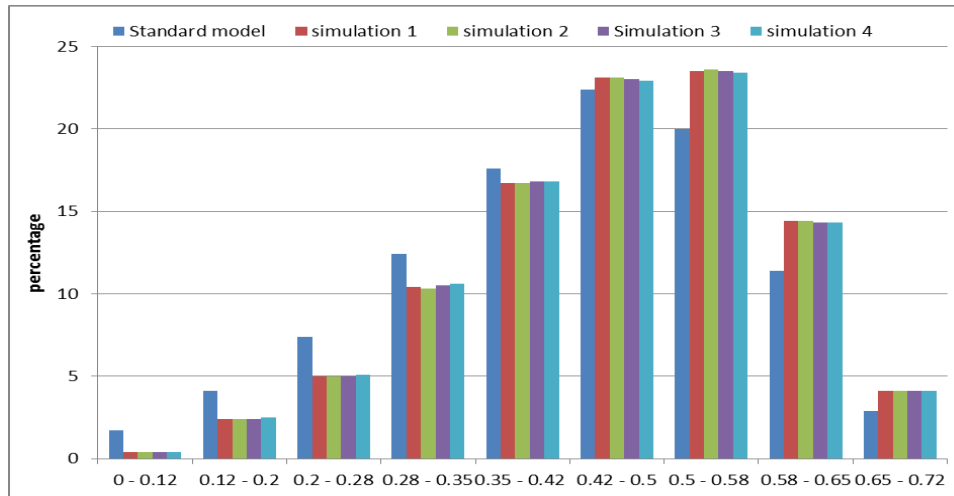


Figure 101 – Water Saturation evolution analysis

The facies distribution and NTG distribution are appreciated bellow, confirming the direct relation with the EoD Definitions, for the Standard model Figure 102 and for the MPS model Figure 104.

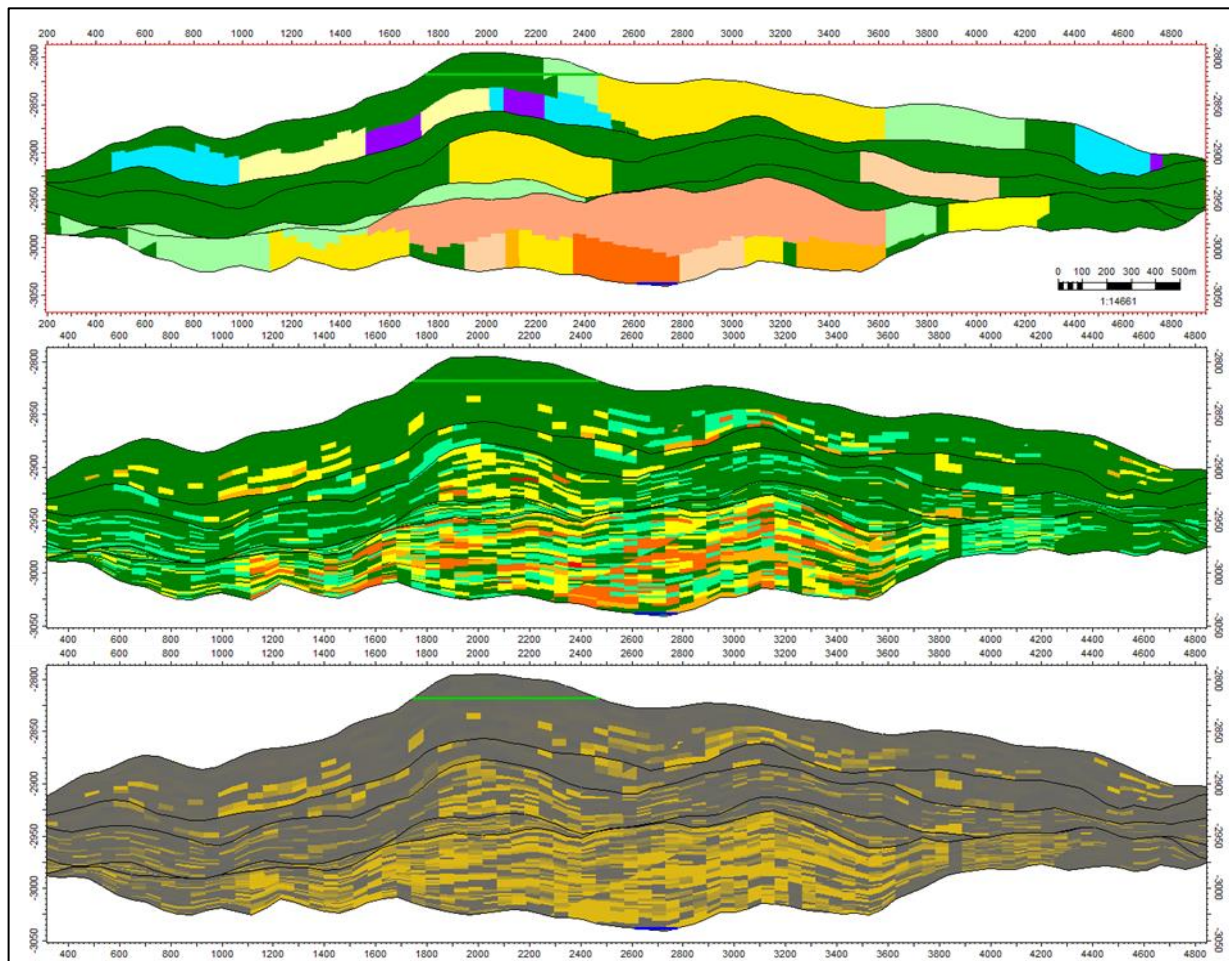


Figure 102 –standard model EoD, facies and NTG distribution



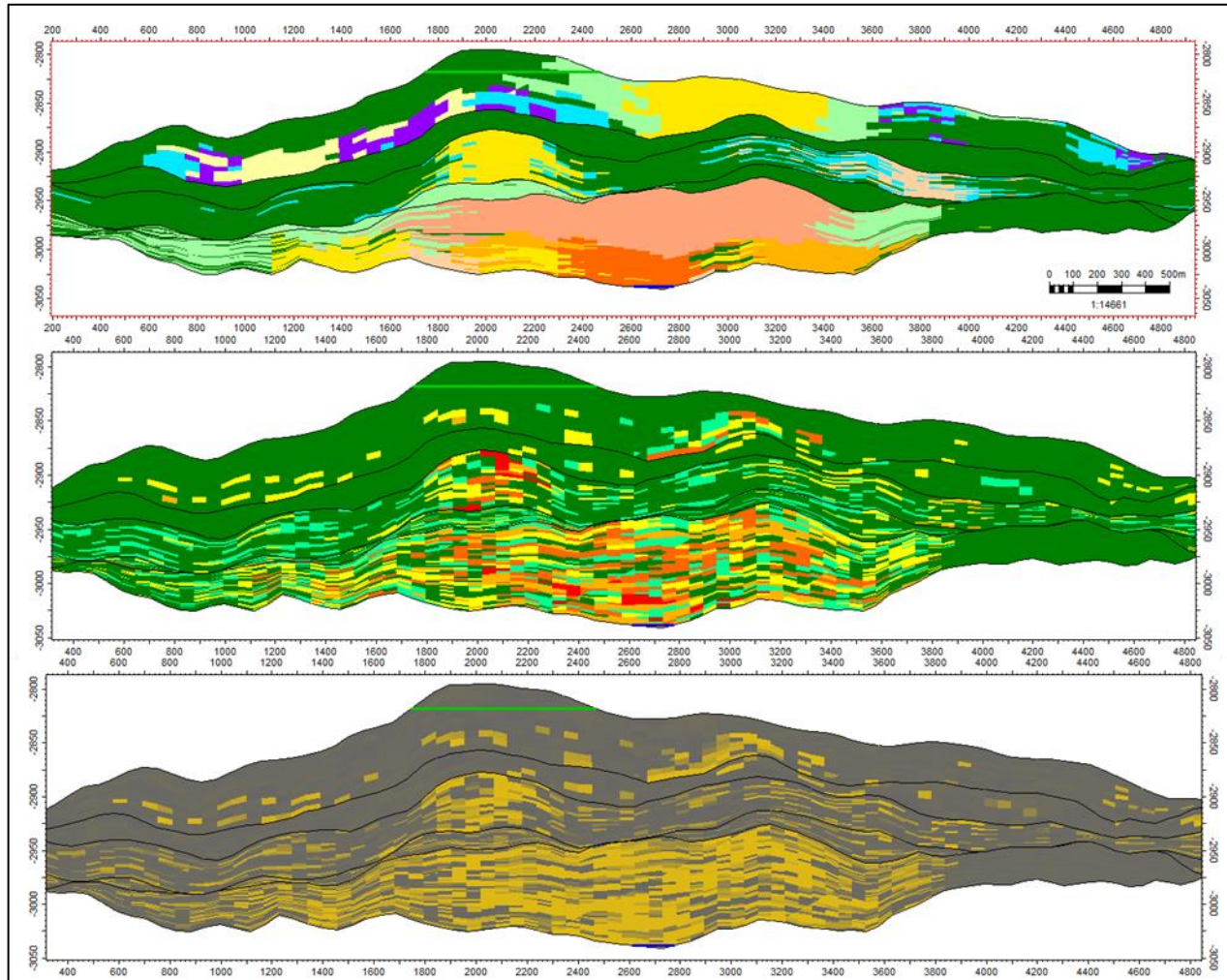


Figure 103 –MPS model EoD, facies and NTG distribution

### 3.2.6 Volumetric (STOIIP)

The volumetric calculation is the last step of the static modelling workflow summarized here below:

- EOD map analysis: leading to both the TIs and the EoD probability volumes generation;
- Geo-body (EoDs) simulation (probabilistic approach): by means of the Multiple Point Statistics (MPS) algorithm;
- Litho-Facies simulation SIS (Reservoir Characterization): based on the modeled geobodies, following the facies modelling workflow (algorithm and parameters) of the standard model;
- Petrophysical model: NTG, Porosity and Water saturation distributed as per the standard model workflow (algorithm and parameters).

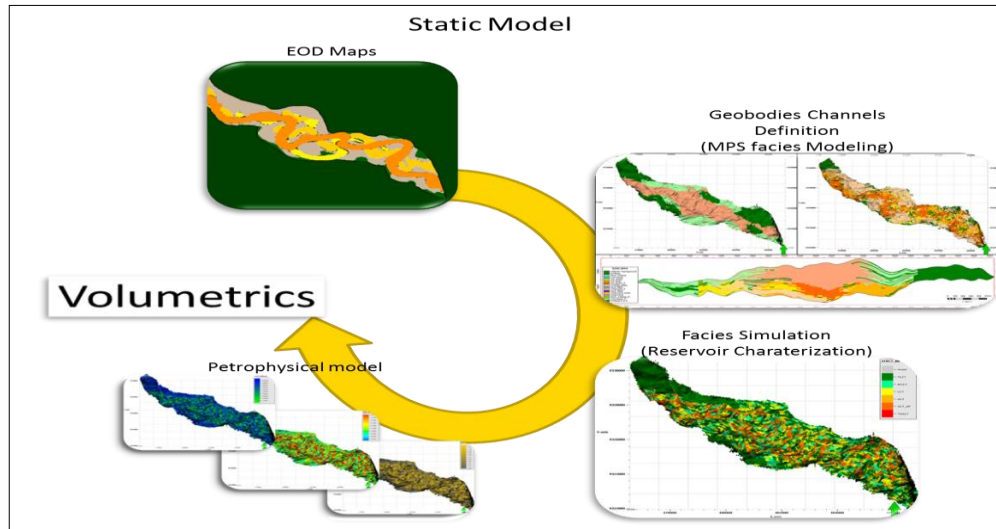


Figure 104 – Petrel MPS static model workflow

For each one of the sensitivity performed on the EoD model, the facies and petrophysical property distributions were carried out and finally a STOIIP value extracted by zone.

The volume calculation considers the same fluid contacts of the standard model: gas-oil contact at -2818 mssl, oil-water contact water at -3038m ssl and the perched water contact at 2997.5 mssl. The table here below shows the STOOIP analysis considering the contribution from each pseudozones.

STOIIP[*10 <sup>6</sup> STB]					
Pseudozones	Standard simulation	Simulation 1	Simulation 2	Simulation 3	Simulation 4
Zone A	51.03	45.78	43.66	40.79	40.43
Zone AB	32.8	29.74	29.7	24.78	25.18
Zone B	43.53	43.23	43.23	43.23	43.53
Zone C	105.25	108.53	105.69	112.29	113.37
Zone CD	72.57	64.83	63.97	64.1	63
Zone D	191.86	157.24	154.5	156.57	157.65
Zone F	116.49	112.01	110.1	108.29	108.67
Zone E	38.57	28	28.05	28.74	29.06
Total STOIIP	652.1	589.36	578.9	578.79	580.89

Table 15 - STOOIP per pseudozones

### 3.2.7 Static volumes comparison (Current vs. MPS workflow)

Below is illustrated the STOIIP variation in each pseudozone: for the reference case (standard model) and the four simulated MPS models.

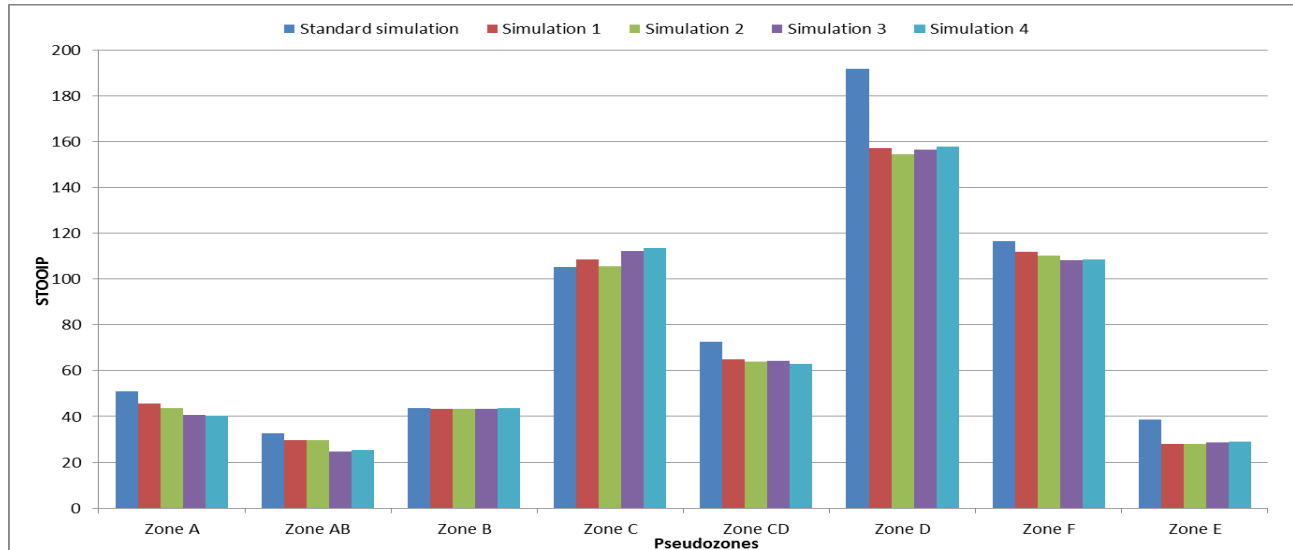


Figure 105 – STOIIP analysis per pseudozone

The STOIIP contribution in each pseudozone is described here below:

- Pseudozone A: a gradual decrease in the STOIIP from the standard model to the fourth simulation from 51 MMSTB to 40.4 MMSTB with a standard deviation up to - 20% from the standard model STOIIP;
- Pseudozone AB: a gradual decrease is experienced as well; simulation one and two with very low differences. Zone AB represents a mud filled channels with a vast levee, with poor sand facies. Low changes are expected, in fact STOIIP variation is from 32.8 MMSTB to 25 MMSTB, standard deviation is -24% from the reference model;
- Pseudozone B: an assign value as VLCT facies was performed (mostly shale) in this zone, as per the standard model. No simulation was performed;
- Pseudozone C: a gradual increase on the STOIIP; on simulation 3 and 4 there was a reduction of the off-axis facies, due to the introduction of levee to the two sandy channels facies, with positive variation on the STOIIP from 105 MMSTB to 113 MMSTB, representing a standard deviation of +8% from the reference STOIIP (standard model);
- Pseudozone CD: STOIIP having a quite smooth variation through the different simulations, the main facies is reach off-axis;
- Pseudozone D: identified by an amalgamated channels facies, represented on Figure 90, and with a high STOIIP. Standard deviation is around 19% from the mean reference standard model that is in line with the geo-body channel definitions from the Training Image;

- Pseudozone F: an amalgamation of channels, respecting the superposition principle, which represents a cycle of stacked channels (sandy facies);
- Pseudozone E: the northern section of the field, characterized by a vast crevasse and a channel EoD. This level has a high standard deviation of 27% from the reference STOIP, corresponding to a variation from 38 MMSTB to 28 MMSTB.

	Simulaion 1	Simulation 2	Simulation 3	Simulation 4
Zone A	-10.288	-14.442	-20.067	-20.772
Zone AB	-9.329	-9.451	-24.451	-23.232
Zone B	-0.689	-0.689	-0.689	0.000
Zone C	3.116	0.418	6.689	7.715
Zone CD	-10.666	-11.851	-11.671	-13.187
Zone D	-18.044	-19.473	-18.394	-17.831
Zone F	-3.846	-5.485	-7.039	-6.713
Zone E	-27.405	-27.275	-25.486	-24.656

Table 16- Pseudozones STOIP St. Deviation from the standard model

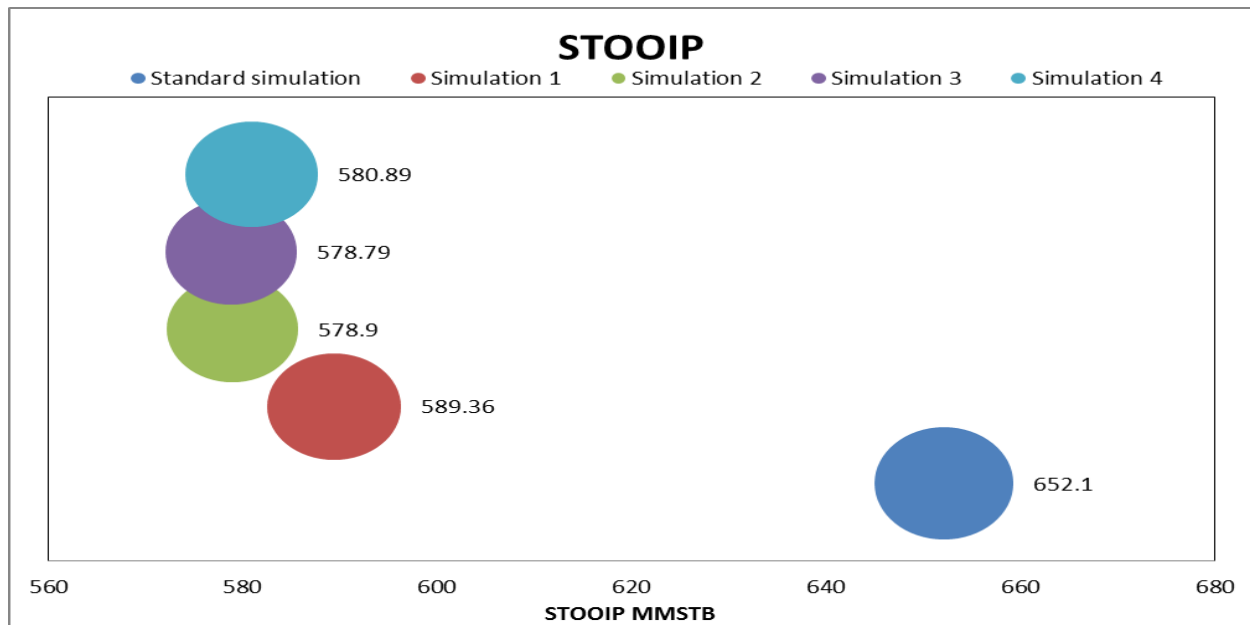


Figure 106 – STOOIP analysis

STOIP[*10 <sup>6</sup> STB]					
STOIP	Standard model	Simulation 1	Simulation 2	Simulation 3	Simulation 4
	652.1	589.36	578.9	578.79	580.89
STOIP (%)	100.00	90.38	88.77	88.76	89.08
ST. Deviation		9.62	11.23	11.24	10.92

Table 17- STOOIP Standard Deviation from the reference standard model

The STOIP differences and the standard deviation from the reference STOIP can be appreciated in Table 17.



## 4 UNCERTAINTY AND OPTIMIZATION ANALYSIS

Out of the different MPS simulations performed, the third one best represents the geological settings and the sedimentological model. It is the coupled effect of the combination between the most representative training image and the right weight correction balance.

A risk analysis has been performed, on the basal levels, representing the amalgamated complex channels system. It has to be considered that all the wells found massive sand facies in level D and F and all the wells were completed in the these pseudozones (D and F).

Computational capability available to run different sensitivities on a reasonable time frame (few hours ~70 hours) is a constraint, which does not allow running a risk analysis on the full model, including all the pseudozones (it could take several days).

### 4.1 Risk analysis (RA) purpose

The purpose of the RA is to analyze the selected EoDs/Facies ratio of the main channels and its impact on the STOIP. This has been performed in the standard model and in the MPS reference model (3rd simulation model).

### 4.2 Standard model RA workflow

A set of the 6 channels, representing the amalgamated basal sand level D, E and F, was selected and the facies fraction of the referred EoDs was analyzed.

Eod\Facies	VLCT	MXDT	LCT	HCT	HCT_HP	TRAC
CH_AXIS_3	27	15	26	10	22	
CH_AXIS	18.56	13.93	14.11	28.66	23.26	1.48
CH_AXIS_1F	12.97	16.18	9.71	39.69	14.26	7.19
CHANNEL4_F	45	15	25	15		
CHANNEL_E_N	20.3	56.39	23.31			
CHANNEL_D	26.5	17	19	10.5	27	

Table 18- RA variables to be simulated

The FF reference variable (Mode) in each EoDs was defined, selecting the available best sandy facies (high concentration turbidity\_ high porosity (HCT\_HP)). If this reference facies is not present in an EoD the second best facies is selected, as highlighted in bold in Table 18.

The uncertainty analysis was made on the main FF variable (Mode) and an expression based on the Mode was applied to the others FF on the same EoD to maintain the same ratio among the facies in the EoD as in the standard model. In this way, changing the variable on the main FF on the EoD, the other facies fraction of the same EoD will directly respect the changes in main FF ratio.

EoD CH_AXIS_3	
HCT_HP	\$HCTHP_CHA3
HCT	$(100 - \$HCTHP\_CHA3) * (10/78)$
LCT	$(100 - \$HCTHP\_CHA3 - \$HCT\_CHA3) * (26/68)$
MXDT	$(100 - \$HCTHP\_CHA3 - \$HCT\_CHA3 - \$LCT\_CHA3) * (15/42)$
VLCT	$(100 - \$HCTHP\_CHA3 - \$HCT\_CHA3 - \$LCT\_CHA3 - \$MXDT\_CHA3)$
EoD CH_AXIS	
HCT_HP	\$HCTHP_CHA
HCT	$(100 - \$HCTHP\_CHA) * (28.66/76.74)$
LCT	$(100 - \$HCTHP\_CHA - \$HCT\_CHA) * (14.11/48.08)$
MXDT	$(100 - \$HCTHP\_CHA - \$HCT\_CHA - \$LCT\_CHA) * (13.93/33.97)$
VLCT	$(100 - \$HCTHP\_CHA - \$HCT\_CHA - \$LCT\_CHA - \$MXDT\_CHA) * (18.56/20.04)$
TRAC	$(100 - \$HCTHP\_CHA - \$HCT\_CHA - \$LCT\_CHA - \$MXDT\_CHA - \$VLCT\_CHA)$
EoD CH_AXIS_1F	
HCT_HP	\$HCTHP_CHA1F
HCT	$(100 - \$HCTHP\_CHA1F) * (39.69/85.74)$
LCT	$(100 - \$HCTHP\_CHA1F - \$HCT\_CHA1F) * (9.71/46.05)$
MXDT	$(100 - \$HCTHP\_CHA1F - \$HCT\_CHA1F - \$LCT\_CHA1F) * (16.18/36.34)$
VLCT	$(100 - \$HCTHP\_CHA1F - \$HCT\_CHA1F - \$LCT\_CHA1F - \$MXDT\_CHA1F) * (12.97/20.16)$
TRAC	$(100 - \$HCTHP\_CHA1F - \$HCT\_CHA1F - \$LCT\_CHA1F - \$MXDT\_CHA1F - \$VLCT\_CHA1F)$
EoD CH_4F	
HCT	\$HCT_CH4F
LCT	$(100 - \$HCT\_CH4F) * (25/85)$
MXDT	$(100 - \$HCT\_CH4F - \$LCT\_CH4F) * (15/60)$
VLCT	$(100 - \$HCT\_CH4F - \$LCT\_CH4F - \$MXDT\_CH4F)$
EoD CH_E_N	
LCT	\$LCT_CHEN
MXDT	$(100 - \$LCT\_CHEN) * (56.39/76.69)$
VLCT	$(100 - \$LCT\_CHEN - \$MXDT\_CHEN)$
EoD CH_D	
HCT_HP	\$HCTHP_CHD
HCT	$(100 - \$HCTHP\_CHD) * (10.5/73)$
LCT	$(100 - \$HCTHP\_CHD - \$HCT\_CHD) * (19/62.5)$
MXDT	$(100 - \$HCTHP\_CHD - \$HCT\_CHD - \$LCT\_CHD) * (17/43.5)$
VLCT	$(100 - \$HCTHP\_CHD - \$HCT\_CHD - \$LCT\_CHD - \$MXDT\_CHD)$

Table 19- EoD and facies fractions algorithm

With the algorithm implemented, corresponding to 29 variables to be simulated, the risk analysis was made by means of the Monte-Carlo uncertainty sampling method. 300 runs were made, which also corresponds to 300 samples per variable, considering one sample for each variable in one run.

The sensitivity was performed in around 15 hours, with an average of 3 minutes of simulation per sample.

Create new:

Edit existing:

Task:  No. of runs:

Base case ☒ Variables ☐ Uncertainty ☐

	Type	Pr	Int	Name	Base value	Distribution	Arguments
1	Uncertain		<input type="checkbox"/>	SHCTHP_CHA3	22	Triangular	Min 12 Mode 22 Max 32
2	Expression		<input type="checkbox"/>	SHCT_CHA3	10		(100-SHCTHP_CHA3)*(10/78)
3	Expression		<input type="checkbox"/>	SLCT_CHA3	26		(100-SHCTHP_CHA3-SHCT_CHA3)*(26/68)
4	Expression		<input type="checkbox"/>	SMXDT_CHA3	15		(100-SHCTHP_CHA3-SHCT_CHA3-SLCT_CHA3)*(15/42)
5	Expression		<input type="checkbox"/>	SVLCT_CHA3	27		100-SHCTHP_CHA3-SHCT_CHA3-SLCT_CHA3-SMXDT_CHA3
6	Uncertain		<input type="checkbox"/>	SHCTHP_CHA	23.26	Triangular	Min 13 Mode 23.26 Max 33
7	Expression		<input type="checkbox"/>	SHCT_CHA	28.66		(100-SHCTHP_CHA)*(28.66/76.74)
8	Expression		<input type="checkbox"/>	SLCT_CHA	14.11		(100-SHCTHP_CHA-SHCT_CHA)*(14.11/48.08)
9	Expression		<input type="checkbox"/>	SMXDT_CHA	13.93		(100-SHCTHP_CHA-SHCT_CHA-SLCT_CHA)*(13.93/33.97)
10	Expression		<input type="checkbox"/>	SVLCT_CHA	18.56		(100-SHCTHP_CHA-SHCT_CHA-SLCT_CHA-SMXDT_CHA)*(18.56/20.04)
11	Expression		<input type="checkbox"/>	STRACT_CHA	1.48		100-SHCTHP_CHA-SHCT_CHA-SLCT_CHA-SMXDT_CHA-SVLCT_CHA
12	Uncertain		<input type="checkbox"/>	SHCTHP_CHA1F	14.26	Triangular	Min 4 Mode 14.26 Max 24
13	Expression		<input type="checkbox"/>	SHCT_CHA1F	39.69		(100-SHCTHP_CHA1F)*(39.69/85.74)
14	Expression		<input type="checkbox"/>	SLCT_CHA1F	9.71		(100-SHCTHP_CHA1F-SHCT_CHA1F)*(9.71/46.05)
15	Expression		<input type="checkbox"/>	SMXDT_CHA1F	16.18		(100-SHCTHP_CHA1F-SHCT_CHA1F-SLCT_CHA1F)*(16.18/36.34)
16	Expression		<input type="checkbox"/>	SVLCT_CHA1F	12.97		(100-SHCTHP_CHA1F-SHCT_CHA1F-SLCT_CHA1F-SMXDT_CHA1F)*(12.97/20.16)
17	Expression		<input type="checkbox"/>	STRACT_CHA1F	7.19		100-SHCTHP_CHA1F-SHCT_CHA1F-SLCT_CHA1F-SMXDT_CHA1F-SVLCT_CHA1F
18	Uncertain		<input type="checkbox"/>	SHCT_CH4F	15	Triangular	Min 5 Mode 15 Max 25
19	Expression		<input type="checkbox"/>	SLCT_CH4F	25		(100-SHCT_CH4F)*(25/85)
20	Expression		<input type="checkbox"/>	SMXDT_CH4F	15		(100-SHCT_CH4F-SLCT_CH4F)*(15/60)
21	Expression		<input type="checkbox"/>	SVLCT_CH4F	45		100-SHCT_CH4F-SLCT_CH4F-SMXDT_CH4F
22	Uncertain		<input type="checkbox"/>	SLCT_CHEN	23.31	Triangular	Min 13 Mode 23.31 Max 33
23	Expression		<input type="checkbox"/>	SMXDT_CHEN	56.39		(100-SLCT_CHEN)*(56.39/76.69)
24	Expression		<input type="checkbox"/>	SVLCT_CHEN	20.3		100-SLCT_CHEN-SMXDT_CHEN
25	Uncertain		<input type="checkbox"/>	SHCTHP_CHD	27	Triangular	Min 17 Mode 27 Max 37
26	Expression		<input type="checkbox"/>	SHCT_CHD	10.5		(100-SHCTHP_CHD)*(10.5/73)
27	Expression		<input type="checkbox"/>	SLCT_CHD	19		(100-SHCTHP_CHD-SHCT_CHD)*(19/62.5)
28	Expression		<input type="checkbox"/>	SMXDT_CHD	17		(100-SHCTHP_CHD-SHCT_CHD-SLCT_CHD)*(17/43.5)
29	Expression		<input type="checkbox"/>	SVLCT_CHD	26.5		100-SHCTHP_CHD-SHCT_CHD-SLCT_CHD-SMXDT_CHD

Run Test Status: **Test OK** Options: ☒

Apply OK Cancel

Figure 107 – Uncertainty and optimization window RA Standard model

### 4.3 MPS model Risk Analysis workflow

On the MPS model approach, the probabilistic geo-body definition was analyzed risking the EoD fraction in the Training Image and performing also the FF analysis on the channels EoD as per the standard model RA.

	\$CHD	\$CHEN	\$RoA	\$CHA1F	\$CHA	\$CHA3	\$CH4F	\$offaxis	FRACTIONS
D	80							20	100
E		33	15					52	100
F				30	18	6	40	6	100

Table 20 – Training Image input facies fractions

The same principle as per the standard model RA was applied, the uncertainty was made on main EoD fractions (Mode) and an expression based on the Mode was applied to the others EoD fractions on the same training image to maintain the same ratio among the EoD.

Pseudozone D	
\$CHD	\$CHD_D
\$offaxis	(100-\$CHD_D)
Pseudozone E	
\$CHEN	\$CHEN_E
\$RoA	(100-\$CHEN_E)*(15/67)
\$offaxis	(100-\$CHEN_E-\$RoA_E)
Pseudozone F	
\$CH4F	\$CH4F_F
\$CHA3	(100-\$CH4F_F)*(6/60)
\$CHA	(100-\$CH4F_F-\$CHA3_F)*(18/54)
\$CHA1F	(100-\$CH4F_F-\$CHA3_F-\$CHA_F)*(30/36)
\$offaxis	100-\$CH4F_F-\$CHA3_F-\$CHA_F-\$CHA1F_F

Table 21- Training image D, E and F facies fraction algorithm

The second section is aimed to run also the sensitivity on the facies fractions FFs inside the channel EoDs, as per the standard model RA algorithm (the same variable range from the mode, and the same algorithm for the other variables) (Table 19).

With the variables implemented, corresponding to 7 variables on the TI and to 29 variables on the probabilistic EoDs facies fractions, making a total of 36 variables, the RA was performed by means of the Monte-Carlo uncertainty sampling method with 500 samples, corresponding to 500 runs, which will consider one sample per each variable per run.

The sensitivity was performed in around 58 hours, with an average of 7 minutes of simulation per sample.



Create new:

Edit existing:

Task:  No. of runs:

Base case ☐ Variables ☐ Uncertainty ☐

	Type	Pr	Int	Name	Base value	Distribution	Arguments					
1	Uncertain			\$CHD_D	80	Triangular	Min	70	Mode	80	Max	90
2	Uncertain			\$CHEN_E	33	Triangular	Min	23	Mode	33	Max	43
3	Expression			\$RoA_E	15		(100-\$CHEN_E)*(15/67)					
4	Uncertain			\$CH4F_F	40	Triangular	Min	35	Mode	40	Max	45
5	Expression			\$CHA3_F	6		(100-\$CH4F_F)*(6/60)					
6	Expression			\$CHA_F	18		(100-\$CH4F_F-\$CHA3_F)*(18/54)					
7	Expression			\$CHA1F_F	30		(100-\$CH4F_F-\$CHA3_F-\$CHA_F)*(30/36)					
8	Uncertain			\$HCTHP_CHA3	22	Triangular	Min	12	Mode	22	Max	32
9	Expression			\$HCT_CHA3	10		(100-\$HCTHP_CHA3)*(10/78)					
10	Expression			\$LCT_CHA3	26		(100-\$HCTHP_CHA3-\$HCT_CHA3)*(26/68)					
11	Expression			\$MXDT_CHA3	15		(100-\$HCTHP_CHA3-\$HCT_CHA3-\$LCT_CHA3)*(15/42)					
12	Expression			\$VLCT_CHA3	27		100-\$HCTHP_CHA3-\$HCT_CHA3-\$LCT_CHA3-\$MXDT_CHA3					
13	Uncertain			\$HCTHP_CHA	23.26	Triangular	Min	13	Mode	23.26	Max	33
14	Expression			\$HCT_CHA	28.66		(100-\$HCTHP_CHA)*(28.66/76.74)					
15	Expression			\$LCT_CHA	14.11		(100-\$HCTHP_CHA-\$HCT_CHA)*(14.11/48.08)					
16	Expression			\$MXDT_CHA	13.93		(100-\$HCTHP_CHA-\$HCT_CHA-\$LCT_CHA)*(13.93/33.97)					
17	Expression			\$VLCT_CHA	18.56		(100-\$HCTHP_CHA-\$HCT_CHA-\$LCT_CHA-\$MXDT_CHA)*(18.56/20.0)					
18	Expression			\$TRAC_CHA	1.48		100-\$HCTHP_CHA-\$HCT_CHA-\$LCT_CHA-\$MXDT_CHA-\$VLCT_CHA					
19	Uncertain			\$HCTHP_CHA1F	14.26	Triangular	Min	4	Mode	14.26	Max	24
20	Expression			\$HCT_CHA1F	39.69		(100-\$HCTHP_CHA1F)*(39.69/85.74)					
21	Expression			\$LCT_CHA1F	9.71		(100-\$HCTHP_CHA1F-\$HCT_CHA1F)*(9.71/46.05)					
22	Expression			\$MXDT_CHA1F	16.18		(100-\$HCTHP_CHA1F-\$HCT_CHA1F-\$LCT_CHA1F)*(16.18/36.34)					
23	Expression			\$VLCT_CHA1F	12.97		(100-\$HCTHP_CHA1F-\$HCT_CHA1F-\$LCT_CHA1F-\$MXDT_CHA1F)*					
24	Expression			\$TRAC_CHA1F	7.19		100-\$HCTHP_CHA1F-\$HCT_CHA1F-\$LCT_CHA1F-\$MXDT_CHA1F-\$					
25	Uncertain			\$HCT_CH4F	15	Triangular	Min	5	Mode	15	Max	25
26	Expression			\$LCT_CH4F	25		(100-\$HCT_CH4F)*(25/85)					
27	Expression			\$MXDT_CH4F	15		(100-\$HCT_CH4F-\$LCT_CH4F)*(15/60)					
28	Expression			\$VLCT_CH4F	45		100-\$HCT_CH4F-\$LCT_CH4F-\$MXDT_CH4F					
29	Uncertain			\$HCTHP_CHD	27	Triangular	Min	17	Mode	27	Max	37
30	Expression			\$HCT_CHD	10.5		(100-\$HCTHP_CHD)*(10.5/73)					
31	Expression			\$LCT_CHD	19		(100-\$HCTHP_CHD-\$HCT_CHD)*(19/62.5)					
32	Expression			\$MXDT_CHD	17		(100-\$HCTHP_CHD-\$HCT_CHD-\$LCT_CHD)*(17/43.5)					
33	Expression			\$VLCT_CHD	26.5		(100-\$HCTHP_CHD-\$HCT_CHD-\$LCT_CHD-\$MXDT_CHD)					
34	Uncertain			\$LCT_CHEN	23.31	Triangular	Min	13	Mode	23.31	Max	33
35	Expression			\$MXDT_CHEN	56.39		(100-\$LCT_CHEN)*(56.39/76.69)					
36	Expression			\$VLCT_CHEN	20.3		100-\$LCT_CHEN-\$MXDT_CHEN					

Run Test Status: **Test OK** Options: ☐

Apply OK Cancel

Figure 108 – Uncertainty and optimization window RA MPS 3rd model

## 4.4 Result comparison

For the standard model a histogram on the STOIIP was achieved with a P10, P50 and P90 probability volumes.

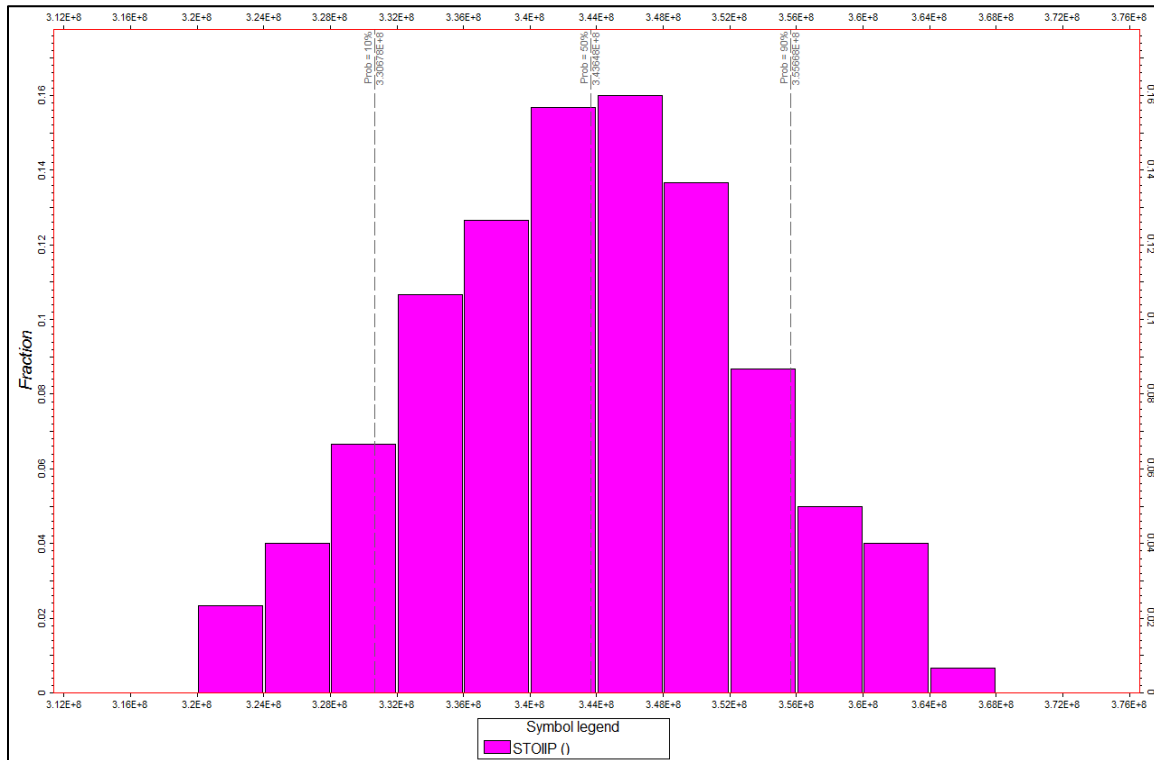


Figure 109 – Standard model uncertainty analyze histogram P10, P50 and P90

P10	P50	P90
330.6	343.6	355.6
-3.78%		3.49%

Table 22- Standard model RA STOOIP P10, P50 and P90

The STOIIP of the base case is 347 MMSTB, the P50 on the RA is in line with the base case. The facies variation impact on the STOIIP is acceptable with a standard deviation from P50 around 3.7% to P10 and P90.

The MPS model histogram on the STOOIP was achieved with a P10, P50 and P90 probability volumes.

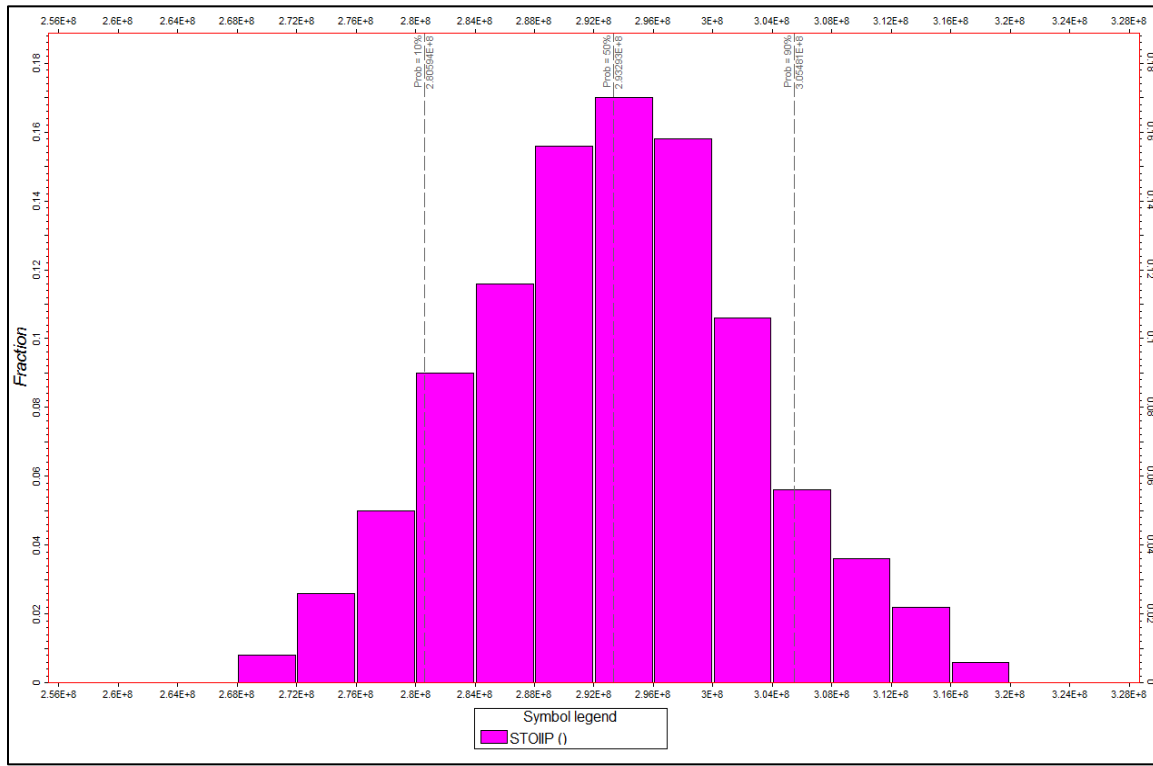


Figure 110 – MPS model uncertainty analyze histogram P10, P50 and P90

P10	P50	P90
280.6	293.3	305.5
-4.33%		4.20%

Table 23- MPS model RA STOOIP P10, P50 and P90

The MPS STOIIP base case is 293.6 MMSTB, the P50 on the RA is in line with the base case, a standard deviation from P50 of 4.3% to P10 and P90 is observed.

On the MPS model RA the STOIIP standard deviation is higher than on the standard model RA, from an average 3.7 % to 4.3%, which is acceptable, considering that on the MPS RA the sensitivity was made with a high number of variables (36) corresponding to the EoD fraction as input for the training image and the facies fraction in the channel EoDs.

The standard model RA was made with less variables (29), corresponding to the facies fraction in the channel's EoDs.

Since the facies fraction algorithm in the channels EoDs was the same applied in both sensitivities, the difference between the two standard deviation values is linked to the RA performed on the MPS model in the EoD input fractions in the training image.

## 5 CONCLUSION AND WAY FORWARD

Multiple-point statistics (MPS) is a facies modeling technique based on multiple point statistics instead of the conventional variogram-based technique founded on bi-point statistics. Through the use of a Training Image (i.e. conceptual model), which describes the geometrical and statistical characteristics of the facies to be modelled, this technology enables to model non-linear facies, geo-body shapes such as sinuous channels, and to capture complex spatial relationships between multiple facies.

This was achieved extending the stochastic simulation approach to the sedimentological model by means of the MPS approach. In fact the Environment of Deposition (EoD) coming from the sedimentological interpretation have been used to build the training images (conceptual models) for each zone, as result a probabilistic EoD (Geo-body) was achieved. Instead of being the product of a deterministic interpretation.

The facies and petrophysical properties have been distributed following the same approach (parameters and process) of the standard modelling, in order to properly evaluate the impact of the MPS algorithm on the STOIP.

The MPS model from a volumetric perspective is a conservative model compare with the standard one, given very similar percentages of EoDs. This is mainly due to the 3D definition of the sedimentological features. The MPS algorithm allows a very detailed geological modelling in terms of both shapes and spatial relationship among the EoDs and the geo-bodies, which are better geologically represented. This affects the facies and petrophysical properties distribution.

The external constraint in the MPS model have a huge influence, they work as a guiding tool for the geo-body distribution within the MPS approach, they allow constraining the simulation by modulating the strength of the secondary variable by means of a weigh factor value ranging from 0 to 1, In this way, depending on the maturity of the studies carried out on the field, the stochastic contribution of the algorithm can be fine-tuned, but always honoring the well data. High values of the weight factor will decrease the training image performance that will lead to a close match to the standard model and the geological meaning of the model is compromised.

The weight factor representing the 3D probability volume as external constraint will work in a simplified way accounting for the non-stationary features of the data related with the environment of deposition (EoD), represented in the MPS model.

A remarkable advantage of MPS methodology with respect to the standard model is the possibility to easily update the sedimentological model once new wells are available. If the well results show a different sedimentological behavior (i.e. a different EoD than expected) a new deterministic interpretation will not be needed. It will be enough up-scaling the EoD in the 3D grid and run the EoD simulation that is already considering the geological features.

Before going more in detail, it is important to remember that the “MPS modelling workflow” is very similar to the standard one. The main and most important difference is the EoD modelling way. The deterministic interpretation of the standard model has been replaced by a stochastic simulation (MPS based) driven by an external probabilistic constraint. This step has been tested with several sensitivities that lead to a volumetric analyze and finishing with



risk analysis focus on the impact on the volume based on the sensitivities on the deterministic and probabilistic EoDs and MPS Geo-body definition.

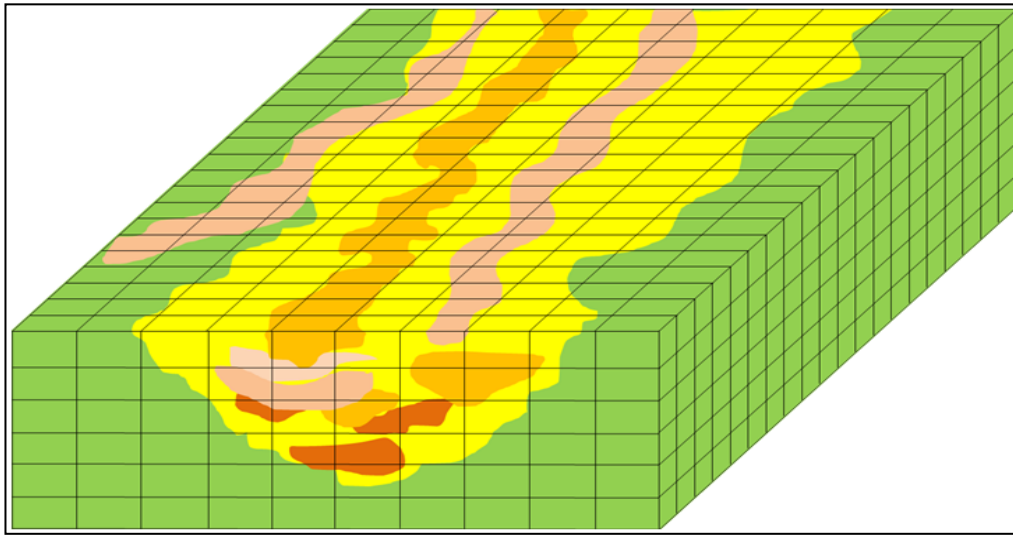


Figure 111 – MPS Concept model (with stacked geo-bodies)

The detailed results of the work are listed here below:

- The MPS technology has a better definition of the geological shapes and a robust simulation of sedimentological model considering the detail input parameters on the training image and external constraints;
- the definition of the TIs by means of the object modelling stochastic algorithm allows capturing and reproducing the stratigraphic and depositional principles (superposition, cross-cutting, intrusive relation);
- In the MPS model is easy to update the sedimentological model with new well data, which in reservoir development scenario can be a very important tool on the local model update to better understand the reservoir in an operational time frame;
- The EoD definition can be modified or optimized to seismic resolution, considering the vertical orientation of the sedimentological model;
- Training Image definition is a time consuming iterative process, many sensitivities are needed to get the right spatial configuration and distribution;
- The EoD probability volume (3D external trend property), requires a smoothness sensitivity on the EoD model definition, which to be performed a good understanding of the sedimentological model is needed. This is an iterative process and it is clearly time consuming;
- Being the sedimentological model closer to the real depositional behavior, a more realistic output from the model in term of well prognosis (facies and petrophysical properties) can be achieved;
- MPS simulation is a time consuming algorithm in terms of both training image definition and facies simulation. This has to be taken into account especially while planning a Risk Analysis.

MPS implementation in the reservoir model can be achieved easily once a few sedimentological data are available. Moreover it allows a faster and simpler updating of the model as well as the possibility to define the strength of the external deterministic constraints on the stochastic simulation, always honoring well data.

It is important to highlight that a proper computational capacity is needed to run this kind of simulation and it is even more critical when performing a complete reservoir Risk Analysis.

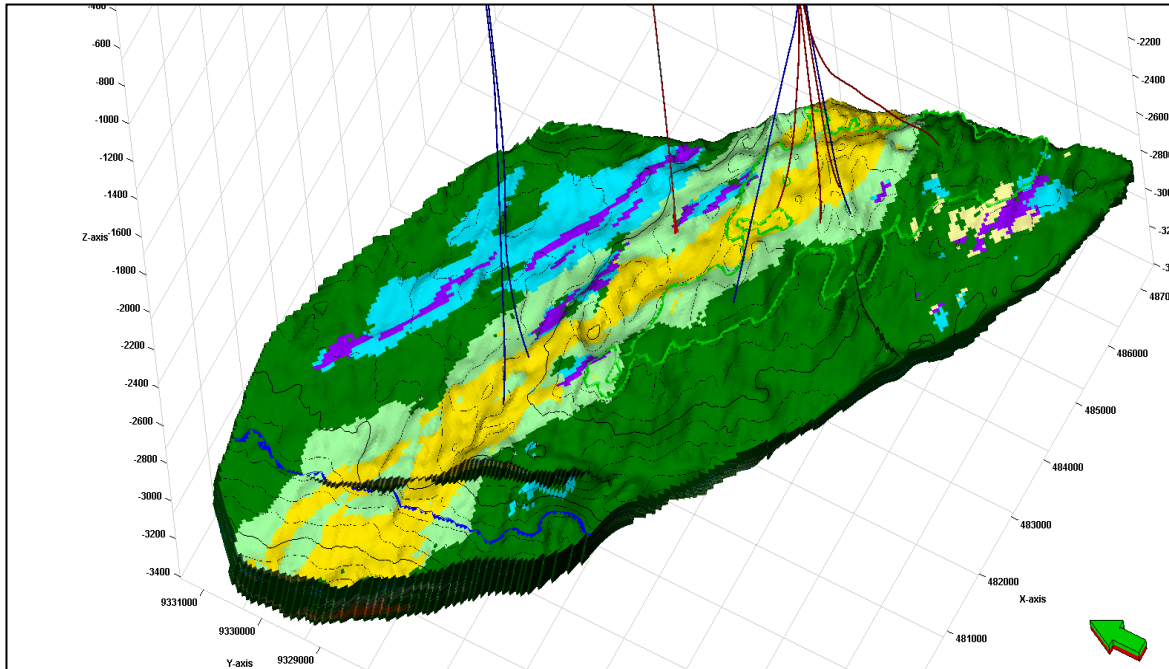


Figure 112 – MPS model

To complete the study a reservoir dynamic simulation should be performed (initialization, History Match and forecast) in order to verify if the dynamic behavior of the field is better matched and forecasted by a static model, which reproduces with more details the geological features and their spatial relationships.

These could influence the way forward on the pre-development and development campaign of a field, based on the better geological representation of the subsurface, the model conservative output and a robust dynamic model.



## ACKNOWLEDGEMENTS

There are so many wonderful people from teachers to class mates that were a key element on Politecnico di Torino. Thanks for helping me during the last two year during the amazing Master Program in Petroleum Engineering.

The professors who brought the exiting engineering curiosity to the class, making the two year path memorable.

The outstanding class mates which through discussions and an exchange of experiences added value to the learning curve.

First, I would like to thanks my direct supervisor Tomasi Andrea for his guidance, technical discussions and Support over the last four months, your support was essential to my success.

I also would like to say thank you to my Politecnico supervisor, Professor Stefano Lo Russo for his patient and will to help and support during the last four months.

The learning curve is just a derivative of the wiliness to do so; the petroleum engineering course is a strong back bone for a carrier on the oil and gas industry.

Great appreciation to ENI Angola and the Reservoir manager **Ilario Franco**, for the opportunity on this project allowing the use of an Angola offshore field data.

Big thanks for the amazing engineers on the reservoir department that within they time gave me technical support.



## REFERENCES

- [1] - Tahmasebi P, Multiple point statistics: a Review 2018, P 618-620, Department of Petroleum Engineering, University of Wyoming, Laramie. WY 8271, USA [https://doi.org/10.1007/978-3-319-78999-6\\_30](https://doi.org/10.1007/978-3-319-78999-6_30).
- [2] - S. Lyster, A Comparison of MPS Algorithms 2008, P 113-1. [http://www.ccgaberta.com/ccgresources/report10/2008-113\\_mps\\_comparison.pdf](http://www.ccgaberta.com/ccgresources/report10/2008-113_mps_comparison.pdf).
- [2] - A. S. Høyer, G. Vignoli, T. M. Hansen, L. T. Vu, D. A. Keefer, F. Jørgenden, Multiple point Statistical simulation for hydrogeological models: 3-D training image development and conditioning strategies, Hydrology Earth System Science, 21, 6069-6089, 2017 <https://doi.org/10.5194/hess-21-6069-2017>.
- [3] - A.G. Journel, Multiple-point Geostatistics: a State of the Art, 2003, Stanford Center for Reservoir forecasting [https://pangea.stanford.edu/departments/ere/dropbox/scrf/documents/reports/16/SCRF2003\\_Report16/SCRF2003\\_Andre\\_Journel.pdf](https://pangea.stanford.edu/departments/ere/dropbox/scrf/documents/reports/16/SCRF2003_Report16/SCRF2003_Andre_Journel.pdf).
- [4] - Y. Yin, W.Feng, A location-based multiple point statistics method: modelling the reservoir with non-stationary characteristics, <https://doi.org/10.1515/geo-2017-0048>.
- [5] - J. Caers, T. Zhang, Multiple-point geostatistics: a quantitative vehicle for integrating geologic analogs into multiple reservoir models 2006, Stanford University, Stanford Center for Reservoir forecasting, CA 94305-2220, <https://pdfs.semanticscholar.org/3115/99f2be14da9271e04fb07a16785329e4da17.pdf>.
- [6] - Petrel 20117.1 User guide, training image scale. Schlumberger;
- [7] - Cabaça Reservoir studies LM22, Eni Angola,